land

MDPI

Article

Navigating Ecological–Economic Interactions: Spatiotemporal Dynamics and Drivers in the Lower Reaches of the Jinsha River

Zhongyun Ni [1], Yinbing Zhao [1,2,3,*], Jingjing Liu [1], Yongjun Li [1], Xiaojiang Xia [1] and Yang Zhang [1,4]

[1] College of Geography and Planning, Chengdu University of Technology, Chengdu 610059, China; nizhongyun2012@mail.cdut.edu.cn (Z.N.)
[2] State Key Laboratory of Urban and Regional Ecology, Research Center for Eco-Environmental Sciences, Chinese Academy of Sciences, Beijing 100085, China
[3] Human Geography Research Center of Qinghai-Tibet Plateau and Its Eastern Edge, Chengdu University of Technology, Chengdu 610059, China
[4] School of Architecture, Southeast University, Nanjing 210096, China
* Correspondence: zhaoyinbing06@cdut.cn

Abstract: The lower reaches of the Jinsha River, serving as a vital ecological barrier in southwestern China and playing a crucial role in advancing targeted poverty alleviation efforts, remain underexplored in terms of the coupling between ecological and economic development, creating a gap in understanding the region's sustainable development potential. This study combines the remote sensing ecological index (RSEI) derived from MODIS data and the biodiversity richness index (BRI) based on land use data to create the ecological environment index (EEI) using a weighted approach. It also develops the economic development index (EDI) from economic data using the entropy weight method. By integrating the EEI and EDI, the study calculates key metrics, including the ecological–economic coupling degree (EECD), coupling coordination degree (EECCD), and relative development degree (EERDD), and examines their spatiotemporal changes from 2000 to 2020. Additionally, the study applies a geographic detector model to identify the spatial drivers of the EEI, an obstacle factor diagnosis model to pinpoint the main barriers to EDI, and a neural network model to uncover the underlying forces shaping EECCD. The results indicate that: (I) From 2000 to 2020, the overall improvement rate of the ecological and economic subsystems was greater than that of the ecological–economic coupling system. The entire region is still in the Running-In Stage, and the coordination level has been upgraded from near imbalance to marginal coordination. About 85% of the counties' EERDDs are still in the EDI Behind EEI Stage. (II) The structural composition of the EEI shows a pattern of low Dry Hot Valley Area and high in other areas, mainly driven by natural factors, although human activities had a notable impact on these interactions. (III) Originating from an impact model primarily driven by economic factors and supplemented by ecological factors, both EDI and EECCD exhibit a pattern of high in the south and low in the north, with improvements spreading northward from the urban area of Kunming. The development gradient differences between 24 poverty-stricken counties and 16 non-poverty-stricken counties have been reduced. (IV) For the six types of ecological–economic coupling development zones, it is essential to adopt localized approaches tailored to the differences in resource and environmental characteristics and development stages. Key efforts should focus on enhancing ecological protection and restoration, increasing financial support, implementing ecological compensation mechanisms, and promoting innovative models for sustainable development.

Keywords: ecological environment index; economic development index; coupling coordination degree; geographic detector; obstacle recognition; neural network model; natural and anthropogenic drivers; development gradient; targeted poverty alleviation

check for updates

Citation: Ni, Z.; Zhao, Y.; Liu, J.; Li, Y.; Xia, X.; Zhang, Y. Navigating Ecological–Economic Interactions: Spatiotemporal Dynamics and Drivers in the Lower Reaches of the Jinsha River. *Land* **2024**, *13*, 2159. https://doi.org/10.3390/land13122159

Academic Editors: Yinghui Zhang, Jingzhe Wang, Yangyi Wu, Ivan Lizaga and Zipeng Zhang

Received: 3 November 2024
Revised: 2 December 2024
Accepted: 8 December 2024
Published: 11 December 2024

Copyright: © 2024 by the authors. Licensee MDPI, Basel, Switzerland. This article is an open access article distributed under the terms and conditions of the Creative Commons Attribution (CC BY) license (https://creativecommons.org/licenses/by/4.0/).

1. Introduction

The ecological and economic environments exhibit a mutual relationship of influence and constraint, wherein they foster and propel each other's growth to a certain degree. Engaging in research on the coupled development of the ecological economy holds immense significance for advancing harmonious coexistence between humanity and nature, as well as bolstering the overall competitiveness of regions [1,2]. To characterize the relationship between the ecological and economic environments, researchers often use both single and composite indicators, such as the environmental Kuznets curve [3,4], human development index (HDI) [5,6], green GDP [7,8], ecological footprint [9], eco-efficiency index [10,11], sustainability index [12,13], natural capital index [14,15], sustainable development indicators (SDIs) [16], ecosystem service valuation (ESV) [17,18], coupling degree [19], coupling coordination degree (CCD) [20,21], and relative development degree [22]. These indicators provide a variety of evaluation perspectives, offering researchers nuanced insights into the ecological–economic interplay. The CCD is widely employed to assess the coordinated development between systems or among elements within a system. However, there remains a gap in optimizing the selection of evaluation indicators, improving data accuracy, and refining data processing methods, all of which are essential to further enhance the precision and reliability of CCD analyses.

Based on the above indicators, different analysis models were constructed to further explore the coupling mechanism between the ecological and economic environments. System dynamics models simulate the impacts of various economic conditions on ecological–economic systems [23,24]. The input–output model analyzes industrial linkages and resource usage, guiding industrial optimization and resource allocation strategies [25]. The grey correlation degree model quantifies the influence of multiple factors on ecological–economic development through ranking analysis, offering policy insights [26,27]. The ecological footprint model compares human resource consumption with ecological carrying capacity to guide sustainable development efforts [28,29]. Moreover, the coupling coordination model, which constructs a comprehensive evaluation index system for ecological–economic systems, calculates the degree of coupling and coordination to assess development trends and levels [30,31]. Additionally, various methods have been employed to analyze the causes or driving forces of changes in economic subsystems, ecological environment subsystems, or ecological–economic coupling systems, including the fixed effects regression model [32], the ordinary least squares regression model [33], the geographically weighted regression model [34], and obstacle factor analysis [35]. Simultaneously, neural network models are gaining increasing recognition for their advanced pattern recognition capabilities in analyzing changes and complex interactions within ecological and economic systems [36,37]. However, these models present significant gaps in both dynamic change monitoring and model interpretability. Consequently, the accuracy of ecological–economic coupling evaluations and predictions remains constrained, undermining the scientific foundation for effective policy formulation.

Research on the coupling development of ecological and economic systems spans multiple spatial and temporal scales, each reflecting different ecological, regional, and economic dynamics. Key scales include the global scale [38,39], which addresses global ecological–economic interactions like carbon emissions and resource use patterns; the national or regional scale [40,41], focusing on the impacts of large-scale policies on sustainability; the county or city level [42], examining localized ecological and economic interrelations driven by regional policies and practices; and the urban scale, where studies focus on urban growth, resource management, and environmental preservation [43]. Research at the watershed or environmental region scale [44,45] closely aligns with the comprehensive and dynamic nature of natural ecological processes, providing a practical framework for addressing the challenges of economic development more effectively. In China, significant focus has been placed on studying the ecological and economic coupling within major regions such as the Yellow River Basin and the middle and lower reaches of the Yangtze River Basin [46–49]. However, there has been relatively limited research in

areas like the lower reaches of the Jinsha River, located in the upper Yangtze River Basin, despite the ecological and economic significance of these regions.

The lower reaches of the Jinsha River are vital for biodiversity conservation in the Hengduan Mountains and soil conservation in the dry hot valleys of Sichuan and Yunnan. Despite its ecological fragility, the region is rich in species diversity. As a key ecological barrier in the Yangtze River Basin, safeguarding the environment here is crucial for ensuring the ecological security of the entire Yangtze River Economic Belt and, by extension, the nation [50]. Moreover, this region is abundant in mineral, tourism, agriculture, forestry, and hydropower resources. The combined installed capacity of the four hydropower stations—Wudongde, Baihetan, Xiluodu, and Xiangjiaba—equals that of two Three Gorges Dams [51]. As resource development and ecological protection efforts have advanced, the region has experienced industrial upgrades and transformation, with poverty alleviation efforts in Wumeng and Daliang Mountains further complicating the interaction between its ecological and economic environments [52]. While past research has predominantly focused on the ecological environment [53,54], the coupling effects between ecology and economy remain underexplored. This gap limits the support needed to consolidate poverty alleviation achievements and foster regional development.

This study investigates the ecological and economic development challenges in the lower reaches of the Jinsha River by integrating a wide range of data sources, including ecological environment, terrain and climate, land resources and utilization, economic indicators, urbanization and population dynamics, infrastructure, and accessibility. Leveraging this integration, the study establishes a comprehensive evaluation index system to assess ecological–economic coupling. It thoroughly examines the spatiotemporal evolution patterns of ecological and economic subsystems, as well as the broader ecological–economic coupling system. Additionally, it explores the driving mechanisms behind these changes and offers strategic recommendations for sustainable future development.

2. Study Area and Data Sources

2.1. Study Area

Located in southwestern China, the lower reaches of the Jinsha River (LR-Jinsha) refer specifically to the basin stretching from the confluence of the Yalong River in Panzhihua City to the confluence of the Minjiang River in Yibin (Figure 1a). This study focuses on the counties (districts) within the administrative boundaries of the lower Jinsha River basin. The research area is geographically defined by coordinates 100°57′–104°38′ E and 24°29′–28°53′ N, covering an area of 81,035 km^2. It spans seven cities (prefectures) in Sichuan and Yunnan provinces, comprising a total of 40 counties (districts), including 16 A-class regions (non-poverty areas) and 24 B-class regions (lifted out of poverty by 2020) (Figure 1b). This regional classification is primarily based on factors such as geographical location, resource availability, economic development levels, poverty status, poverty alleviation goals, policy orientation, and regional development strategies. The 16 A-class regions include Anning, Chenggong, Dongqu, Fumin, Guandu, Huidong, Huili, Jinning, Ningnan, Panlong, Renhe, Shuifu, Songming, Wuhua, Xishan, and Yuanmou. The 24 B-class regions include Butuo, Daguan, Dayao, Dongchuan, Huize, Jinyang, Leibo, Ludian, Luquan, Meigu, Mouding, Pingshan, Puge, Qiaojia, Suijiang, Wuding, Xundian, Yanjin, Yao'an, Yiliang, Yongren, Yongshan, Zhaojue, and Zhaoyang.

The research area features significant variations in altitude and terrain, with steeper slopes in the central and western regions and gentler slopes in the eastern region. The landform is divided into five zones: the Wumeng Mountain Area, Sichuan Basin, Southwest Sichuan Mountain Area, Dry Hot Valley Area, and Plateau Basin Valley Area (Figure 2a). The region predominantly falls within the subtropical monsoon climate zone, characterized by uneven precipitation distribution. The annual average precipitation exceeds 800 mm, and the average annual temperature is approximately 13–14 °C. It is further categorized into three subzones: North Subtropical Zone, Central Subtropical Zone, and South Subtropical Zone (Figure 2a).

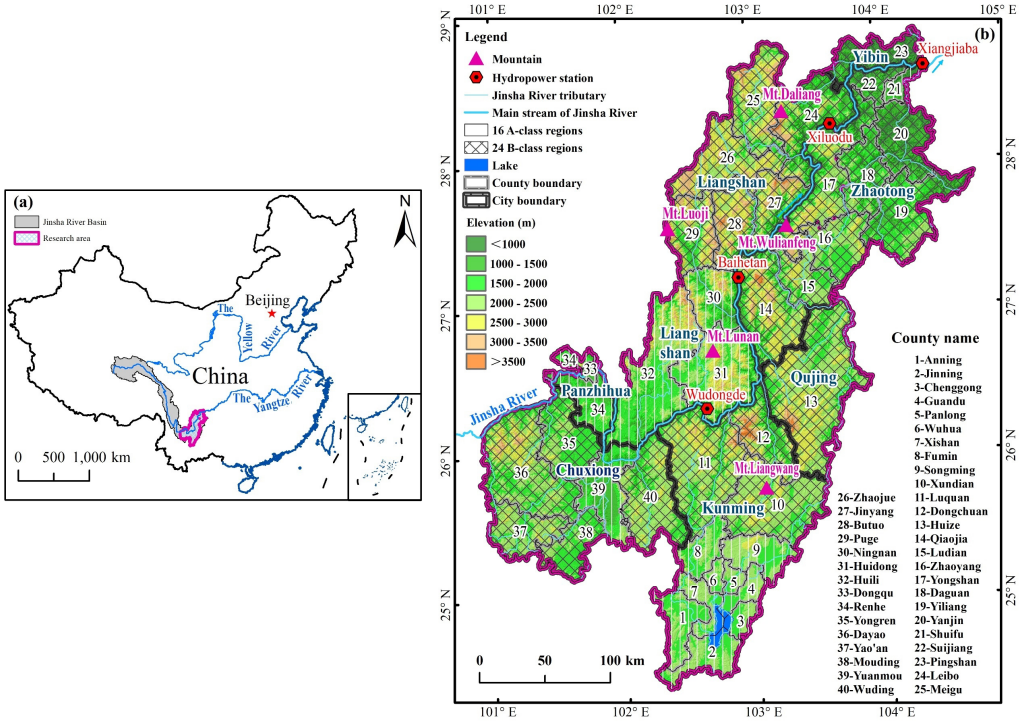


Figure 1. Location of the study area. (**a**) Location of the study area in China; (**b**) administrative division of the study area.

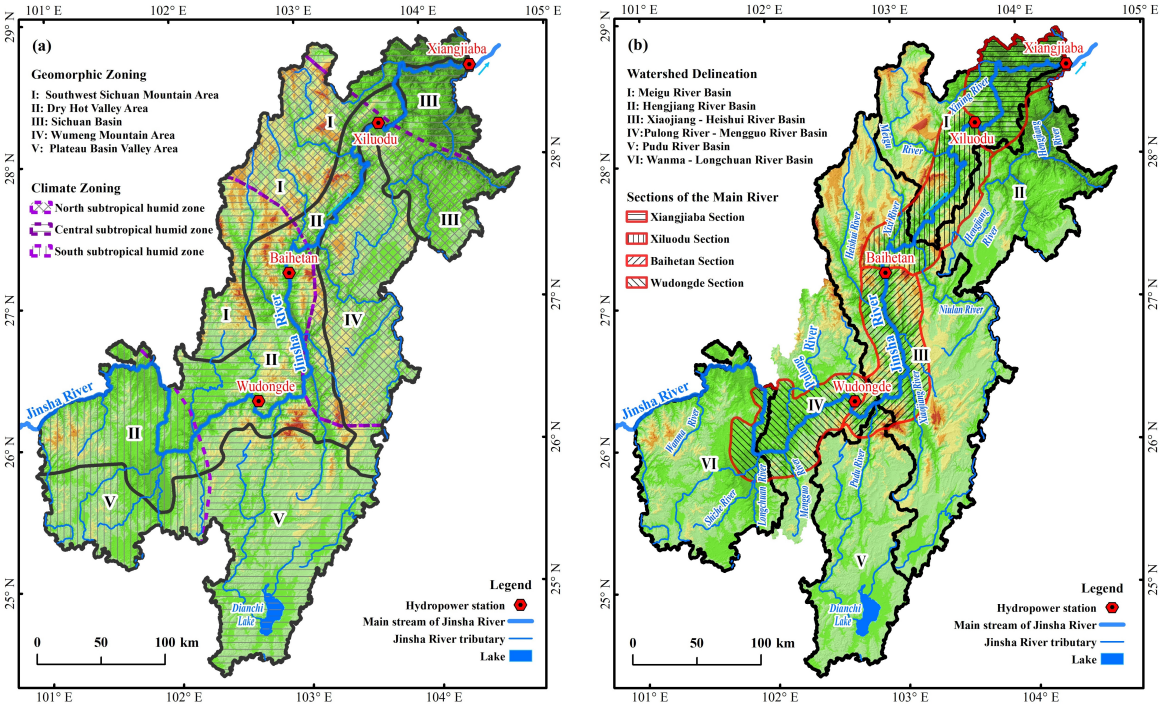


Figure 2. Subdivision of the research area: (**a**) Geomorphic and climatic zoning; (**b**) watershed zoning and main stream segmentation.

The water system in the study area is divided into six sub-basins: Meigu River Basin, Hengjiang River Basin, Xiaojiang Heishui River Basin, Pulong River Mengguo River Basin, Pudu River Basin, and Wanma Longchuan River Basin (Figure 2b). Additionally, based on the locations of four major cascade hydropower stations downstream on the Jinsha River, the river is segmented into four sections: Xiangjiaba Section, Xiluodu Section,

Baihetan Section, and Wudongde Section (Figure 2b). According to the "National Ecological Function Zoning" issued by China in 2015, the research area is recognized as an important zone for soil conservation, biodiversity preservation, agricultural production, and urban agglomeration. It is classified as both extremely important and relatively important for ecological protection. This complex ecological and economic landscape forms the basis for the integrated development of ecology and economy in the region.

2.2. Data Sources

To identify the ecological–economic coupling system and its dynamic changes, this study primarily gathers time-series data for five key periods: 2000, 2005, 2010, 2015, and 2020. The collected data encompass evaluations of ecological environment quality, assessments of economic development levels, and the driving factors influencing ecological environment changes, economic growth, and the causes of ecological–economic coupling (Table 1). The selection of these specific years is guided by considerations such as the research objectives, data availability, policy and economic contexts, and the evolving dynamics of the ecological–economic coupling system.

Table 1. Calculation and analysis data of ecological–economic coupling system.

No.	Data	Type	Data Sources	Spatial Resolution
1	Gross value of primary industry ①	Statistical	Sichuan Statistical Yearbook (2001–2021) and Yunnan Statistical Yearbook (2001–2021)	County
2	Second gross domestic product ①	Statistical		County
3	Gross value of the tertiary industry ①	Statistical		County
4	Urbanization rate ①	Statistical		County
5	Per capita cropland area ①	Statistical	China Regional Economic Statistical Yearbook (2001–2021)	County
6	Total GDP ①	Statistical		County
7	Per capita GDP ①	Statistical		County
8	Total retail sales of consumer goods ①	Statistical		County
9	Nighttime light index ①③	Grid	Institute of Geographic Sciences and Resources, Chinese Academy of Sciences [a]	1 km
10	Cropland area ②	Grid	Land use dataset created by Yang and Huang (2021) from Wuhan University	1 km
11	Woodland area ②	Grid		
12	Grassland area ②	Grid		
13	Water area ②	Grid		
14	Construction land area ②	Grid		
15	Unused land area ②	Grid		
16	Normalized Difference Vegetation Index (NDVI) ②	Grid	Calculated from Moderate-Resolution Imaging Spectroradiometer (MODIS) data, sourced from the USGS [b]	1 km
17	Wetness Index (WET) ②	Grid		
18	Normalized Difference Built-up and Bareness Index (NDBSI) ②	Grid		
19	Land Surface Temperature (LST) ②	Grid		
20	Annual average temperature ③	Grid	National Qinghai Tibet Plateau Scientific Data Center [c]	1 km
21	Annual precipitation ③	Grid		
22	Elevation ③	Grid	Geographic Spatial Data Cloud [d]	30 m
23	Slope ③	Grid		
24	Aspect ③	Grid		
25	Land use type ③	Grid	Land use dataset created by Yang and Huang (2021) from Wuhan University	30 m
26	Cropland density ③	Grid		1 km
27	Construction land density ③	Grid		
28	Gross domestic product density ③	Grid	Institute of Geographic Sciences and Resources, Chinese Academy of Sciences [a]	1 km

Table 1. *Cont.*

No.	Data	Type	Data Sources	Spatial Resolution
29	Population density ③	Grid	School of Geography and Environmental Sciences at the University of Southampton [e]	100 m
30	Euclidean distance of road ③	Grid	Calculated from road vector data, sourced from National Geomatics Center of China [f]	1 km

[a] https://www.resdc.cn/ (accessed on 26 July 2024); [b] https://earthexplorer.usgs.gov/ (accessed on 26 July 2024); [c] https://data.tpdc.ac.cn/ (accessed on 26 July 2024); [d] http://www.gscloud.cn/ (accessed on 26 July 2024); [e] https://www.worldpop.org/ (accessed on 26 July 2024); [f] http://www.ngcc.cn (accessed on 26 July 2024); Symbol ① indicates that the data are used to analyze obstacles to the economic development index. Symbols ① and ② indicate that the data are used to analyze the Ecological–Economic Coupling Coordination Degree via the neural network model. Symbol ③ represents the driving forces for analyzing the ecological environment index using the geographic detector model.

2.2.1. Basic Geographic Data

In addition to the thematic data listed in Table 1, the basic geographic data used in this article—such as administrative divisions, place names, water systems, mountain ranges, and power stations—are all sourced from the National Geomatics Center of China. Geomorphic divisions [55], climate divisions [56], and other relevant data are also referenced. To ensure the consistency and accuracy of the research data, multi-source heterogeneous spatial data are uniformly processed: the coordinate system used is WGS1984, with the Universal Transverse Mercator (UTM) projection, specifically using UTM 48N Zone. Statistical data are assigned to the corresponding county-level units for use as vector data, while grid data are standardized in spatial resolution using resampling or interpolation methods as required for evaluation and analysis.

2.2.2. Statistical Data

Statistical data are primarily used for evaluating and analyzing the driving factors of economic development levels, assessing the ecological–economic coupling and coordination degree, and analyzing the degree of obstacles. These data mainly come from the Sichuan Statistical Yearbook, Yunnan Statistical Yearbook, China Regional Economic Statistical Yearbook, and local government annual national economic and social development bulletins. To ensure the accuracy of the spatial representation of economic data, all data from the periods 2000, 2005, 2010, 2015, and 2020 were standardized to the spatial scale of counties and districts, totaling 40 evaluation units in the study area. Data on the gross value of primary industry, secondary gross domestic product, gross value of the tertiary industry, urbanization rate, per capita cropland area, total GDP, per capita GDP, and total retail sales of consumer goods were all processed using this method.

2.2.3. Grid Data

The five data generation methods for cropland area, woodland area, grassland area, water area, construction land area, and unused land area are as follows: using a 2 km × 2 km grid, the area of each grid corresponding to the land use type was calculated, then the statistical value was assigned to the center point of the grid. The inverse distance weighted method was applied to interpolate and generate raster data with a spatial resolution of 1 km. Similarly, the two data generation methods for cropland density and construction land density are as follows: using a 1 km × 1 km grid, the area of cropland or construction land corresponding to each grid was calculated, then the inverse distance weighted method was applied to interpolate and generate raster data with a spatial resolution of 1 km. The four data types of NDVI (Normalized Difference Vegetation Index), WET (Wetness Index), NDBSI (Normalized Difference Built-up and Bareness Index), and LST (Land Surface Temperature) were calculated from MODIS (Moderate-Resolution Imaging Spectroradiometer) data. The elevation data came directly from the Digital Elevation Model (DEM), while the

slope and aspect data are derived from the DEM. The data for annual average temperature, annual precipitation, gross domestic product density, and population density were all downloaded and uniformly processed to a spatial resolution of 1 km.

2.2.4. MODIS Data

As a crucial tool for earth science research and application development, the Google Earth Engine (GEE) data processing platform offers extensive data storage and processing capabilities [57]. Users can access a wide variety of remote sensing data stored on the GEE platform in real time, eliminating the need to download and store large amounts of data. This makes data analysis and processing both convenient and efficient. Additionally, GEE provides several effective cloud removals processing solutions, helping users handle obstructions such as clouds and shadows in remote sensing images, thereby enhancing image quality and usability. Due to the vast area of the study region and its complex meteorological conditions, the availability of cloud-free and low-cloud Landsat satellite data is limited. As a result, this study utilizes MODIS data in place of Landsat satellite data. Utilizing this platform, through band operation technology, we achieved minimum cloud amount fusion, obtaining same-season MODIS datasets for five different years—2000, 2005, 2010, 2015, and 2020—as data sources for remote sensing ecological index extraction (Figure A1).

3. Methodology

The technical workflow of this study is presented in Figure 3: (I) We extracted four key components—NDVI, WET, NDBSI, and LST—from the MODIS dataset, which were synthesized to form the remote sensing ecological index (RSEI). (II) Land use data were used to calculate the area proportions of different land types, which were then utilized to construct the biodiversity richness index (BRI). (III) The integration of the RSEI and BRI produced the ecological environment index (EEI), while a geographic detector was applied to analyze the driving forces, leveraging additional datasets. (IV) The economic development index (EDI) was derived from economic dataset, revealing spatiotemporal patterns, and the obstacle degree method was employed to identify key drivers. (V) The EEI and EDI data were used to calculate the ecological–economic coupling degree (EECD), the ecological–economic coupling coordination degree (EECCD), and the ecological–economic relative development degree (EERDD), with the spatiotemporal patterns of these indices analyzed. A neural network model was specifically applied to explore the drivers behind the EECCD. (VI) Tailored development strategies were then proposed based on the characteristics of ecological–economic coupling in the region.

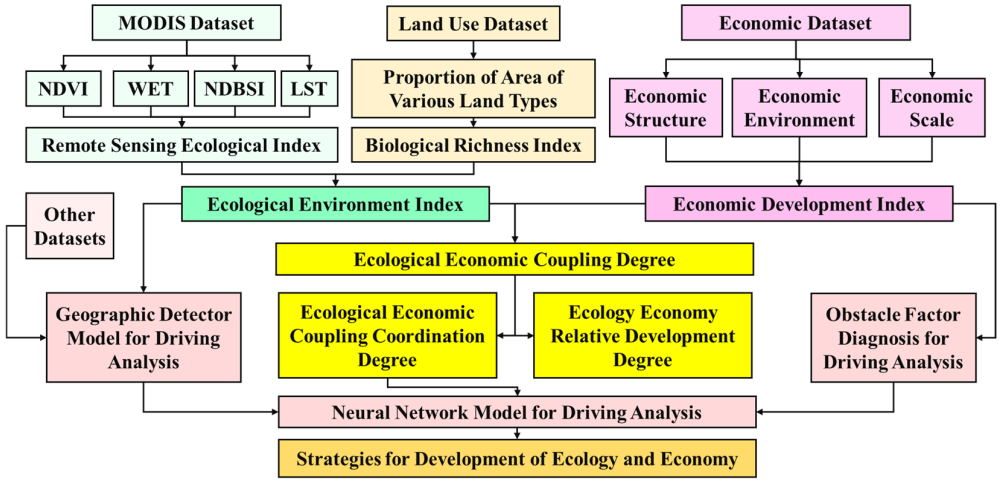


Figure 3. Technical workflow of this study.

3.1. Construction of Evaluation Index System

Following the principles of scientific rigor, representativeness, and comprehensiveness in indicator selection, this study comprehensively examined the current situation of the research area and constructed an ecological–economic coupling system indicator evaluation system based on previous experience (Table 2). The economic subsystem is characterized by three components: economic structure, economic environment, and economic scale [58–60]. Three indicators—total primary industry output, total secondary industry output, and total tertiary industry output—were selected to reflect the economic structure [60], and these indicators were used to generate the economic structure index (EcoESTI). Three indicators—urbanization rate, per capita cropland area, and nighttime light index—were selected to reflect the economic environment [61–63], and these indicators were used to generate the economic environment index (EcoEEI). Three indicators—total GDP, per capita GDP, and total retail sales of consumer Goods—were selected to reflect the economic scale, and these indicators were used to generate the economic scale index (EcoESCI). The ecological subsystem is characterized by the RSEI and the biological richness index (BRI). The RSEI includes four indicators: NDVI, WET, NDBSI, and LST. The biological richness index includes six indicators: cropland area, woodland area, grassland area, water area, construction land area, and unused land area.

Table 2. Evaluation index system for ecological–economic coupling system.

System	Subsystem	First Level Indicator	Second Level Indicator	Code	Weight
Ecological Economic Coupling System	Economic Subsystem	Economic Structure	Total Primary Industry Output	C_{11}	Determined by Entropy Weight Method
			Total Secondary Industry Output	C_{12}	
			Total Tertiary Industry Output	C_{13}	
		Economic Environment	Urbanization Rate	C_{21}	
			Per Capita Cropland Area	C_{22}	
			Nighttime Light Index	C_{23}	
		Economic Scale	Total GDP	C_{31}	
			Per Capita GDP	C_{32}	
			Total Retail Sales of Consumer Goods	C_{33}	
	Ecological Subsystem	Biological Richness Index	Cropland Area	E_{11}	Determined by Analytic Hierarchy Process
			Woodland Area	E_{12}	
			Grassland Area	E_{13}	
			Water Area	E_{14}	
			Construction Land Area	E_{15}	
			Unused land Area	E_{16}	
		Remote Sensing Ecological Index	NDVI	E_{21}	Determined by Principal Component Analysis Method
			WET	E_{22}	
			NDBSI	E_{23}	
			LST	E_{24}	

3.2. Entropy Weight Method

The entropy weight method is an objective weighting technique that assigns weights according to the amount of information each indicator contains. It depends on the degree of data dispersion, which helps to mitigate the overlap of information between indicator variables and reduce human subjectivity. Consequently, it provides an objective reflection of the utility value of the indicators [64]. Due to the inconsistency in the units of different indicators representing economic development levels, direct calculations are not feasible. Therefore, the raw data must first be standardized to eliminate the effects of differing dimensions and the positive or negative orientations of various indicators. Since

a standardized value of "0" can affect subsequent calculations, the positive and negative indicators are calculated separately using Formulas (1) and (2), respectively:

$$x_{ij}^{'} = \frac{X_{ij} - min(X_j)}{max(X_j) - min(X_j)} + a \quad (1)$$

$$x_{ij}^{'} = \frac{max(X_i) - X_{ij}}{max(X_j) - min(X_j)} + a \quad (2)$$

where $x_{ij}^{'}$ represents the standardized value; X_{ij} is the raw value of the system indicator; $max(X_j)$ is the maximum value of the j-th indicator; $min(X_j)$ is the minimum value of the j-th indicator; and $a = 1$.

After completing data standardization, the entropy weight method was used to determine the weights of each indicator. The calculation steps are as follows: calculate the information entropy e_j of the indicators (Formula (3)), calculate the weight w_j of each indicator (Formula (4)), and then determine the economic development level index $F(x)$ using the comprehensive index method after obtaining the weights of the various economic development indicators (Formula (5)).

$$e_j = -k\sum_{i=1}^{m} p_{ij} \ln p_{ij} \quad (3)$$

where $p_{ij} = \frac{x_{ij}^{'}}{\sum_{i=1}^{m} x_{ij}^{'}}$, $k = \frac{1}{\ln m}$.

$$w_j = \frac{1 - e_j}{\sum_{j=1}^{m} (1 - e_j)} \quad (4)$$

$$F(x) = w_j x^{'}{}_{ij} \quad (5)$$

Multiply the weights of the obtained economic indicators with the normalized economic indicators (Table A1), then add them up to obtain the economic development index (EDI).

3.3. Remote Sensing Ecological Index

The remote sensing ecological index (RSEI), introduced by Chinese scholar Xu [65,66], offers a scientific approach to characterizing ecological attributes. It serves as a comprehensive indicator that leverages remote sensing technology and data analysis methods to assess the quality of the regional ecological environment effectively. This index comprises four components: moisture, greenness, dryness, and heat. In this paper, MODIS data are utilized to calculate these various components of the RSEI. The formula is as follows:

$$RSEI = f\,(Moisture, Greenness, Dryness, Heat) \quad (6)$$

Moisture is calculated using the wetness component from the Tasseled Cap Transformation to represent soil moisture, as this component is specifically designed to capture key attributes of soil and plant moisture. Soil moisture conditions are identified as the primary characteristic expressed in this wetness component. The wet component of MODIS data can be calculated as follows [66]:

$$Wet = 0.1147B_1 + 0.2489B_2 + 0.2408B_3 + 0.3132B_4 - 0.3122B_5 - 0.6416B_6 - 0.5087B_7 \quad (7)$$

where B_1 to B_7 represent bands 1 to 7, corresponding to the *red*, NIR_1, *blue*, *green*, NIR_2, short-wavelength infrared 1 ($SWIR_1$), and short-wavelength infrared 2 ($SWIR_2$) bands of the MODIS image, respectively.

Greenness is represented by the Normalized Difference Vegetation Index (NDVI) [67]. Vegetation, being the most sensitive indicator of ecological conditions, is utilized to monitor vegetation changes and synthesize RSEI. The calculation formula is as follows [68]:

$$NDVI = \frac{NIR - Red}{NIR + Red} \tag{8}$$

where NIR and Red are the near-infrared (NIR_1) and red bands of the MODIS image (MOD09A1), respectively.

Dryness is typically represented by the bare Soil Index (SI), which indicates the scarcity of vegetation in the ecological environment [69]. However, a significant portion of the study area is covered by construction land, which can also contribute to soil "dryness". The Index-based Built-up Index (IBI) reflects the condition of the construction land itself to some extent [70]. Therefore, the dryness component can be represented as the average of SI and IBI, termed the Normalized Difference Built-up and Bareness Index (NDBSI) [71], and is calculated using the following formula:

$$BI = \frac{(SWIR + Red) - (NIR + Blue)}{(SWIR + Red) + (NIR + Blue)} \tag{9}$$

$$IBI = \frac{\frac{2SWIR}{SWIR+NIR} - \frac{NIR}{NIR+Red} - \frac{Green}{Green+SWIR}}{\frac{2SWIR}{SWIR+NIR} + \frac{NIR}{NIR+Red} + \frac{Green}{Green+SWIR}} \tag{10}$$

$$NDBSI = \frac{SI + IBI}{2} \tag{11}$$

where Red, $Green$, $Blue$, NIR, and $SWIR$ represent the red, green, blue, near-infrared, and shortwave infrared bands of MODIS images, respectively.

The heat component is represented by Land Surface Temperature (LST). We use the MOD11A2 Daytime Land Surface Temperature (DLST) dataset, derived from the MODIS series, to integrate LST data within the GEE platform [72].

The RSEI is synthesized based on its four components: WET, NDVI, NDBSI, and LST. RSEI synthesis can be performed using various methods such as Principal Component Analysis (PCA) [73], the Analytic Hierarchy Process (AHP) [74], and the entropy weight method (EWM) [75]. In this paper, the well-established PCA method is employed. To facilitate the measurement and comparison of RSEI across different time periods, a normalization method is applied to process the RSEI for each period. The final RSEI values range from [0, 1], with values closer to 1 indicating better ecological conditions.

3.4. Biological Richness Index

Although RSEI provides a multi-dimensional assessment of ecological environment quality, it should be supplemented with additional indices or components, such as the Biological Richness Index (BRI), particularly in regions experiencing significant changes in terrain, climate, and land use types. The BRI measures the richness and scarcity of local species by calculating the differences in species numbers across various land use types. It is a key indicator for evaluating the quality of the regional ecological environment [76]. The calculation formula is as follows:

$$BRI = A_{bri}(0.11 \times CLA + 0.35 \times WLA + 0.21 \times GLA + 0.28 \times WA + 0.04 \times CSLA + 0.01 \times ULA) / Area \tag{12}$$

where BRI stands for the biological richness index, A_{bri} is the normalization coefficient, and CLA, WLA, GLA, WA, $CSLA$, and ULA represent the areas of cropland, woodland, grassland, wetland, construction land, and unused land, respectively. $Area$ denotes the total area of the region.

3.5. Ecological Environment Index

The ecological environment index (EEI) is a comprehensive framework of indicators designed to assess the quality of the ecological environment within a given area. By integrating multiple environmental factors and ecological variables into an assessment system, the EEI aims to translate the state of ecological environmental quality into quantifiable and comparable indicators through scientific algorithms and models. Building on previous research, the EEI is synthesized by combining RSEI and BRI. The calculation formula is as follows:

$$EEI = \alpha \times RSEI + \beta \times BRI \tag{13}$$

where α represents the weight of *RSEI*, and β represents the weight of *BRI*. The weight of *RSEI* and *BRI* is determined using the Analytic Hierarchy Process, with α set to 0.85 and β set to 0.15.

To better observe and analyze the EEI across different periods, the results were classified into five levels at 0.2 intervals: Poor (0.0–0.2), Fair (0.2–0.4), Moderate (0.4–0.6), Good (0.6–0.8), and Excellent (0.8–1.0).

To further investigate changes in EEI this study applies the Theil–Sen median analysis and the Mann–Kendall significance test to evaluate the trends and their statistical significance. The Theil–Sen median analysis, a robust non-parametric method, is utilized to estimate the rate of change in long-term time series data, including meteorological, hydrological, and vegetation data [77]. The calculation formula is as follows:

$$\beta_{EEI} = Median\left(\frac{EEI_j - EEI_i}{j - i}\right),\ 2000 \le i \le j \le 2020 \tag{14}$$

where β_{EEI} indicates the rate of change in EEI during the study period. The variables i and j represent the start and end years, respectively, covering the period from 2000 to 2020. EEI_i and EEI_j correspond to the EEI values in the years i and j, respectively.

The Mann–Kendall significance test is a non-parametric, rank-based method commonly used to detect turning points in long-term time-series data for meteorological, hydrological, and vegetation variables [78]. Based on the significance levels derived from both the β_{EEI} and the Mann–Kendall test, the trends in β_{EEI} are classified into four categories: significant increase ($\beta > 0$, $p < 0.05$), insignificant increase ($\beta > 0$, $p \ge 0.05$), significant decrease ($\beta < 0$, $p < 0.05$), and insignificant decrease ($\beta < 0$, $p \ge 0.05$).

3.6. Coupling Coordination Degree

The intricate nature of the relationship between the ecological and economic systems transcends mere interactions, necessitating a deeper exploration. To this end, this article employs a sophisticated coupling coordination model for an exhaustive analysis. Drawing upon the interconnectedness between these two pivotal systems, we have devised a model that quantifies the extent of their coupling, specifically focusing on the harmony between economic development and ecological environmental protection. The calculation formula is as follows:

$$C = \sqrt{\frac{u_1 \times u_2}{\left[\left(u_1 + u_2\right)/2\right]^2}} = 2\frac{\sqrt{u_1 \times u_2}}{u_1 + u_2} \tag{15}$$

where u_1 represents the comprehensive evaluation index of the economic development subsystem, u_2 represents the comprehensive evaluation index of the ecological environment subsystem, and C denotes the ecological–economic coupling degree (EECD), with a value range of (0, 1]. A higher EECD value indicates a stronger degree of correlation between the two systems. When EECD reaches 1, it signifies that the two systems have achieved the optimal coupling state. The classification of coupling degrees is shown in Table 3.

Table 3. Classification criteria for coupling degree.

EECD	Coupling Stage
(0.0, 0.3]	Low-Level Coupling Stage
(0.3, 0.5]	Antagonistic Stage
(0.5, 0.8]	Running-In Stage
(0.8, 1.0]	High-Level Coupling Stage

As the EECD merely quantifies the strength of correlation between entities without elucidating the directional nature of their impact, it cannot solely determine whether the influence between two systems is positive or negative. In essence, relying solely on the coupling degree is insufficient to ascertain whether the impact is enhancing or detracting. To gain a more precise and objective understanding of the positive interaction dynamics between the two systems, we employ the following ecological–economic coupling coordination degree (EECCD) model, with its calculation formula detailed as follows:

$$EECCD = \sqrt{C \times T} \tag{16}$$

$$T = \alpha u_1 + \beta u_2 \tag{17}$$

where C represents the EECD, and T is the comprehensive evaluation index of the overall benefits of the two systems. α and β are undetermined coefficients, and the sum of the two is 1. Considering the balance between ecosystem and economic development system in evaluation, this article sets $\alpha = \beta = 0.5$. EECCD is a quantitative indicator of the degree of coupling and coordination between economic development and ecological environment protection. Its value directly reflects the degree of coupling and coordination between the two, that is, the quality of interaction and coordination between systems. The specific criteria for dividing EECCD values are detailed in Table 4.

Table 4. Classification of different coordination types.

EECCD	Coordination Level	EECCD	Coordination Level
(0.0, 0.1]	Extreme Imbalance	(0.5, 0.6]	Marginal Coordination
(0.1, 0.2]	Severe Imbalance	(0.6, 0.7]	Elementary Coordination
(0.2, 0.3]	Moderate Imbalance	(0.7, 0.8]	Moderate Coordination
(0.3, 0.4]	Mild Imbalance	(0.8, 0.9]	Effective Coordination
(0.4, 0.5]	Near Imbalance	(0.9, 1]	Optimal Coordination

3.7. Relative Development Degree

While the EECCD offers valuable insights into the intensity of the interconnection between ecological environment quality and economic development, it falls short in distinguishing the nuances between different systems. To address this limitation, this article introduces an ecological–economic relative development degree (EERDD) model, which effectively characterizes the dynamics of leadership and lag between ecological environment quality and economic development. The specific calculation formula for this model is presented in Equation (18).

$$EERDD = \frac{u_1}{u_2} \tag{18}$$

where $EERDD$ denotes the relative development degree, u_1 represents the Economic Development Index (EDI), and u_2 signifies the Ecological Environment Index (EEI). Drawing upon existing research findings [22], the value of EERDD serves as a criterion for categorizing regional economic development types. Specifically, when EERDD > 1.2, it signifies that the region's economic development is ahead of its projected pace, indicating a favorable economic advancement. Conversely, when 0.8 < EERDD $\leq$ 1.2, it indicates a harmonious synchronization between economic development and the ecological environment. Lastly, when EERDD $\leq$ 0.8, it reveals that the region's economic development lags behind its

ecological environment, suggesting a potential need for economic rejuvenation or ecological preservation measures.

3.8. Geographic Detector Model

As a statistical toolkit, geographic detectors not only provide a quantitative assessment of the spatial heterogeneity of geographic elements but also facilitate a deeper analysis of driving mechanisms [79]. This article uses the EEI in the LR-Jinsha as the dependent variable (Y) and considers the factors influencing its changes as independent variables (X). By applying the geographic detector model, the study aims to uncover the potential driving mechanisms behind the spatial distribution patterns of ecological environment quality in the LR-Jinsha. Geographic detectors encompass both single-factor detection and interactive detection methods.

Through single-factor detection, the explanatory power of each driving factor X on the spatial differentiation of ecological environment quality Y is determined, allowing for a quantitative analysis of the relative importance of each factor. The calculation formula is as follows:

$$q = 1 - \frac{\sum_{h=1}^{L} N_h \sigma_h^2}{N_h \sigma^2} \tag{19}$$

where the q value measures the correlation between the ecological environment quality (Y) and the driving factor detection and evaluation indicators (X), with a range from 0 to 1. A higher q value indicates a stronger explanatory power. L represents the number of layers of the driving factor X; N_h and N are the number of sample units in the h-th layer and the entire region, respectively; and σ_h^2 and σ^2 denote the variances of ecological environment quality values for the h-th layer and the entire region, respectively.

The primary aim of interaction detection is to analyze the pairwise interactions between driving factors to determine whether these interactions influence the explanatory power of ecological environment quality. Specifically, it assesses whether interactions strengthen, weaken, or have no impact on the relationship between the factors and ecological environment quality. These interactions can be categorized into five distinct scenarios, each with its specific outcome and corresponding range of q-values, as detailed in Table 5.

Table 5. Five different situations of interaction detection.

Interaction Type	q-Value Range
Nonlinear attenuation	$q(X_1 \cap X_2) < \mathrm{Min}(q(X_1), q(X_2))$
Single-factor nonlinear attenuation	$\mathrm{Min}(q(X_1), q(X_2)) < q(X_1 \cap X_2) < \mathrm{Max}(q(X_1), q(X_2))$
Dual-factor enhancement	$\mathrm{Max}(q(X_1), q(X_2)) < q(X_1 \cap X_2) < q(X_1) + q(X_2)$
Independent	$q(X_1 \cap X_2) = q(X_1) + q(X_2)$
Nonlinear enhancement	$q(X_1 \cap X_2) > q(X_1) + q(X_2)$

Using a geographic detector, the independent impact of various factors on ecological environment quality and their interactive effects were investigated. Based on the study of the ecological environment quality index system in the research area, four factors—climate, topography, land use, and socio-economic factors—were further analyzed. Due to the requirement of geographic detectors for input data to be categorical variables, continuous variables were discretized. Following the principle of maximizing the q-value, two grading strategies were selected: quantile and natural breaks, with a range of 5–12 grading levels. The grading strategies are shown in Table 6, and the results of each factor's processing are provided in Table A1.

To ensure the scientific validity of the research, 32,513 sampling points were randomly set at intervals of 5 km in the research area. After excluding sample points and abnormal data in larger water areas such as the lower reaches of the Jinsha River and Dianchi Lake, 31,882 valid sample points were retained. Finally, the independent variables (X_1–X_{13}) and the dependent variable (Y—EEI) were assigned to the valid sample points, and subsequent correlation calculations and analyses were performed.

Table 6. Grading of ecological environment index (EEI) driving factors.

Factor Type	Driving Factors	Variable Code	Unit	Grading Method	Number of Grades
Climatic	Annual average temperature	X_1	°C	Natural breaks	9
	Annual precipitation	X_2	mm	Natural breaks	9
Topographical	Elevation	X_3	m	Quantile	9
	Slope	X_4	°	Natural breaks	9
	Aspect	X_5	Dimensionless	-	10
Land use	Land use type	X_7	Dimensionless	-	6
	Cropland density	X_8	Dimensionless	Natural breaks	12
	Construction land density	X_9	Dimensionless	Quantile	12
Socio-economic	Nighttime light index	X_{10}	Dimensionless	Quantile	10
	Gross domestic product density	X_{11}	CNY 10,000/km^2	Natural breaks	10
	Population density	X_{12}	Person/km^2	Quantile	10
	Euclidean distance of road	X_{13}	m	Natural breaks	12

3.9. Obstacle Factor Diagnosis

The obstacle factor diagnosis model is utilized to identify the main barriers to the economic development index in the study area. In this model, the factor contribution degree (F_{ij}) quantifies the impact of a single factor on the entire system, representing its weight in achieving the overall objective. The indicator deviation degree (I_{ijt}) measures the gap between a specific indicator and the standards of an economic development system. The degree of impact of the obstacle (O_{ijt}) assesses the influence of F_{ij} and I_{ijt} on the development of economy [80].

$$F_{ij} = W_i \times W_{ij} \tag{20}$$

$$I_{ijt} = 1 - P_{ijt} \tag{21}$$

$$O_{ijt} = I_{ijt} \times \frac{F_{ij}}{\sum_{i=1}^{n} F_{ij} \times I_{ijt}} \times 100\% \tag{22}$$

where n represents the total number of indicators. W_i is the weight of the i-th classification indicator, while W_{ij} denotes the weight of the j-th individual indicator under the i-th classification indicator, P_{ijt} is the normalized value of the single indicator after range normalization. O_{ijt} indicates the degree of obstacle posed by the j-th individual indicator within the i-th classification indicator in the t-th year. The weights W_i and W_{ij} are determined using the economic development index system, ensuring the accuracy and scientific validity of the evaluation.

3.10. Neural Network Model

A neural network model was employed to identify the driving forces of EECCD. This model simulates the connections and mechanisms of human brain neurons by processing information through a highly interconnected network structure. It comprises multiple layers: an input layer, one or more hidden layers, and an output layer. Each layer contains multiple neurons, also known as nodes or units, that transmit information via weighted connections. By incorporating hidden layers and activation functions, the multilayer perceptron (a type of feedforward neural network) can approximate complex nonlinear functions, enabling it to effectively solve intricate problems (Figure 4) [81].

In this study, a multilayer perceptron neural network model was constructed, with 14 factors as independent variables: total primary industry output, total secondary industry output, total tertiary industry output, urbanization rate, per capita cropland area, nighttime light index, total GDP, per capita GDP, total retail sales of consumer goods, BRI, NDVI, WET, NDSBI, and LST. The EECCD was used as the dependent variable. The influence coefficients of the 14 factors were obtained through analysis.

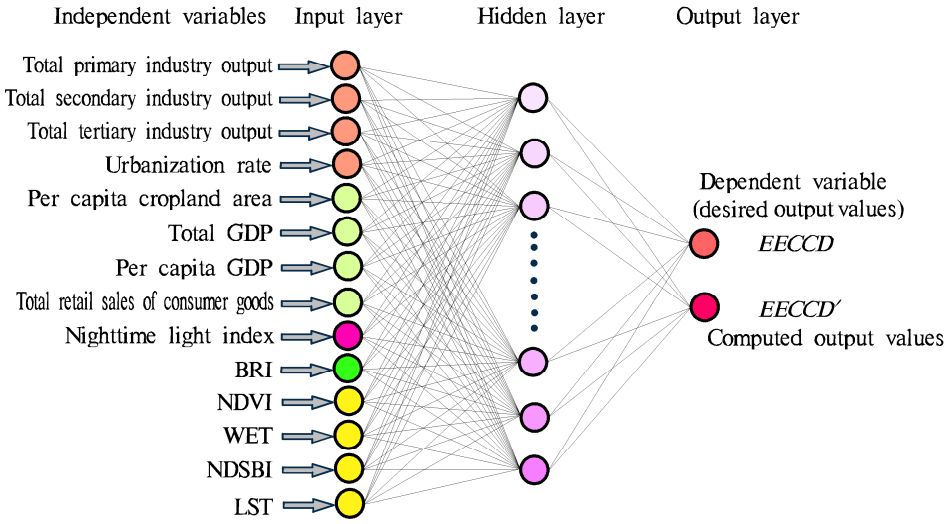


Figure 4. Three-layered feed-forward neural network.

4. Results

4.1. Spatiotemporal Dynamics of Ecological Environment

4.1.1. Spatiotemporal Dynamics in the RSEI

From 2000 to 2020, both the RSEI and its four components exhibited a trend of ecological improvement. The WET component showed an overall upward trend, with a slight decline occurring only between 2010 and 2015, resulting in a net increase of 0.22 (Figures 5a and A3). The NDVI component rose from 0.657 in 2000 to 0.688 in 2020, marking a total increase of 0.031 (Figures 5b and A4). In contrast, the NDBSI component declined from 0.569 in 2000 to 0.555 in 2020, a total decrease of 0.014 (Figures 5c and A5). Similarly, the LST component decreased from 0.553 in 2000 to 0.483 in 2020, a total reduction of 0.070 (Figures 5d and A6).

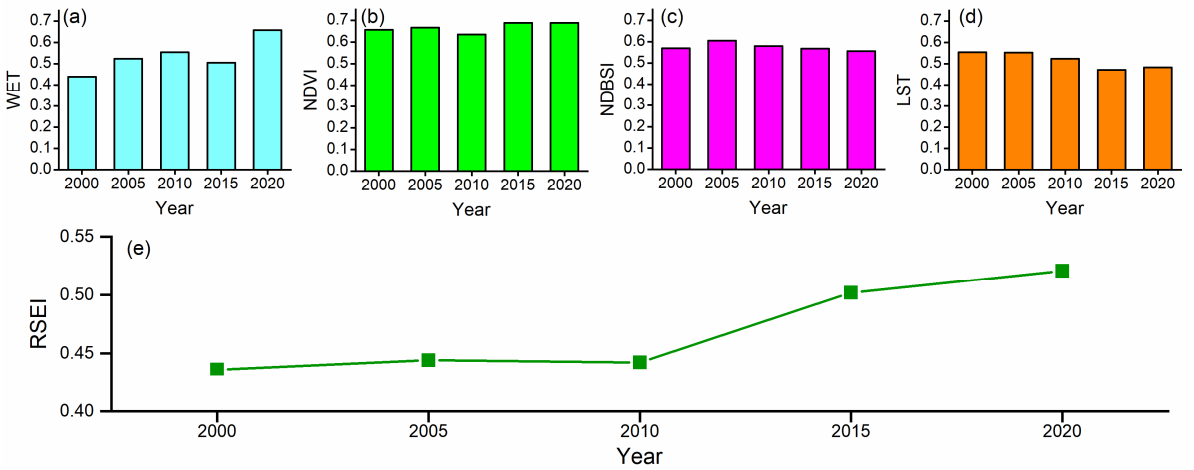


Figure 5. Changes in RSEI and its four components in the entire region from 2000 to 2020: (**a**) WET Variation; (**b**) NDVI Variation; (**c**) NDBSI Variation; (**d**) LST Variation; (**e**) RSEI Variation.

Throughout the period, the RSEI in the study area demonstrated an overall trend of improvement (Figure 5e). Taking 2010 as a pivotal year, two distinct stages can be identified: a phase of low-speed and fluctuating improvement from 2000 to 2010, followed by a phase of rapid and sustained improvement from 2010 to 2020. Specifically, the RSEI value was 0.436 in 2000, rose to 0.444 in 2005, slightly decreased to 0.442 in 2010, then quickly climbed to 0.502 in 2015, and further increased to 0.521 in 2020. From 2000 to 2020, the overall RSEI in the study area increased by 0.085, reflecting a growth rate of 19.50%.

The spatial distribution of the RSEI displayed strong geomorphological zoning characteristics (Figure 6a), with average RSEI values ranked from low to high as follows: the Dry Hot Valley Area, the Wumeng Mountain Area, the Plateau Basin Valley Area, the Southwest Sichuan Mountain Area, and the Sichuan Basin. Across the period from 2000 to 2020, the changes in the RSEI revealed four distinct levels of spatial variability (Figure 6b). Specifically, areas experiencing significant reductions comprised merely 0.15% of the total region, while those with non-significant decreases accounted for 15.02%. Conversely, non-significantly improved regions encompassed 76.38% of the area, and significantly improved zones made up 8.45%. The RSEI variation stages in these five sub-regions were generally consistent with those of the entire region, yet each sub-region exhibited unique patterns of change. The sub-regions were ranked by the intensity of RSEI change from highest to lowest as follows: the Wumeng Mountain Area (22.89%), the Plateau Basin Valley Area (19.44%), the Sichuan Basin (18.70%), the Dry Hot Valley Area (17.62%), and the Southwest Sichuan Mountain Area (11.27%).

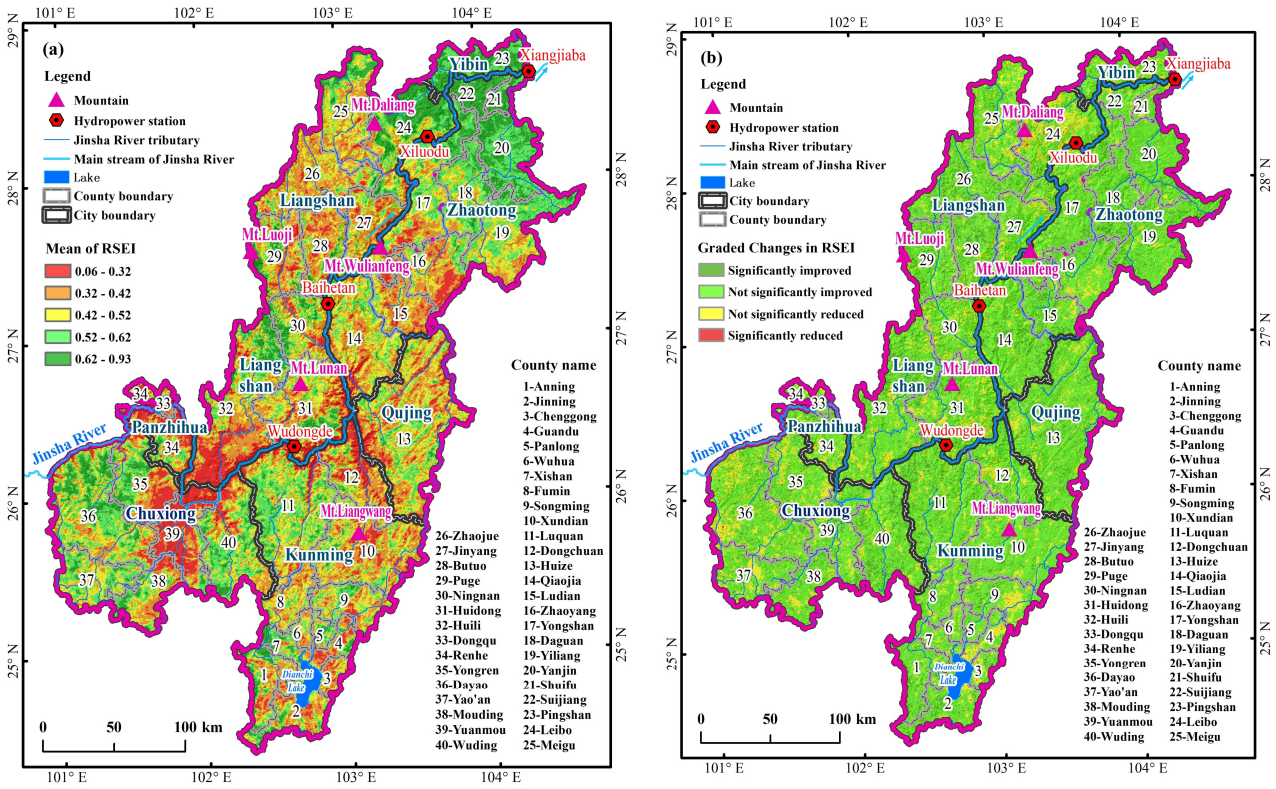


Figure 6. Distribution of RSEI. (**a**) Mean RSEI from 2000 to 2020; (**b**) Classification of RSEI changes from 2000–2020.

4.1.2. Spatiotemporal Dynamics in the BRI

The macro spatial distribution of the BRI remained largely unchanged between 2000 and 2020, showing an overall improving trend. The BRI is primarily influenced by land use types (Figure A7), resulting in a mosaic pattern of various BRI values (Figure 7a). High-value areas are predominantly found in forests, grasslands, and wetlands, while low-value areas are mainly located in cropland, construction land, and unused land. During this period, the BRI exhibited two distinct phases: a relatively stable phase from 2000 to 2005, where no significant changes were observed, and a stable improvement phase from 2005 to 2020. During this latter phase, the BRI increased from 0.426 in 2005 to 0.681 in 2010, continued to 0.691 in 2015, and reached 0.699 in 2020. Analysis of BRI changes reveals that areas with significant reduction and minor reduction accounted for 0.26% and 10.79% of the total region, respectively, primarily in areas where forests, grasslands, and wetlands were converted. Conversely, areas with minor improvement and significant improvement

made up 68.76% and 20.18% of the total area, respectively, with significant improvements mainly occurring in regions where other land types transitioned to forests, grasslands, and wetlands (Figure 7b).

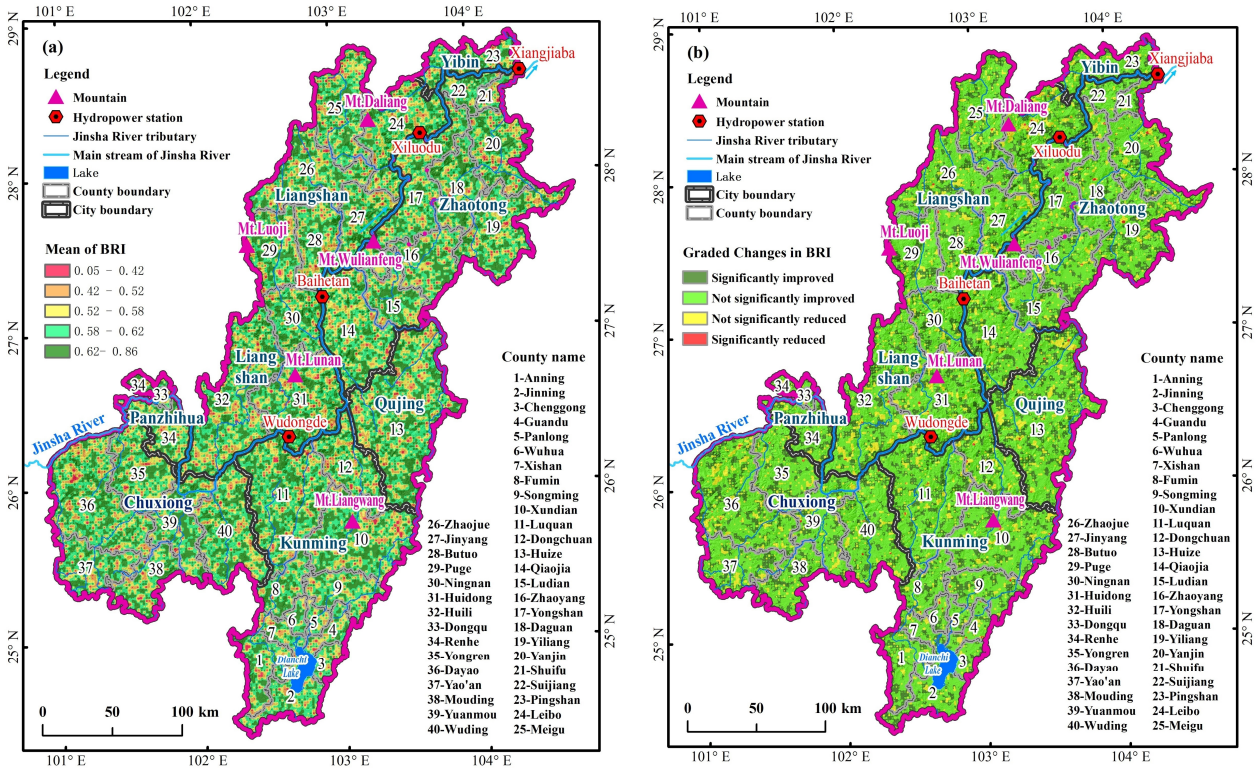


Figure 7. Distribution of BRI. (**a**) Mean BRI from 2000 to 2020; (**b**) classification of BRI changes from 2000 to 2020.

The changes in the BRI are primarily driven by adjustments in land use structure (Figure 8). In 2000, the study area was composed of approximately 55.98% forest land, 27.89% cropland, 15.09% grassland, 0.75% wetland, 0.27% construction land, and 0.02% unused land. By 2020, forest land expanded to 58.37%, cropland increased to 28.61%, grassland decreased to 11.47%, wetland increased to 0.92%, and construction land increased to 0.61%, while unused land remained unchanged at 0.02%. Over the two decades, forest land consistently increased, primarily due to the conversion of cropland and grassland driven by reforestation initiatives. Grassland saw a steady decline, with much of it converting to cropland and wetlands. Cropland remained relatively stable, with notable transitions involving construction land, wetland, forest land, and grassland. Construction land expanded significantly due to urban and rural development, infrastructure projects, and targeted poverty alleviation, mainly at the expense of cropland and grassland. Wetlands experienced growth, largely due to the construction of large-scale hydropower stations and associated water conservancy facilities. These projects included the expansion of reservoir areas at the Xiangjiaba (96 km^2), Xiluodu (134 km^2), Baihetan (1040 km^2), and Wudongde (127 km^2) hydropower stations. Unused land consistently diminished, predominantly transforming into cropland and grassland.

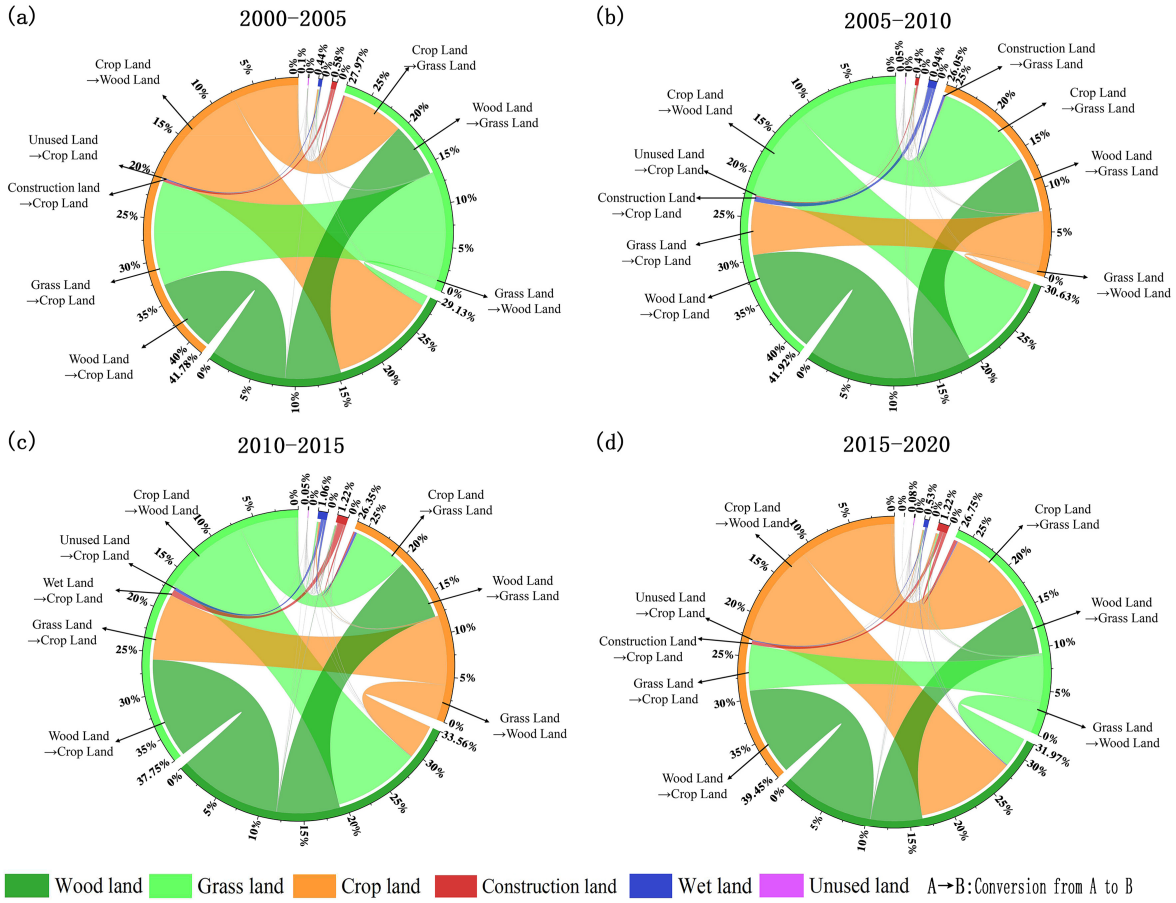


Figure 8. Transfer relationships among various land use types in the study area from 2000 to 2020.

4.1.3. Spatiotemporal Dynamics in the EEI

The EEI in the study area shows a continuous improvement trend, driven by the influence of two components: the RSEI and the BRI. From 2000 to 2020, the EEI increased by approximately 19.95%. The change can be divided into two phases: a slow improvement phase from 2000 to 2010, during which the EEI rose from 0.431 in 2000 to 0.434 in 2005, and further to 0.437 in 2010; and a rapid growth phase from 2010 to 2020, where the EEI increased by 0.068 to reach 0.505 in 2015 and maintained a growth rate of 0.012, reaching 0.517 by 2020.

Based on the five-level classification of EEI (Excellent, Good, Moderate, Fair, and Poor) (Figure 9a), the Poor category accounts for approximately 1.43% of the total area, mainly distributed in the southern part of the study area, near regions like Huili, Yongren, Yuanmou, Luquan, and Dongchuan, close to the main stream of the Jinsha River. The Fair category occupies around 31.38% of the area, primarily located in the central valleys and ridges of the study area. The Moderate category, which dominates the region, covers about 50.50% of the total area and is mainly found in the central and southern parts of the study area. The Good and Excellent categories are primarily concentrated in the northern and western parts, together accounting for 16.69% of the area.

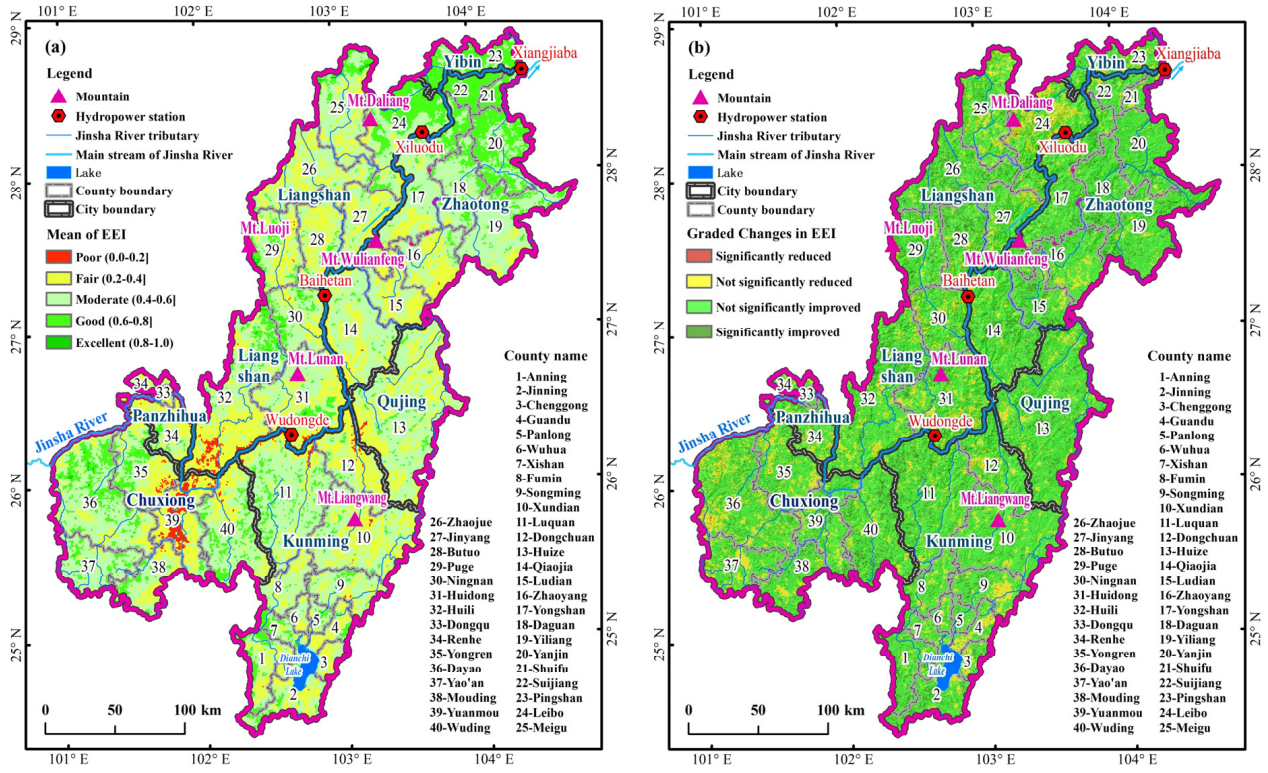


Figure 9. Distribution of EEI. (**a**) Mean EEI from 2000 to 2020; (**b**) classification of EEI changes from 2000 to 2020.

Based on the significance test results of EEI changes, the study area primarily exhibited non-significant and significant improvements in ecological environmental quality (Figure 9b). Significant improvement areas, which account for 8.45% of the total area, are mainly located in the border regions of the Wanma–Longchuan River Basin and Pulong–Mengguo River Basin, the northern part of the Xiaojiang–Heishui River Basin, the Southwest Sichuan Mountain Area, and the central Hengjiang–Luoze River Basin. These improvements are widespread and present in both high and low EEI zones. Non-significant improvement areas dominate the study area, making up 76.38%, and are concentrated in the northeastern low-altitude regions, the Pudu River Basin, and the southern Wumeng Mountain Area. These regions are characterized by forest and grassland, with EEI values generally ranging from moderate to high. Areas showing significant degradation are minimal, covering only 0.15% of the total area, and are sparsely located in the western Wanma–Longchuan River Basin, southeastern Kunming, and northern Meigu River Basin, primarily in forested areas. Non-significant degradation zones make up 15.02% of the study area, typically appearing in patchy distributions in southwestern Chuxiong, northern Liangshan, and around the Dianchi Basin in Kunming, with predominant land uses being cultivation and construction.

The structural composition of the EEI has undergone continuous optimization from 2000 to 2020 (Figure 10). During this period, the proportion of the Poor category decreased from 3% to 1%, while the Fair category declined significantly from 40% in 2000 to 20% in 2020. Meanwhile, the Moderate category showed an increase from 45% in 2000 to 50% in 2020. The Good category also saw notable growth, rising from 11% in 2000 to 28% in 2020. The Excellent category, however, remained relatively stable, fluctuating between 1% and 2% throughout the two decades.

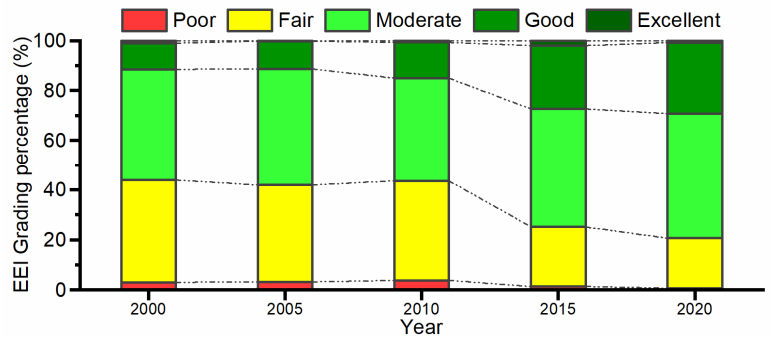


Figure 10. Changes in the percentage composition of five EEI grades from 2000 to 2020.

At the geomorphic zoning scale, the average EEI values and their respective improvement rates are as follows (Figure 11): Sichuan Basin (0.5734, 22%), Southwest Sichuan Mountain Area (0.4957, 18.57%), Plateau Basin Valley Area (0.4743, 20.58%), Wumeng Mountain Area (0.4298, 27.15%), and Dry Hot Valley Area (0.4177, 18.60%). Notably, significant variations in the EEI are observed within both the Southwest Sichuan Mountain Area and the Dry Hot Valley Area.

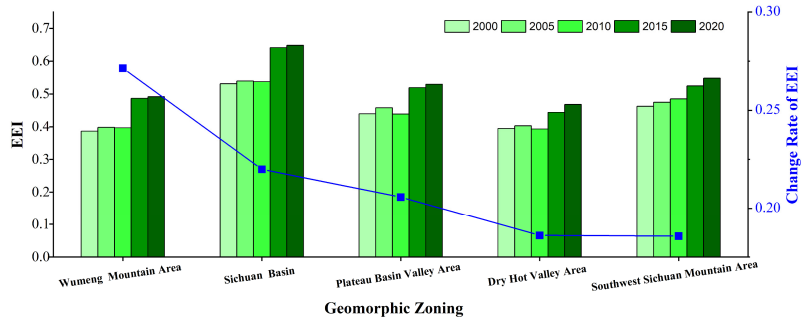


Figure 11. EEI changes in five geomorphic zones from 2000 to 2020.

At the sub-watershed scale (Figure 12), the average EEI values and their respective improvement rates are as follows: Meigu River Basin (0.5331, 10.08%), Hengjiang River Basin (0.5095, 24.26%), Pudu River Basin (0.4751, 22.31%), Wanma-Longchuan River Basin (0.4531, 13.72%), Pulong-Mengguo River Basin (0.4317, 26.06%), and Xiaojiang-Heishui River Basin (0.4267, 23.75%). Notably, considerable variation in EEI is also observed within both the Wanma-Longchuan River Basin and the Pulong-Mengguo River Basin.

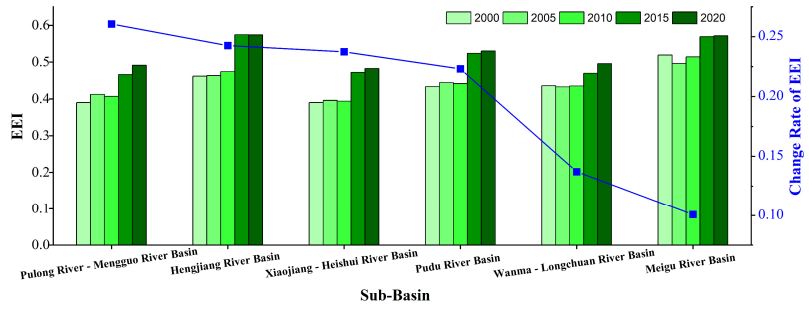


Figure 12. Changes in EEI of six sub-basins from 2000 to 2020.

The distribution and variation of EEI across different sections of the main stream show a clear gradient pattern (Figure 13). In ascending order of elevation, the average EEI is 0.6343 in the Xiangjiaba section, 0.4493 in the Xiluodu section, 0.4041 in the Baihetan section, and 0.3376 in the Wudongde section. From 2000 to 2020, EEI demonstrated a trend of smaller increases in high-value areas and larger increases in low-value areas. Specifically,

the growth rates of EEI were 6.95% in the Xiangjiaba section, 18.70% in the Xiluodu section, 19.81% in the Baihetan section, and 25.76% in the Wudongde section.

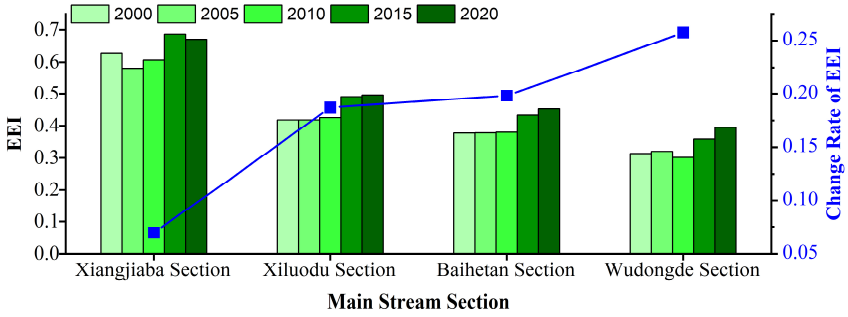


Figure 13. EEI changes in four sections of the main stream from 2000 to 2020.

From 2000 to 2020, the county-level EEI exhibited an overall improvement trend, with a noticeable shift in EEI levels from Fair to Moderate and Good (Figure 14, Table A2). In 2000, four counties—Suijiang, Shuifu, Pingshan, and Leibo—were classified as Good, while 22 counties were classified as Moderate. Fourteen counties, including Huidong, Chenggong, Renhe, Butuo, Zhaoyang, Ludian, Dongchuan, and Yuanmou, were classified as Fair. By 2020, the counties classified as Good had expanded to include Suijiang, Yanjin, Shuifu, Pingshan, Daguan, and Leibo. The number of counties classified as Moderate increased to 33, while the Fair classification was reduced to just one county: Yuanmou.

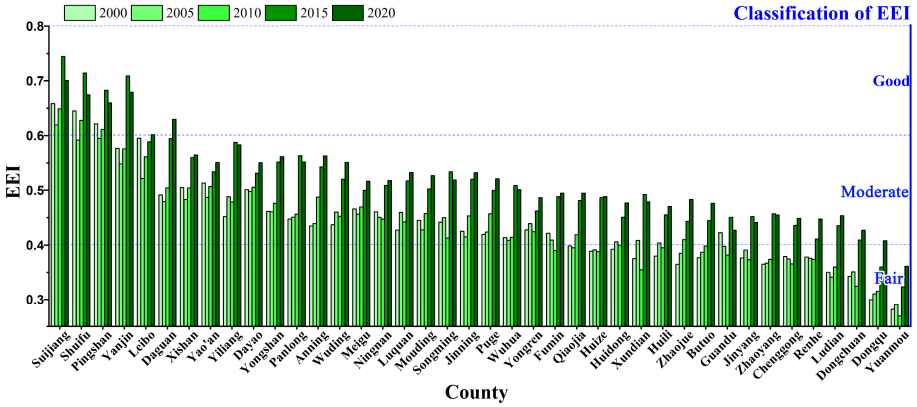


Figure 14. Changes in EEI from 2000 to 2020.

4.2. Spatiotemporal Dynamics of Economic Development

4.2.1. Spatiotemporal Dynamics in the Economic Structure Index

Using the economic structure index (EcoESTI) to analyze the spatiotemporal changes in the economic structure subsystem, the study area exhibited a consistent upward trend in EcoESTI from 2000 to 2020, with the most significant growth occurring between 2015 and 2020 (Figure 15, Table A3). The region's average EcoESTI increased from 0.0680 in 2000 to 0.075 in 2005, remained steady at 0.075 in 2010, rose slightly to 0.076 in 2015, and reached 0.092 in 2020. This reflects a total increase of 0.0270 over the two decades, representing a growth rate of 39.74%.

Between 2000 and 2020, eight counties—Guandu, Wuding, Xishan, Panlong, Dongqu, Anning, Zhaoyang, and Huili—achieved an average EcoESTI value exceeding 0.1000, indicating strong development potential in agriculture, forestry, mineral resources, water resources, and tourism. These counties are primarily located in the southern and central parts of the study area. In contrast, nine counties—Leibo, Yongren, Puge, Zhaojue, Jinning, Meigu, Daguan, Butuo, and Suijiang—recorded an average EcoESTI value below 0.050, highlighting significant opportunities to improve resource endowments, infrastructure,

and industrial structures. These counties are mainly concentrated in the northern part of the study area.

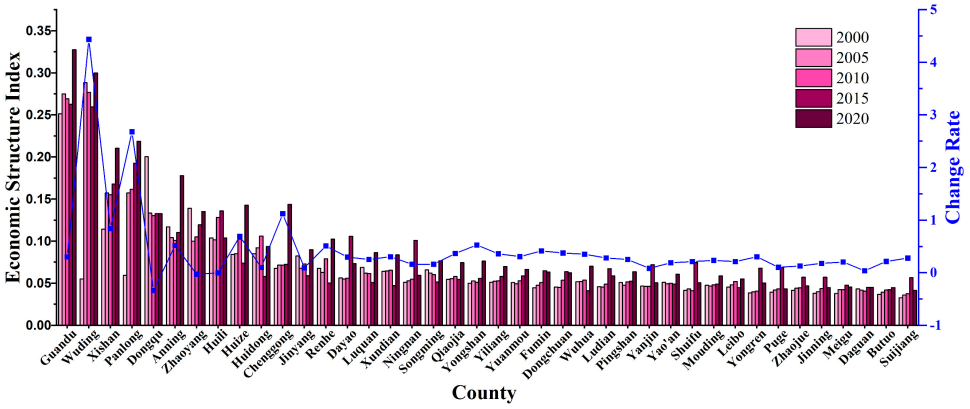


Figure 15. Changes in economic structure index (EcoESTI) from 2000 to 2020.

4.2.2. Spatiotemporal Dynamics in the Economic Environment Index

The average economic environment index (EcoEEI) for the region in 2000, 2005, 2010, 2015, and 2020 was 0.1041, 0.0917, 0.0983, 0.0958, and 0.0978, respectively, indicating a slight decline followed by a rebound in 2020 (Figure 16, Table A4). Spatially, the EcoEEI displays a clear north-south differentiation, with lower values in the north and higher values in the south, roughly divided by a line formed by Ningnan, Huidong, and Dongchuan. From 2000 to 2020, ten counties—Dongqu, Wuding, Panlong, Guandu, Chenggong, Xishan, Anning, Renhe, Jinyang, and Songming—consistently maintained an average EcoEEI above 0.1000. In contrast, five counties—Zhaojue, Pingshan, Qiaojia, Yiliang, and Yanjin—had an average EcoEEI below 0.060.

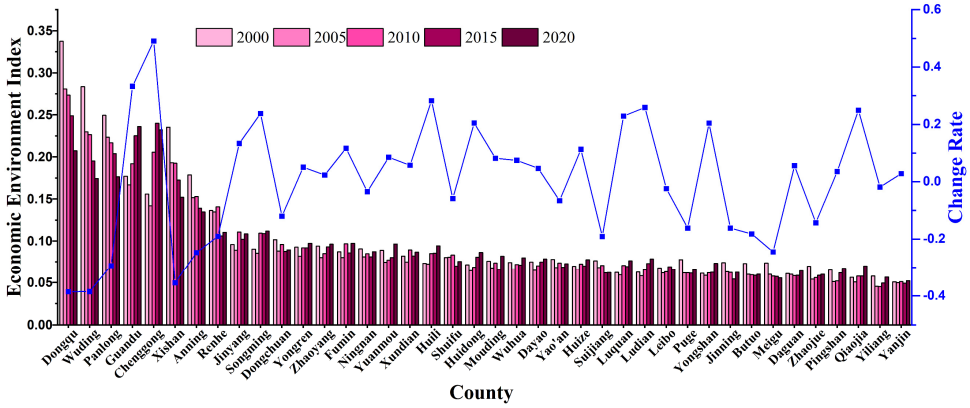


Figure 16. Changes in economic environment index (EcoEEI) from 2000 to 2020.

Between 2000 and 2020, 22 counties experienced positive EcoEEI growth, with five counties—Chenggong, Guandu, Huili, Ludian, and Qiaojia—achieving growth rates exceeding 25%, largely due to urbanization and infrastructure development that offset the impact of reduced per capita cropland. Conversely, 18 counties saw a negative EcoEEI growth rate, with five counties—Anning, Panlong, Xishan, Wuding, and Dongqu—experiencing declines of more than 25%, primarily due to factors such as reforestation, grassland restoration, and the reduction of per capita cropland caused by construction projects.

4.2.3. Spatiotemporal Dynamics in the Economic Scale Index

The economic scale index (EcoESCI) in the research area exhibited a continuous growth trend from 2000 to 2020 (Figure 17, Table A5). The average EcoESCI values for the region were 0.0793, 0.0922, 0.0963, 0.1073, and 0.1094 in 2000, 2005, 2010, 2015, and

2020, respectively, representing an overall growth rate of 37.96% over the two decades. The spatial distribution of EcoESCI revealed a pattern of higher values in the central region and lower values in the northern and southern regions.

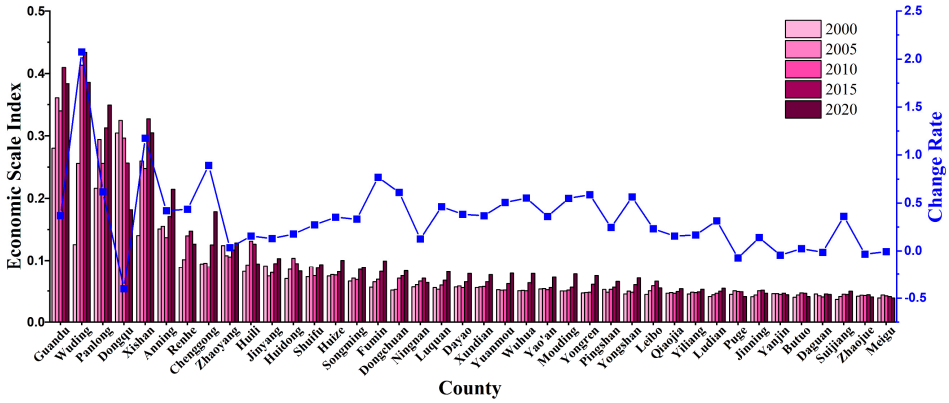


Figure 17. Changes in economic scale index (EcoESCI) from 2000 to 2020.

Between 2000 and 2020, ten counties, including Guandu, Wuding, Panlong, Dongqu, Xishan, Anning, Renhe, Chenggong, Zhaoyang, and Huili, achieved an average EcoESCI value greater than 0.1000. Conversely, eleven counties, including Qiaojia, Yiliang, Ludian, Puge, Jinning, Yanjin, Butuo, Daguan, Suijiang, Zhaojue, and Meigu, had an average EcoESCI value below 0.0500.

Over the same period, 36 counties experienced positive EcoESCI growth. Notably, Wuding and Xishan counties recorded significant growth rates of 207.46% and 117.77%, respectively. In contrast, counties located in the Daliangshan and Wumeng mountainous areas, such as Meigu, Daguan, Zhaojue, Yanjin, Puge, and Dongqu, exhibited growth rates below 0, with Dongqu experiencing a notable decline of −40.31%.

4.2.4. Spatiotemporal Dynamics in the EDI

The EDI in the study area, influenced by the combined effects of the economic structure, economic environment, and economic scale subsystems, exhibited a consistent growth trend from 2000 to 2020 (Figure 18, Table A6). The average EDI values for the entire region were 0.152, 0.159, 0.171, 0.186, and 0.203 in 2000, 2005, 2010, 2015, and 2020, respectively. This reflects an overall increase of 0.051, or approximately 33.55%, over the two decades. Analyzing the distribution of EDI levels across forty counties, in 2000, twenty-six counties had an EDI value below 0.1, eight counties had an EDI between 0.1 and 0.25, and six counties had an EDI above 0.25. By 2020, the number of counties with an EDI value below 0.1 decreased to eleven, while those with an EDI between 0.1 and 0.25 increased to twenty-two, and those with an EDI above 0.25 increased to seven.

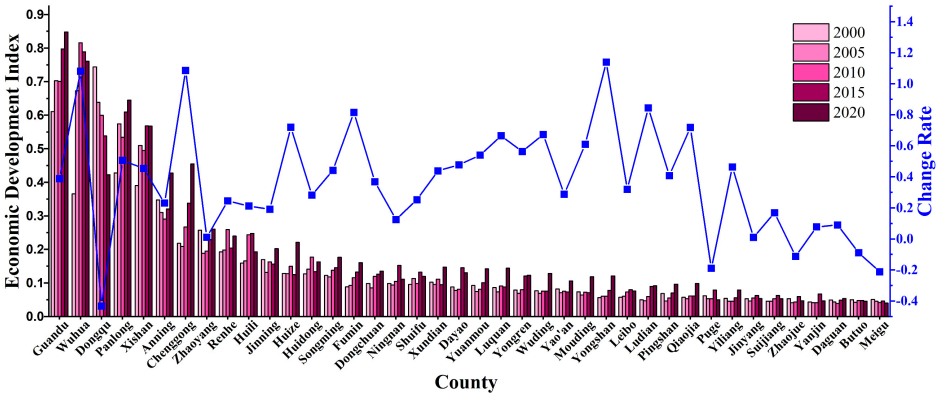


Figure 18. Changes in the EDI from 2000 to 2020.

Throughout the period of EDI change, counties with higher EDI rankings displayed variability in their rankings, while those with lower rankings exhibited lagging or declining trends. Counties with mid-range EDI rankings generally maintained stable growth. From 2000 to 2020, a total of 35 counties experienced positive EDI growth rates, with Yongshan, Chenggong, and Wuhua showing growth rates exceeding 100%. Conversely, Yanjin, Jinyang, and Zhaoyang had growth rates below 10%. Five counties experienced a decline in EDI, including Butuo, Zhaojue, Puge, and Meigu in Liangshan Prefecture, and Dongqu in Panzhihua, with Dongqu experiencing the most significant decrease at 43.15%.

The EDI exhibits a distinct spatial differentiation between the northern and southern regions (Figure 19). In the study area, a spatial differentiation pattern of EDI has formed along the line connecting Puge, Butuo, Leibo, and Ludian. South of this line lies the high EDI value zone and relatively high-growth area, while the area along the line and to the north, mainly encompassing the Daliangshan and Wumeng mountainous regions, is characterized by low EDI values and slow development. Additionally, EDI values and growth rates gradually decrease as one moves from the central areas of Zhaoyang in Zhaotong, Huili, Dongqu, and Renhe in Panzhihua, and Anning, Chenggong, Guandu, and Xishan in Kunming towards the surrounding regions.

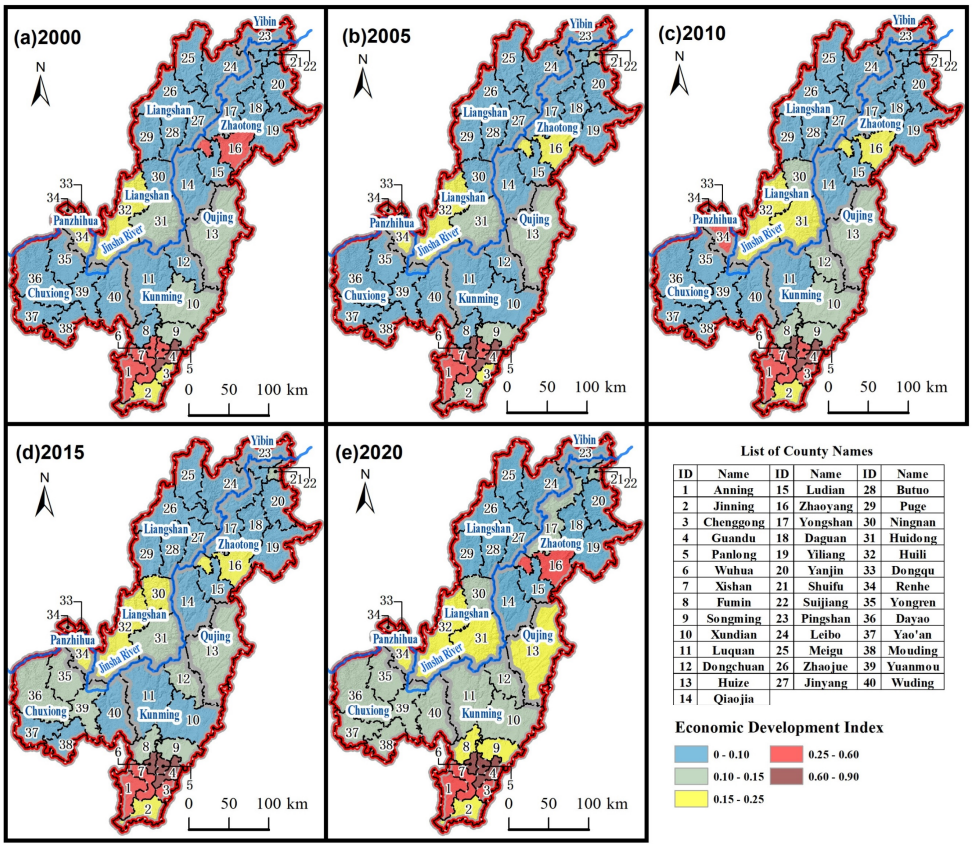


Figure 19. Distribution of EDI changes from 2000 to 2020.

Moran's index analysis of the EDI data from five periods between 2000 and 2020 shows an increase from 0.801 in 2000 to 1.543 in 2020, indicating a growing positive spatial correlation of EDI among the counties in the study area, with similar values becoming more spatially clustered (Figure A8).

4.3. Spatiotemporal Dynamics of Ecology–Economy Coupling

4.3.1. Spatiotemporal Dynamics in the EECD

During the period from 2000 to 2020, the overall ecological–economic coupling degree (EECD) in the study area remained at a high level, showing a slight decline followed by a

modest increase (Figure 20, Table A7). The average EECD across the study area remained relatively stable, with a slight overall increase from 0.7668 in 2000 to 0.7883 in 2020. The number of counties in the High-Level Coupling Stage increased gradually, rising from 17 counties in 2000 to 20 counties by 2015, where it stabilized through 2020. The number of counties in the Running-In Stage fluctuated slightly, decreasing from 22 counties in 2000 to 20 counties by 2015, where it also stabilized through 2020. The Antagonistic Stage was nearly absent, with only one county (Suijiang) in this stage in 2000, and none in subsequent years. Additionally, sample data from 40 counties show that the EECD metric is only able to roughly depict the High-Level Coupling Stage and Running-In Stage, falling short in capturing the nuanced differences in ecological–economic interactions between counties.

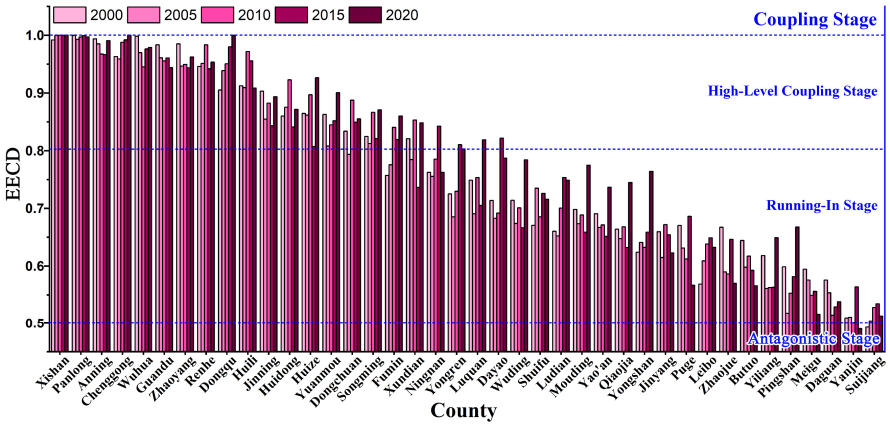


Figure 20. Changes in EECD from 2000 to 2020.

4.3.2. Spatiotemporal Dynamics in the EECCD

From 2000 to 2020, the average EECCD in the study area showed an overall increasing trend. The average EECCD was 0.472 in 2000, slightly decreased to 0.468 in 2005, and then increased to 0.481 in 2010. During the period from 2000 to 2010, the entire area was predominantly in the near imbalance stage. By 2015, the EECCD surged to 0.514 and further increased to 0.531 by 2020, with the entire area predominantly entering the marginal coordination stage from 2015 to 2020. From 2000 to 2020, the EECCD increased by 0.059, representing an approximate growth of 12.50%.

The average EECCD and its rate of change across 40 counties from 2000 to 2020 did not exhibit a linear negative correlation (Figure 21, Table A8), indicating the varying impacts of economic development history and stages among these counties. In the 24 B-class regions, the average EECCD was 0.4205 in 2000, slightly declined to 0.4077 in 2005, rebounded to 0.4197 in 2010, surged to 0.4524 in 2015, and continued to rise to 0.4715 in 2020, marking an overall increase of 12.13% from 2000 to 2020. During the same period, the 16 A-class regions exhibited a steady upward trajectory, with the average EECCD increasing from 0.5501 in 2000 to 0.5591 in 2005, 0.5736 in 2010, 0.6064 in 2015, and 0.6191 in 2020, reflecting a total increase of 12.54%. Among the top twenty counties in terms of EECCD growth rate, twelve were poverty-alleviated counties, with six counties—Yongshan, Ludian, Huize, Qiaojia, Wuding, and Luquan—ranking within the top 10 at 1st, 4th, 5th, 7th, 8th, and 9th, respectively. Conversely, eight of the counties ranked 31st to 40th were also poverty-alleviated counties, underscoring the disparity in EECCD changes among these regions.

The coordination levels of counties in the study area have consistently improved over time (Figures 22 and 23, Table A9). The number of counties classified as Mild Imbalance and Near Imbalance decreased from 30 in 2000 to 18 in 2020. However, four poverty-alleviated counties—Meigu, Zhaojue, Jinyang, and Butuo—remain in the Mild Imbalance category. In contrast, the number of counties under Marginal Coordination increased from four in 2000 to fifteen in 2020, marking a critical transitional phase in the development of ecology–economy coupling. The number of counties classified as Elementary Coordination

and Moderate Coordination remained stable, at six and seven counties each. In 2000, Guandu was the only county classified under Moderate Coordination. Starting in 2005, this category expanded to include Panlong, Wuhua, and Xishan in Kunming, a classification that persisted through 2020. By then, Anning in Kunming was also included, bringing the total number of counties under Moderate Coordination to five.



Figure 21. Comparison of average EECCD and its change rate from 2000 to 2020.

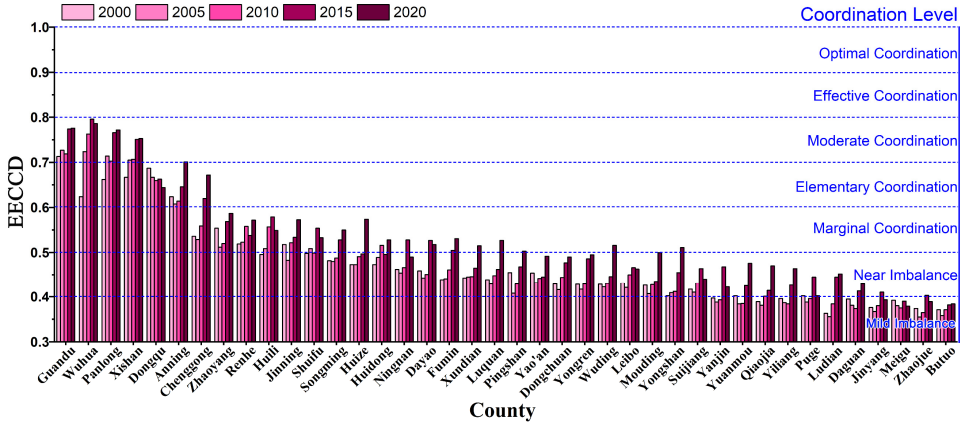


Figure 22. EECCD changes and comparison with coordination level in 40 counties from 2000 to 2020.

From 2000 to 2020, the distribution of the average EECCD in the study area displayed a spatial pattern with higher values in the south and lower values in the north (Figure 24a). The southern counties of Guandu (0.742), Wuhua (0.739), Panlong (0.723), and Xishan (0.717) in Kunming were classified as having a Moderate Coordination level, representing the highest average EECCD values in the region during this period. Dongqu (0.644) in Panzhihua and Anning (0.639) in Kunming were at the Elementary Coordination level. In the northern part of the study area, the counties of Butuo (0.373), Zhaojue (0.377), Meigu (0.383), Jinyang (0.385) in Liangshan Prefecture, and Daguan (0.398) in Zhaotong were classified as Mild Imbalance level, indicating the lowest EECCD values. Nine counties, including Chenggong and Huidong, were at the Marginal Coordination level, while twenty counties, such as Ningnan, Puge, and Ludian, were at the Near Imbalance level, predominantly located in the southwestern, central-northern, and northern regions. Regarding the Jinsha River main stream segmentation, EECCD values were relatively high throughout most areas, except for regions east and north of the Baihetan Hydropower Station, with particularly high values near Panzhihua. The hot spot analysis revealed a prominent hot spot area centered around Kunming and cold spot areas in Zhaojue and Butuo, whereas the remaining counties did not display significant clustering of either hot spots or cold spots (Figure 24b).

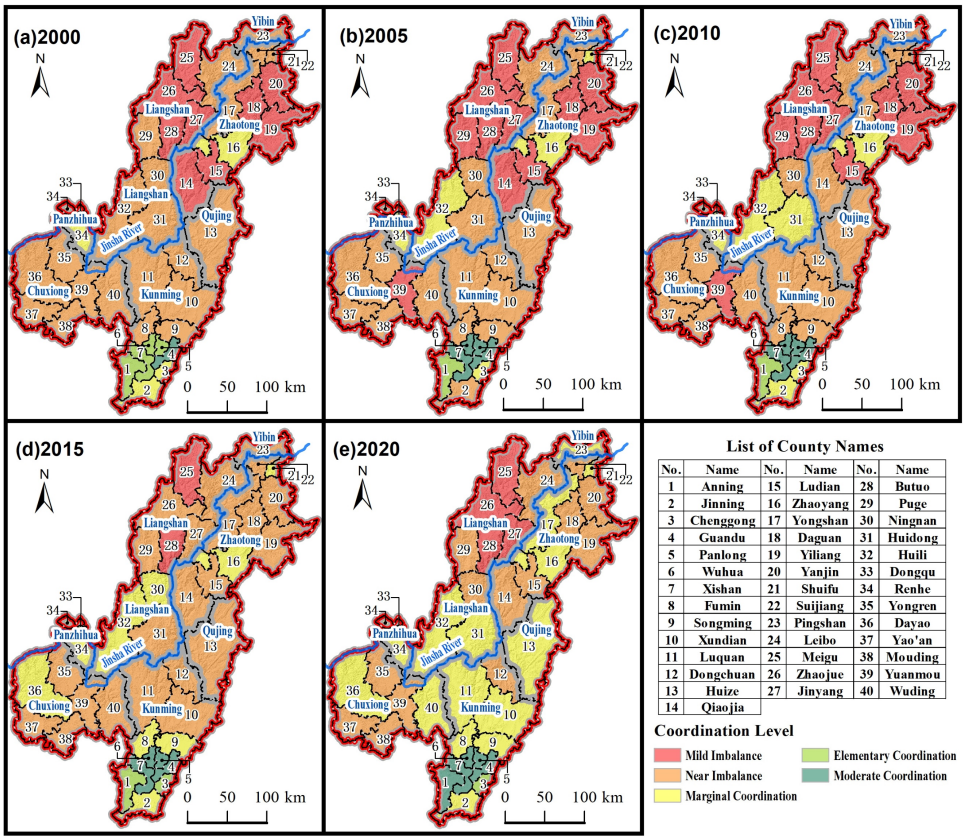


Figure 23. Spatial distribution of EECCD from 2000 to 2020.

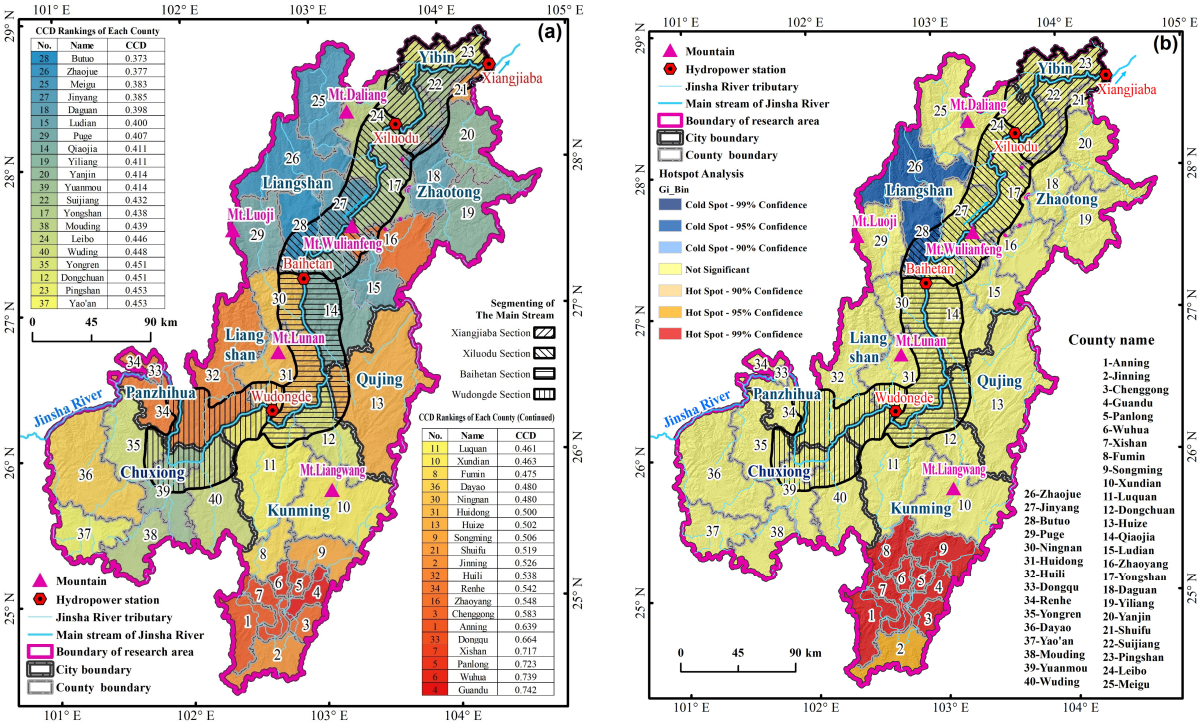


Figure 24. Spatial distribution of EECCD. (**a**) Average EECCD from 2000 to 2020; (**b**) hot spot analysis of average EECCD from 2000 to 2020.

4.3.3. Spatiotemporal Dynamics in the EERDD

From 2000 to 2020, although the ecological–economic relative development degree (EERDD) growth in the 24 B-class regions lagged behind that of the 16 A-class regions, a positive trend was still apparent. The average EERDD in the 24 B-class regions for 2000, 2005, 2010, 2015, and 2020 was 0.1801, 0.1554, 0.1746, 0.1705, and 0.2004, respectively, demonstrating an initial decline followed by a subsequent increase, culminating in an overall growth of 11.27%. In comparison, the average EERDD in the 16 A-class regions during the same period was 0.6128, 0.7381, 0.7889, 0.7039, and 0.7254, respectively, showing a pattern of increase, decline, and then increase, with a total growth of 18.37%. Overall, the EERDD development in these 16 counties was significantly better than in the 24 B-class regions.

According to the EERDD stage criteria, economic development in most counties within the study area continues to lag behind ecological environment improvements (Figure 25, Table A10). From 2000 to 2020, only two to four counties consistently maintained an EERDD classified as the "EDI Leads EEI Stage", with just one county remaining in this stage by 2020. Dongqu was in the "EDI Leads EEI Stage" from 2000 to 2015 but shifted to the "EDI and EEI Synced Stage" by 2020. Wuhua remained in the "EDI Leads EEI Stage" from 2005 to 2020. Panlong entered the "EDI Leads EEI Stage" in 2005, downgraded to the "EDI and EEI Synced Stage" in 2015, but returned to the "EDI Leads EEI Stage" in 2020. During this period, only one to four counties were classified under the "EDI and EEI Synced Stage", while the remaining counties, including all 24 B-class regions, were in the "EDI Behind EEI stage".

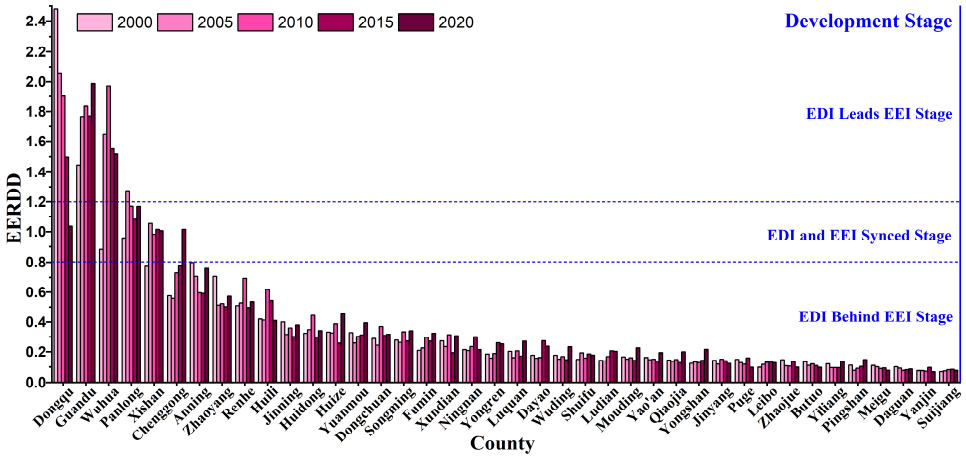


Figure 25. Ranking of ecological–economic relative development degree (EERDD) averages from 2000 to 2020.

Analyzing the EERDD growth rate from 2000 to 2020 reveals that counties with stronger economic foundations exhibited higher improvement rates (Figure 26, Table A11). Among the twenty-four B-class regions, eight—Yanjin, Jinyang, Daguan, Zhaoyang, Butuo, Meigu, Zhaojue, and Puge—experienced negative growth rates. Similarly, among the sixteen non-poverty-stricken counties, four—Huili, Jinning, Anning, and Dongchuan—also recorded negative growth rates. A negative growth rate indicates that economic development is relatively lagging, suggesting that the improvement rate of EEI exceeded the growth rate of EDI. Notably, among the 24 B-class regions, Yongshan, Ludian, Qiaojia, Yongren, Huize, and Mouding ranked among the top 10 counties in terms of EERDD growth rate.

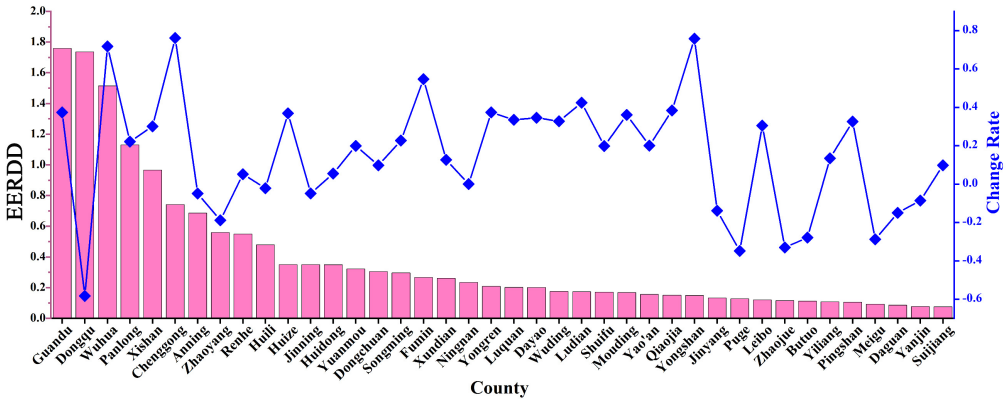


Figure 26. Comparison of average EERDD and its change rate in 40 counties from 2000 to 2020.

5. Discussion

5.1. Analysis of Spatiotemporal Dynamics in Ecological Environment

5.1.1. Single-Factor Driving Force Analysis

The primary factors driving the ecological environment index, ranked by their impact, include climatic, topographic, land use, and socioeconomic variables (Figure 27). These factors, listed from highest to lowest influence, are annual average temperature, aspect, elevation, land use type, nighttime light index, annual precipitation, cropland density, population density, GDP density, slope, Euclidean distance from roads, and construction land density. Natural conditions are the dominant factors influencing the spatial differentiation of the ecological environment index in the study area, with significant variation in the driving forces among different natural factors. Annual average temperature emerges as the strongest driver, with a *q*-value as high as 0.496, followed by slope (*q*-value of 0.378) and elevation (*q*-value of 0.304). The *q*-values for annual precipitation and slope are both below 0.2, indicating a relatively weak driving effect on the ecological environment index.

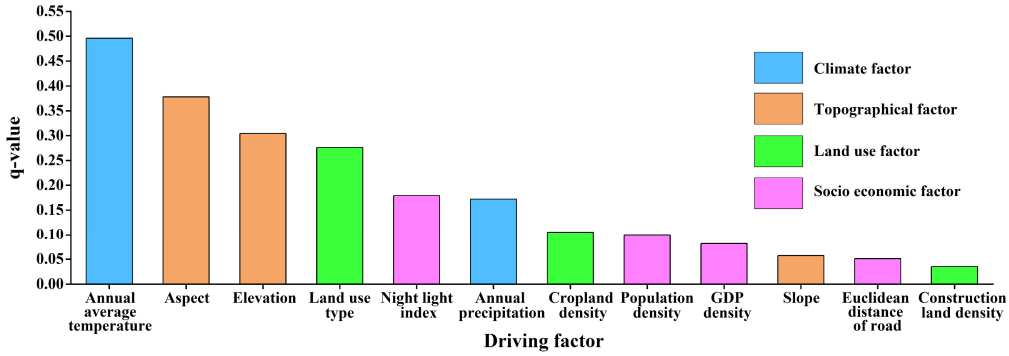


Figure 27. Ranking of single-factor driving force analysis results for changes in EEI.

Climatic Factors

Annual precipitation and annual average temperature are key indicators for evaluating hydrothermal conditions, and their impacts on the ecological environment of the study area vary significantly [82]. Among these factors, the influence of annual average temperature and its variations is more pronounced. High annual average temperatures predominantly occur in the dry-hot valley region of the LR-Jinsha [83], particularly in the border areas of Panzhihua, Chuxiong Prefecture, and Liangshan Prefecture. These elevated temperatures pose challenges for improving the ecological environment index. Compared to precipitation, temperature in the LR-Jinsha exerts a more substantial impact on the ecological environment. This is mainly because temperature fluctuations directly affect vegetation growth, soil moisture levels, and ecosystem stability, while the effects of changes in precipitation are relatively indirect and complex. Additionally, the combined effects

of global warming and human activities have heightened the sensitivity of the ecological environment to temperature changes in the region [84].

Topographical Factors

Among the topographic factors, the *q*-values of aspect and elevation both exceed 0.3, indicating their significant driving influence on the ecological environment index in the study area. In contrast, the slope factor has a comparatively minor impact, with a *q*-value of only 0.057. Aspect plays a critical role in determining the amount of solar radiation received by different areas [85]. In the mountainous regions of the LR-Jinsha, southern-facing slopes tend to be warmer and drier, while northern-facing slopes are cooler and wetter. This variation affects key ecological elements such as soil moisture, vegetation coverage, and evapotranspiration rates, all of which are vital for shaping the region's ecological environment [86]. Elevation also leads to temperature fluctuations, influencing the distribution of vegetation, soil types, and biodiversity [87]. The wide elevation range in the LR-Jinsha creates diverse microclimates, which have a substantial impact on the area's ecological dynamics. While slope is important for processes like soil erosion, water runoff, and land stability, its broader influence on climate and ecological variables is more localized. Compared to altitude and aspect, slope has a more limited impact on the region's ecological landscape [88].

Anthropogenic Factors

From 2000 to 2020, the influence of human activities on the ecological environment exhibited a downward trend. Among the contributing factors, land use, which captures the effects of various human activities [89], had a notably strong impact, with a *q*-value of 0.276. To address the region's fragile ecological conditions and mitigate the adverse effects of human activity, national and local governments launched large-scale initiatives, such as returning farmland to forests and enhancing ecological protection [90,91]. These efforts led to a marked increase in forest land and water bodies, both of which possess essential ecological source properties. Additionally, these projects facilitated the optimization of the quantity and spatial distribution of construction land.

The *q*-value of the nighttime light index, which reflects the activity of the local economy and the intensity of human activities [92], is 0.179, ranking second. The driving force of factors such as population density, GDP density, Euclidean distance of roads, and construction land density gradually weakened, with their *q*-values not reaching 0.1. This may be due to the limited accuracy of the relevant data and the concentrated reflection of human activities in a relatively confined space, which contrasts with the larger spatial scope of the study area, leading to a decrease in explanatory power.

5.1.2. Two-Factor Interaction Analysis

The Two-Factor Interaction Analysis presents a better explanatory effect [93]. As illustrated in Figure 28, the interaction between annual average temperature (X_1) and nighttime light index (X_{10}) is the most significant, with a *q*-value of 0.671. This is followed by the interaction between annual average temperature and elevation (X_3), with a *q*-value of 0.635, and the interaction between annual average temperature and construction land density (X_9), with a *q*-value of 0.165. These findings indicate that temperature is a crucial factor affecting the ecological environment index of the study area [94]. Comparative analysis shows that in univariate analysis, the impact of construction land density (X_9) and nighttime light index (X_{10}) on the ecological environment is relatively small. However, when considering the interaction effect, the *q*-value of the interaction between these factors significantly increases with the annual average temperature.

The interaction between natural elements and human activity elements exhibits a dual-factor enhancement effect, significantly driving the quality of the ecological environment [95]. Specifically, the interaction between annual precipitation (X_2) and aspect (X_5) with other factors exerts a significant influence on the ecological environment. This

is primarily due to their capacity to enhance soil moisture, support vegetation growth, and promote biodiversity, leading to an overall positive effect on the ecosystem [96]. In the interaction between annual average temperature and other factors, the *q*-values of interaction with Euclidean distance of roads (X_{13}) and cropland density (X_8) are slightly lower at 0.485 and 0.496, respectively. However, the *q*-values of interaction with other human activity factors are all over 0.515. The interaction between slope (X_4) and land use type (X_7) is the strongest among all interactions, with a *q*-value as high as 0.576. This result reveals the combined effect of slope and human activity-related factors, which has a more profound impact on the spatial analysis of EEI in the study area [97].

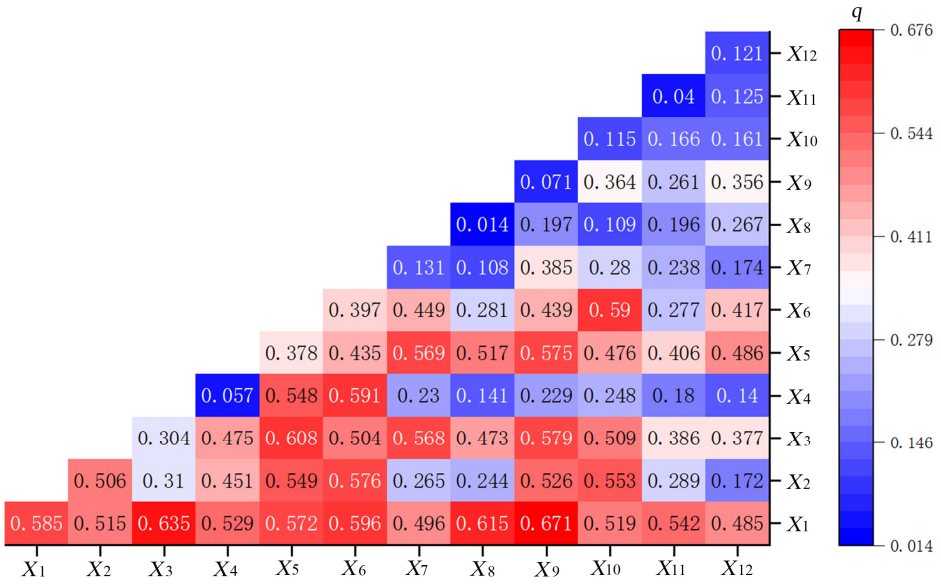


Figure 28. Detection results of the interaction between ecological environment driving factors.

5.2. Analysis of Spatiotemporal Dynamics in Economic Development

5.2.1. Analysis of Influencing Factors at the Subsystem Level

The obstacle factor diagnosis method was applied to calculate the factor contribution degrees of three subsystems—economic structure, economic environment, and economic scale—to the EEI in the 24 B-class and 16 A-class regions, respectively. The analysis revealed that the factor contribution degree of the economic structure increased, the economic environment's contribution degree decreased, and the economic scale's contribution degree fluctuated before stabilizing (Figure 29).

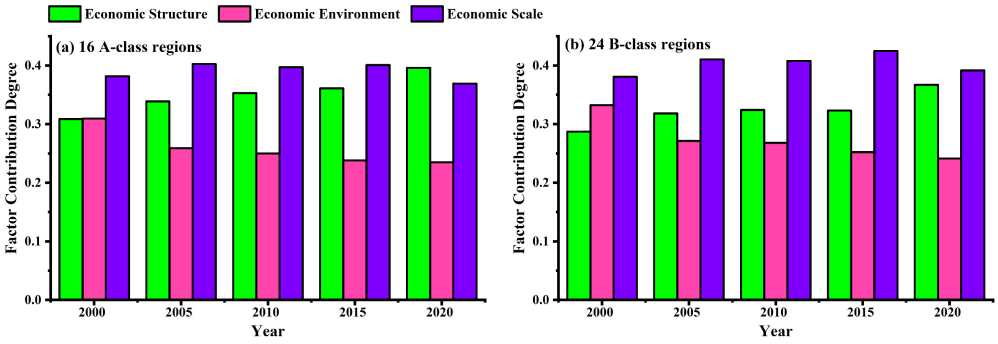


Figure 29. Factor contribution degrees of three subsystems—economic structure, economic environment, and economic scale—to EEI. (**a**) 16 A-class regions; (**b**) 24 B-class regions.

Economic Structure

Both types of regions showed an increase in the factor contribution degree of economic structure. In the B-class regions, it rose from 28.72% in 2000 to 36.69% in 2020, while in

the A-class regions, it increased from 30.87% in 2000 to 39.61% in 2020. The economic structure factor contribution in the 16 A-class regions was generally higher than in the 24 B-class regions, and the rate of increase was also greater. This reflects a common challenge across both regions: optimizing and upgrading industrial structures [98]. Traditional industries, such as agriculture and low-end manufacturing, still constitute a significant proportion of the economic structure and lack support from high value-added and high-tech industries. This leads to lagging industrial optimization and represents a major obstacle to economic development [99]. In the 16 A-class regions, where the economic foundation is relatively strong, the traditional industrial structure no longer meets the needs of high-quality development. Thus, economic structural optimization has become a more significant barrier to further development [100]. Additionally, in some counties, there is a large gap in urban and rural economic structures and a low level of urbanization, hindering effective industrial upgrading and structural adjustment.

Economic Environment

The obstacles related to the economic environment showed a continuous downward trend. The factor contribution degree of the economic environment to economic development levels in both types of regions decreased steadily over time. In B-class regions, it fell from 33.23% in 2000 to 24.14% in 2020; in A-class regions, it dropped from 30.95% in 2000 to 23.49% in 2020. However, the decline in the 16 A-class regions was slightly less pronounced than in the 24 B-class regions. This trend can be attributed to improvements in infrastructure, policy environment, and business environment optimization. The implementation of poverty alleviation and rural revitalization policies has significantly enhanced infrastructure—such as transportation, energy, and communication—as well as public services like education and healthcare in the 24 B-class regions [101]. These improvements reduce the barriers posed by the economic environment to economic development. The government has also provided more policy support to the 24 B-class regions, including infrastructure investment, tax incentives, and talent recruitment, which have effectively improved the economic environment. In the 16 A-class regions, local governments have prioritized optimizing the business environment through various measures such as introducing one-stop government services, streamlining administrative approval processes, refining business environment policies, enhancing the efficiency of government services, and innovating service models [102]. These initiatives have collectively contributed to reducing barriers within the economic environment.

Economic Scale

The contribution of economic scale exhibited fluctuations but showed a general trend towards stabilization over time. In both A- and B-class regions, the contribution of economic scale to the EDI remained consistently significant, although with some variation. In the 24 B-class regions, the contribution primarily ranged between 38% and 42% throughout the study period, while in the 16 A-class regions, it ranged from 36.90% to 40.24%. This trend reflects the relatively modest economic base in both types of regions. Notably, the limited economic scale and fragile industrial foundation in the 24 B-class regions present substantial constraints on expanding economic growth. For instance, by 2020, the average GDP and total retail sales of consumer goods in these 24 regions represented only 25% of the average in China's western region, with per capita GDP standing at just 44% of the national average.

Additionally, the economic growth models across both types of counties are relatively homogeneous, often relying on a few key industries. When these industries face growth bottlenecks or slow down, they have a more substantial impact on the overall economic scale, as seen in regions such as Dongchuan and Butuo. In areas with less favorable geographic conditions, such as Leibo, Jinyang, Meigu, Puge, and Zhaojue, a shrinking demographic dividend and limited resources further hinder the expansion and development of economic scale.

Overall Analysis

Compared to the 16 A-class regions, the economic environment factor contribution degree in the 24 B-class regions has decreased more significantly, whereas the economic structure factor contribution degree is more prominent in the 16 A-class regions. This suggests that the 24 B-class regions are more reliant on improvements in infrastructure and the business environment, while the 16 A-class regions more urgently require economic structural transformation and optimization. The reasons for this include the following: First, the 24 B-class regions are in the early stages of economic development, where the role of infrastructure and environmental improvements is relatively substantial. The 16 A-class regions, having reached a certain level of economic development, rely more on industrial upgrading and economic restructuring for higher-quality development [103]. Second, government support policies for the 24 B-class regions have primarily focused on infrastructure, public services, and improving the business environment, whereas for the 16 A-class regions, the emphasis has been on guiding economic structural optimization and fostering innovation-driven development [104].

5.2.2. Analysis of Influencing Factors at the Indicator Level

Using the obstacle factor diagnosis method, we analyzed the impact of nine economic factors on the EDI and found notable differences between the 16 A-class and 24 B-class regions (Figure 30). In the 16 A-class regions, the average influence of each factor on EDI, ranked from highest to lowest, is as follows: social consumption (17.05%), human activity intensity (15.75%), tertiary industry (16.72%), total GDP (13.73%), secondary industry (13.31%), urbanization rate (5.91%), per capita cropland (4.16%), per capita GDP (8.24%), and primary industry (5.93%). In contrast, in the 24 B-class regions, the factors' average influence is ranked as: human activity intensity (17.65%), social consumption (16.57%), tertiary industry (15.31%), total GDP (13.12%), secondary industry (12.51%), urbanization rate (7.04%), per capita GDP (10.62%), primary industry (4.58%), and per capita cropland (2.22%).

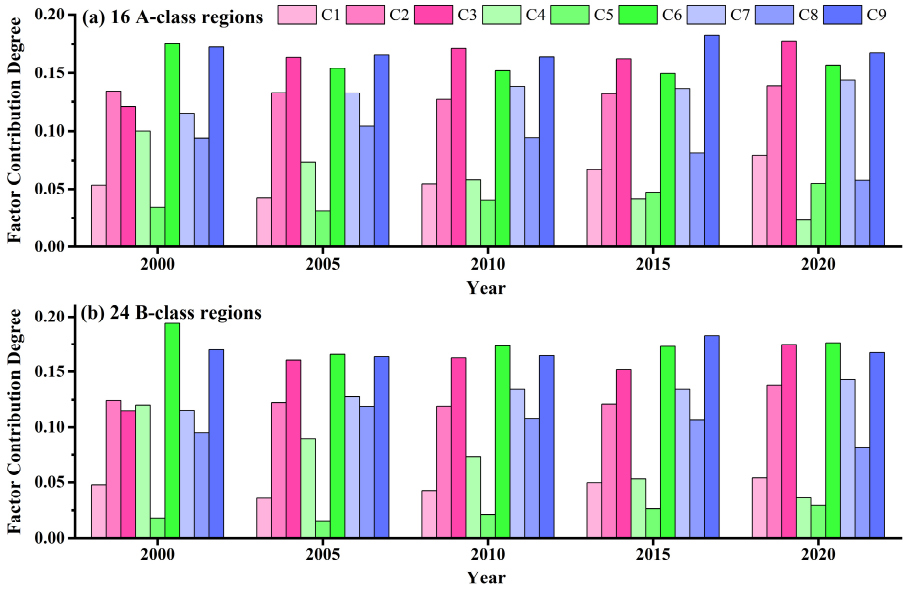


Figure 30. Contribution of 9 economic factors to EEI: (**a**) 16 A-class regions; (**b**) 24 B-class regions. C1 denotes total output value of primary industry, C2 denotes total output value of secondary industry, and C3 denotes total output value of tertiary industry. C4 represents urbanization rate, C5 represents per capita cultivated land area, and C6 represents nighttime light index. C7 indicates total GDP, C8 indicates GDP per capita, and C9 indicates total retail sales of consumer goods.

The influence of the four factors—human activity intensity, social consumption, tertiary industry, and total GDP—is similar in both types of regions, indicating that these

factors play a crucial role in the economic development across the LR-Jinsha. This suggests that economic activities, consumer spending capacity, and the growth of the service industry significantly impact the economic landscape of the entire region. As the economy develops and social consumption levels increase, the role of the tertiary industry and human activity intensity in driving regional economic growth becomes increasingly prominent [105,106].

There are notable differences in the influence of certain factors between the two types of regions. In the 24 B-class regions, the urbanization rate and secondary industry exert a stronger influence, reflecting that these regions are still in the early stages of urbanization and industrialization. Here, enhancing the level of urbanization and establishing a robust industrial base play a crucial role in driving economic growth. Over time, the marginal effect of urbanization has gradually diminished, which explains the recent downward trend in its impact [107]. Conversely, in the 16 A-class regions, the primary industry and per capita cropland exert a more pronounced influence. This indicates a stronger reliance on natural or agricultural resources for economic development, highlighting the dependence of these regions on the agricultural economy and related sectors. This pattern is particularly evident in regions such as Huidong, Huili, Renhe, Ningnan, and Yuanmou, where agriculture plays a pivotal role in supporting local economies.

The impact of per capita GDP differs between the two types of regions. In the 24 B-class regions, the influence of per capita GDP is generally higher than in the 16 A-class regions. The fluctuations in per capita GDP in the 24 B-class regions suggest that economic development and wealth accumulation per capita in these areas may be influenced by factors such as resource allocation, infrastructure development, and policy support [108].

5.3. Analysis of Spatiotemporal Dynamics in Ecology–Economy Coupling

5.3.1. Analysis in 16 A-Class Regions

The impact factors of EECCD in 16 A-class regions exhibited significant dynamic changes from 2000 to 2020 (Figure 31). The influence of the secondary industry and the nighttime light index, which indicates human activity intensity, weakened over this period. Conversely, the influence of factors such as the tertiary industry, WET, and per capita cropland area gradually increased. These changes in the weight of economic restructuring and ecological factors reflect adjustments in development strategies and environmental policies during the ecological–economic coupling process in these regions.

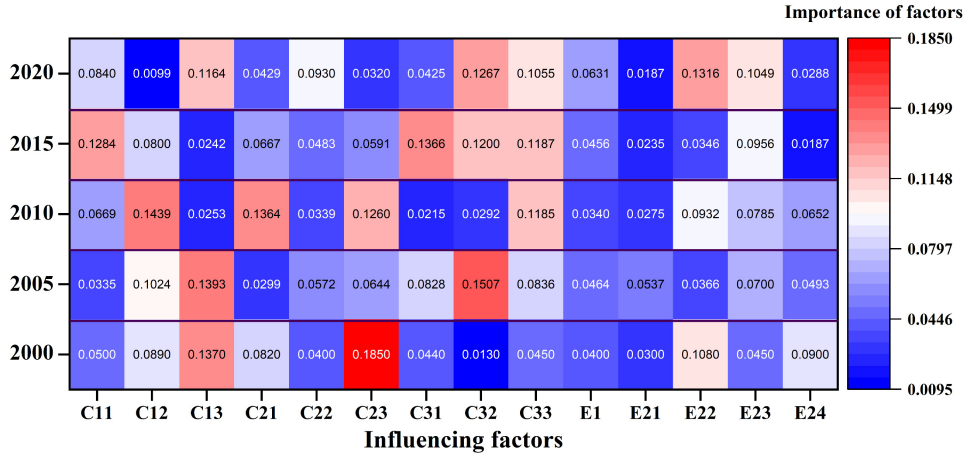


Figure 31. The importance of influencing factors on EECCD in 16 A-class regions from 2000 to 2020. C11 denotes total output value of primary industry, C12 denotes total output value of secondary industry, and C13 denotes total output value of tertiary industry. C21 represents urbanization rate, C22 represents per capita cultivated land area, and C23 represents nighttime light index. C31 indicates total GDP, C32 indicates GDP per capita, and C33 indicates total retail sales of consumer goods. E1 stands for BRI, E21 stands for NDVI, E22 stands for WET, E23 stands for NDSBI, and E24 represents LST.

In terms of economic structure, from 2000 to 2020, the impact of the total output value of the primary industry on the coupling and coordination degree of ecological economy fluctuated upward, while the impact of the secondary industry first rose and then fell. The impact of the tertiary industry once decreased but later rebounded, showing the impact of changes in industrial structure on EECCD. The impact of the primary industry on EECCD showed a fluctuating upward trend from 2000 to 2020, reaching a peak of 0.1284 in 2015, indicating that the impact of the ecological–economic coupling of agricultural activities was gradually increasing, but there was a certain decline in 2020. The influence of the secondary industry gradually increased in 2005 and 2010, reaching a peak of 0.1439 in 2010, but then significantly decreased to 0.0099 in 2020. This reflects the gradual shift of the economic center of gravity in these regions from industry to other industries. The influence of the tertiary industry was relatively high in 2000 and 2005, and then significantly decreased in 2010 and 2015, but it rebounded to 0.1164 in 2020, reflecting that the service industry has become an important factor affecting the coupling of ecological economy to a certain extent.

In terms of economic environment, from 2000 to 2020, the impact of urbanization rate on the coupling of ecological economy fluctuated significantly, while the impact of per capita cropland area first decreased and then increased. The explanatory power of nighttime light index as an indicator of economic activity gradually weakened. The impact of urbanization rate on the coupling degree was 0.0820 in 2000, but it dropped to a minimum of 0.0299 in 2005, then reached a peak of 0.1364 in 2010, and then declined again. This indicates that there are significant fluctuations in the impact of urbanization on the coupling of ecological and economic development. The impact of per capita cropland area showed a trend of first decreasing and then increasing, reaching a peak of 0.0930 in 2020, which may be related to the rational use and optimal management of agricultural resources in the region. The intensity of human activities had the greatest impact in 2000, reaching 0.1850, and then showed a general downward trend. This indicates that, over time, the explanatory power of nighttime light index as a proxy for economic activity on the coupling of ecological and economic development has gradually weakened.

From the perspective of economic indicators, the impact of the three factors on the coupling of ecological economy fluctuates. The increase in economic aggregate does not fully and continuously improve EECCD, while per capita income and consumption have a more significant impact in specific years. The impact of total GDP on the coupling of ecological economy fluctuates, reaching a peak of 0.1366 in 2015, but then declining. the increase in economic aggregate does not necessarily continuously improve the coupling degree of ecological economy. The impact of per capita GDP is more significant in 2005 and 2020, which are 0.1507 and 0.1267 respectively, reflecting that the per capita income level has a more significant impact on EECCD at specific stages. The impact of total retail sales of consumer goods began to increase significantly in 2005, reaching 0.0836, and remained at a high level of 0.1187 and 0.1055 in 2015 and 2020, indicating that the impact of consumption on the coupling of ecological and economic development is gradually increasing. From 2000 to 2020, the average total retail sales of consumer goods in 16 counties increased by 17.43 times.

From the perspective of BRI, its impact on EECCD remained relatively stable throughout the entire time period, but slightly increased to 0.0631 in 2020. This indicates that the importance of land use and its derivative BRI is gradually increasing. Especially in urban and rural construction land, cultivated land, and their peripheral areas within the district, such as Panzhihua [109] and Kunming City [110].

The impact of each RSEI component on the coupling of ecology and economy showed different trends, indicating that the changes in the four factors had different effects on the coupling of ecology and economy in different periods. The impact of the NDVI has gradually weakened, from 0.0300 in 2000 to 0.0187 in 2020, indicating that the impact of vegetation coverage on the coupling of ecological economy has gradually decreased. The impact of WET reached a peak of 0.1080 in 2000, then declined and rose again to 0.1316 in 2020, indicating that the impact of WET on ecological economy has significantly changed

over different time periods. The impact of the NDSBI is gradually increasing, indicating that land use change has an increasingly important impact on EECCD. The impact of LST was higher in 2000, at 0.0900, and then gradually decreased. Over time, the direct impact of changes in LST on EECCD has weakened.

5.3.2. Analysis in 24 B-Class Regions

From 2000 to 2020, the impact of various economic factors on EECCD in the 24 B-class regions exhibited significant variations across different years (Figure 32). The influence of the secondary industry has gradually increased, while the marginal effect of urbanization has decreased. The growth of economic aggregates and per capita income continues to be the primary driving force. Although the role of ecological environment indicators has risen, their overall impact remains relatively low.

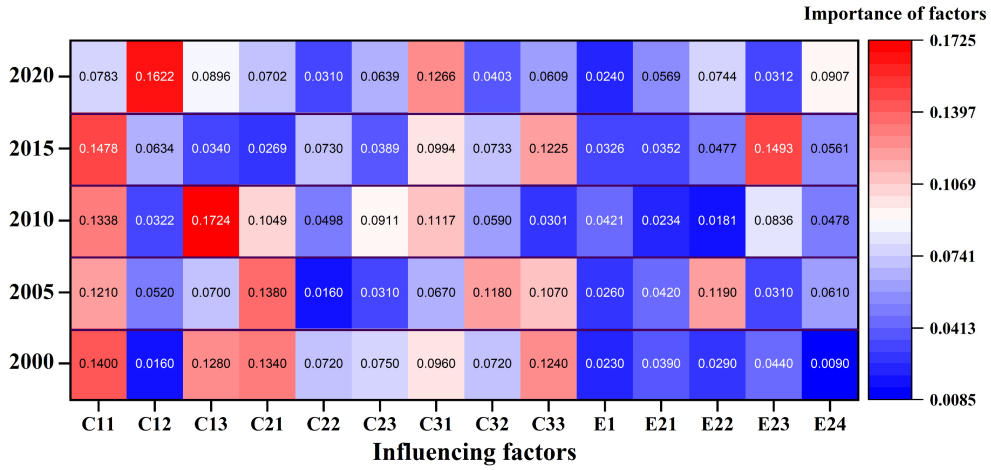


Figure 32. Importance of influencing factors on EECCD in 24 B-class regions from 2000 to 2020. C11 denotes total output value of primary industry, C12 denotes total output value of secondary industry, and C13 denotes total output value of tertiary industry. C21 represents urbanization rate, C22 represents per capita cultivated land area, and C23 represents nighttime light index. C31 indicates total GDP, C32 indicates GDP per capita, and C33 indicates total retail sales of consumer goods. E1 stands for BRI, E21 stands for NDVI, E22 stands for WET, E23 stands for NDSBI, and E24 represents LST.

From the perspective of the economic structure's components on EECCD, the roles of the three industrial sectors have been evolving over time. The primary industry had a significant impact on EECCD from 2000 to 2015, but its influence declined sharply by 2020, reflecting a shift towards an upgraded regional industrial structure and a reduced role of the primary sector. In contrast, the impact of the secondary industry on EECCD has been increasing, particularly in 2020, when it became one of the main influencing factors. This underscores the growing importance of industrialization in promoting EECCD. Meanwhile, the impact of the tertiary industry peaked in 2010 but then gradually weakened, likely due to the saturation of the service sector and adjustments or transformations in the economic structures of various counties.

From the perspective of the economic environment's impact on EECCD, the marginal effect of the urbanization rate is diminishing, the influence of per capita cropland area remains limited, and the relationship between economic activity—represented by the night-time light index—and EECCD is complex. From 2000 to 2010, the impact of the urbanization rate on EECCD was relatively stable but then significantly decreased, indicating either a diminishing marginal effect of urbanization or an increase in environmental problems associated with urbanization. The impact of per capita cultivated land area has consistently been low and fluctuating, reflecting the limited role of agricultural resources on EECCD and constraints from factors such as land use changes and agricultural policies. The nighttime light index, an indirect measure of economic activity, peaked in 2010 and then declined,

highlighting the intricate relationship between economic activity intensity and EECCD, influenced by economic structure, energy efficiency, and policy regulation.

The impact of economic scale on EECCD has been stable and rising, with total GDP and per capita GDP consistently driving EECCD forward. The influence of total GDP peaked in 2020, while per capita GDP reached its highest point in 2005 and then slightly declined but remained high. In contrast, the impact of total retail sales of consumer goods, which was relatively stable from 2000 to 2015, declined in 2020, likely due to changes in consumption patterns and policy regulation [111].

From 2000 to 2020, the impact of the BRI on EECCD remained relatively low and exhibited significant fluctuations, indicating its limited contribution to ecological and economic coupling coordination. This could be attributed to the gradual harmonization of land use changes, ecological protection efforts, ecological restoration, and human activity intensity with ecological and economic development during the initiative's implementation. These areas likely underwent a period of adjustment where the BRI's influence on ecological sustainability and economic growth became more coordinated over time, leading to fluctuating but overall moderate impacts [112].

The four components of the RSEI currently have a low but increasing impact on EECCD, reflecting the effectiveness of ecological protection and restoration efforts, as well as the influence of climate warming. While the impacts of the NDVI, the WET, and the NDSBI are relatively low, they are trending upward, indicating that the role of the ecological environment in EECCD has strengthened following the implementation of ecological protection and restoration projects. Although the impact of LST is also relatively low, it is rising, likely due to global warming and regional human activities, which could further affect both the ecological environment and economic development [113].

5.3.3. Comparative Analysis

Overall, there are distinct differences in the impact of ecological and economic factors on the EECCD between the 24 B-class regions and the 16 A-class regions from 2000 to 2020 (Figure 33). The poverty-alleviated counties are more reliant on the primary industry, economic scale, and urbanization, with ecological and environmental factors playing a relatively minor role. In contrast, the 16 A-class regions are more influenced by economic factors such as consumption, human activity intensity, and the tertiary industry, while ecological and environmental factors have a comparatively more prominent impact.

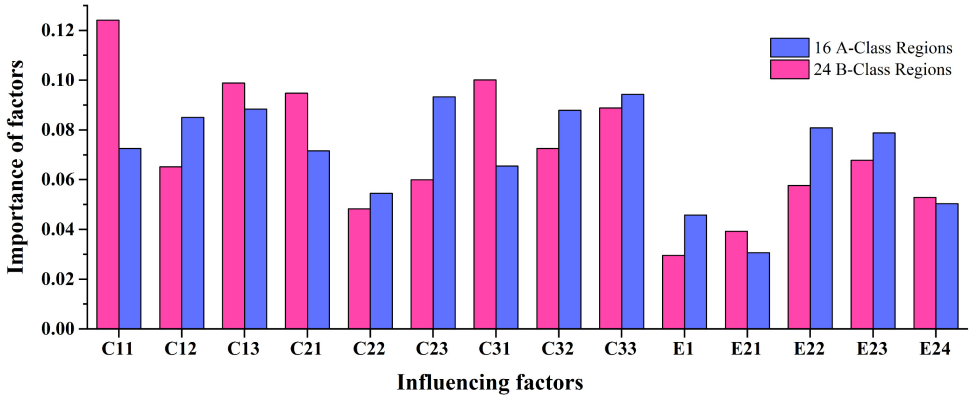


Figure 33. Comparison of importance of 16 A-Class regions and 24 B-Class regions from 2000 to 2020. C11 denotes total output value of primary industry, C12 denotes total output value of secondary industry, and C13 denotes total output value of tertiary industry. C21 represents urbanization rate, C22 represents per capita cultivated land area, and C23 represents nighttime light index. C31 indicates total GDP, C32 indicates GDP per capita, and C33 indicates total retail sales of consumer goods. E1 stands for BRI, E21 stands for NDVI, E22 stands for WET, E23 stands for NDSBI, and E24 represents LST.

The impact of economic structure on the coupling of ecological economy differs significantly between the 24 B-class regions and the 16 A-class regions. In the poverty-alleviated counties, the total primary industry output has the greatest influence on ecological–economic coupling, with a value of 0.1242, which is substantially higher than that in non-poor counties. This suggests that agriculture remains a crucial factor supporting economic development in these areas, with agricultural output making a significant contribution to the coupling of ecology and economy. The impact of total GDP is the second highest in poverty-alleviated counties, at 0.1001, indicating that overall economic growth is more vital in these regions due to their relatively weaker economic foundation [114]. The overall economic growth has a notable effect on enhancing the coupling and coordination of the ecological economy in these counties. In contrast, in the 16 A-class regions, the impact of total tertiary industry output (0.0884) and total secondary industry output (0.0850) is more prominent, reflecting a greater reliance on the service and industrial sectors for promoting economic development and ecological–economic coupling. Meanwhile, the influence of the primary industry in the 16 A-class regions is comparatively smaller, at 0.0726, indicating a shift in their economic structure towards the secondary and tertiary sectors, driven by modern industrial growth [115].

The influence of consumption and human activity intensity on the EECCD is notable. In the 24 B-class regions, the effects of total retail sales of consumer goods (0.0889) and nighttime light index (0.0600) are relatively minor. This suggests that consumption and overall human activity in these areas are less dynamic compared to the 16 A-class regions, resulting in a limited impact on EECCD. Conversely, in the 16 A-class regions, total retail sales of consumer goods (0.0943) and nighttime light index (0.0933) are the highest, indicating that consumption levels and comprehensive human activities play a crucial role in the EECCD of these regions. This reflects a greater dependence on consumption and market vitality in the economies of these areas [116].

Economic efficiency and industrial transformation positively impact the EECCD [117]. In the 24 B-class regions, the effects of per capita GDP (0.0725) and total secondary industry output (0.0652) are relatively modest. This is attributed to the weaker economic efficiency and industrial base in these counties, where economic growth is more reliant on the expansion of the primary industry and, to some extent, the overall economic scale. Conversely, in the 16 A-class regions, the impact of per capita GDP (0.0879) is more pronounced, indicating that economic development in these regions is more focused on enhancing economic efficiency and per capita income, such as Dongchuan, Zhaoyang, and Wuding. Additionally, the substantial effect of total secondary industry output (0.0850) in these 16 counties suggests that industrialization plays a significant role in contributing to EECCD [118].

There are differences in the roles of the RSEI and the BRI in influencing EECCD. In the 24 B-class regions, the impacts of WET (0.0576), NDSBI (0.0678), and LST (0.0529) are relatively small, indicating that changes in ecological factors have limited effects on EECCD, with economic factors playing a more dominant role. The influence of the BRI (0.0295) and the NDVI (0.0393) is the lowest in both types of counties, suggesting that improvements in natural ecological indicators have a less significant impact on EECCD in these areas. In contrast, in the 16 A-class regions, WET (0.0808) and NDSBI (0.0788) have a more substantial impact on EECCD, highlighting the importance of ecological environmental governance, as changes in ecological indicators contribute more to EECCD coordination. While the effects of the NDVI (0.0307) and the BRI (0.0458) remain relatively small, they are slightly higher than in poverty-alleviated counties, reflecting the positive impact of improved vegetation cover and biodiversity on EECCD in these regions [119].

The impacts of urbanization and land use on EECCD differ across regions [120]. In the 24 B-class regions, the urbanization rate (0.0948) plays a more significant role, as these areas are still experiencing rapid urbanization, which strongly drives economic growth. Being in the accelerating stage of urbanization, these regions benefit from increased economic development and industrial restructuring, alongside improvements in resource allocation efficiency and ecological governance. In contrast, in the 16 A-class regions, the effects

of urbanization rate (0.0716) and per capita cropland area (0.0545) are less pronounced, suggesting that urbanization and agricultural land use have a relatively limited impact on EECCD in these areas.

5.4. Implications and Limitations

5.4.1. Implications

To foster coordinated ecological and economic development in the LR-Jinsha, future efforts should focus on strengthening infrastructure construction, enhancing the transportation network, and improving internal and external connectivity to reduce geographical constraints. Financial, tax, and monetary support must be provided to solidify the achievements of targeted poverty alleviation. Increased investment in education and the promotion of science and technology are critical. It is also essential to further develop and utilize resources such as tourism, minerals, water conservancy, photovoltaics, agriculture, and traditional Chinese medicine, while continuously advancing ecological engineering. By leveraging ecological economics and ecological compensation, the industrial structure can be optimized. Based on the spatial–temporal evolution of economic development levels, ecological environment indices, and the EECCD, the development paths in the study area can be categorized into six types (Figure 34).

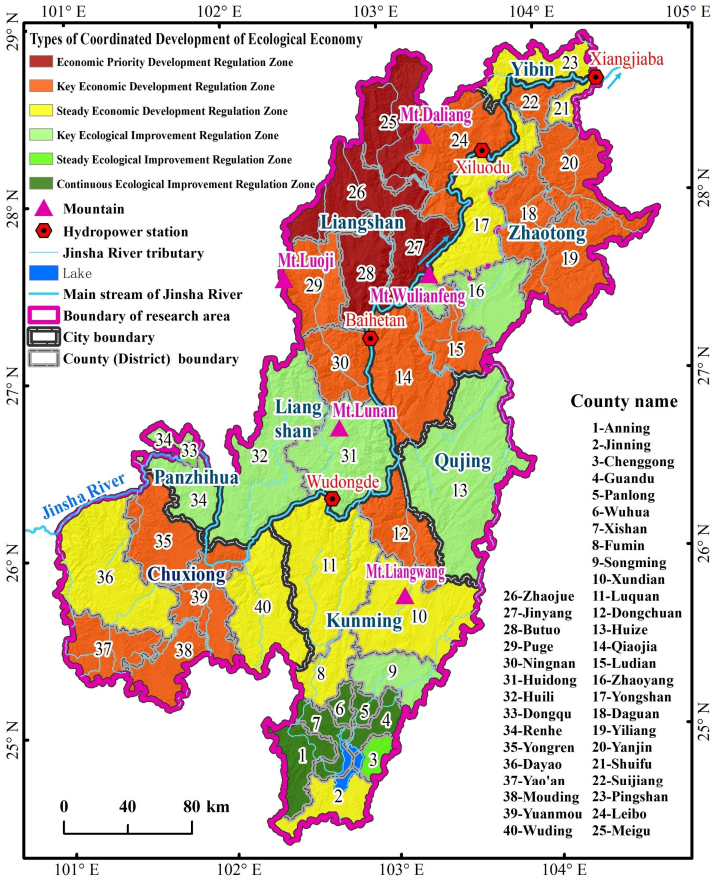


Figure 34. Coordinated development path of ecological environment and economic environment.

Economic Priority Development Regulation Zone: Situated in the southwestern mountainous region of Sichuan, primarily encompassing Meigu, Zhaojue, Butuo, and Jinyang counties in Liangshan Prefecture, these areas should prioritize economic growth while improving the synergy between ecological quality and economic development. Emphasis should be placed on advancing industrial transformation and upgrading, reinforcing the modernization of traditional industries, fostering the development of emerging industries, and promoting infrastructure and industrial park construction.

Key Economic Development Regulation Zone: The most extensive category, encompassing counties such as Mouding, Yaoan, Yongren, and Yuanmou in Chuxiong Prefecture; Leibo, Ningnan, and Puge in Liangshan Prefecture; and Daguan, Ludian, Qiaojia, Suijiang, Yanjin, and Yiliang in Zhaotong City. These regions are characterized by lower levels of economic development but possess significant growth potential. Strengthening economic growth while aligning it with ecological improvements is crucial. To achieve this, it is essential to enhance infrastructure development, improve the investment environment, optimize the industrial structure, and foster the growth of unique local industries. Moreover, regional cooperation and coordinated development are key strategies for unlocking the full potential of these areas.

Steady Economic Development Regulation Zone: Includes Dayao and Wuding counties in Chuxiong Prefecture, Fumin, Jinning, Luquan, and Xundian counties in Kunming City, as well as Shuifu and Yongshan counties in Zhaotong City. These areas are transitioning from an eco-economic imbalance to a more coordinated state. To further advance this transition, steady economic growth is essential to foster a more balanced relationship between ecological and economic factors. Key priorities include optimizing the industrial structure, enhancing ecological protection and restoration efforts, and promoting regional coordination and development strategies.

Key Ecological Improvement Regulation Zone: Covers counties like Songming, Huidong, Huili, and Renhe District, along with Huize County and Zhaoyang District. This zone prioritizes ecological protection and is essential for enhancing the overall ecological quality of the Jinsha River basin. Further efforts are needed to strengthen ecological protection and restoration, optimize industrial and energy structures, improve the ecological environment governance system, and promote regional cooperation and collaborative governance.

Steady Ecological Improvement Regulation Zone: Located in Chenggong District of Kunming City and Dong District of Panzhihua City, where positive eco-economic coordination trends are observed. Steady ecological improvements are necessary to further advance towards coordination. Further efforts are needed to strengthen ecological environment protection and governance, optimize industrial and energy structures, and promote coordinated development of ecological economy.

Continuous Ecological Improvement Regulation Zone: Includes Anning City, Guandu, Panlong, Wuhua, and Xishan districts in Kunming City. These areas exhibit a high degree of internal coordination and therefore necessitate ongoing efforts to enhance ecological quality. Key priorities include strengthening water resource protection and governance, improving air quality, implementing ecological restoration and greening initiatives, advancing pollution control measures, and promoting the development of a green economy.

Meanwhile, the regions designated for prioritized economic development and regulation must balance economic growth with ecological preservation, addressing challenges such as underdeveloped infrastructure and a lack of industrial diversity. Regions marked for steady economic development regulation need to accelerate the transformation of coordination mechanisms and ensure effective policy implementation. Areas with a focus on ecological enhancement face issues like fragile ecosystems and funding shortages. Regions aimed at stable ecological improvement must work to raise public environmental awareness and expedite progress in coordination efforts. Finally, areas striving for continuous ecological advancement should innovate ecological development models to meet higher environmental quality standards.

5.4.2. Limitations

The coupling development of ecological and economic systems has diverse and complex roles and feedback mechanisms. This article constructs a dataset and uses various methods to explore the spatiotemporal changes and driving forces of the ecological and economic coupling system in the LR-Jinsha region, which has different resource endowments, environmental conditions, development history, and development models. However, there

are still some aspects that need improvement. This paper is limited by the availability and consistency of data, and the selection of economic factors can be further increased, such as the proportion of R&D funds in GDP, the proportion of fixed assets investment in GDP, trade balance, labor productivity, employment rate, unemployment rate, human development index, etc. As economic data mostly belongs to statistical data, obtaining raster data or rasterizing data is one of the directions for improvement. The length of research can be extended to before and after 2000–2020, and simulation prediction research can be conducted on this basis to enhance decision support for research results. For ecological and economic coupled development systems that combine natural and social attributes, the potential of machine learning and other methods can be further explored to identify the relationships and processes between complex systems. Furthermore, additional research is required to refine the methodological framework for analyzing the spatiotemporal coupling mechanisms between ecology and economy. Such efforts aim to offer a distinctive ecological and economic perspective for understanding the processes and impacts of the human–environment coupling system.

6. Conclusions

This article integrates multiple datasets and methodological models to identify the spatiotemporal changes and driving factors of the ecological environment subsystem, economic environment subsystem, and the ecological–economic coupling system. Here are the key findings:

From 2000 to 2020, the overall improvement rates of the ecological and economic subsystems surpassed that of the ecological–economic coupling system, with a 19.95% increase in the EEI, a 33.55% rise in the EDI, and a 12.50% improvement in the EECCD. The entire region remains in the Running-In Stage, with the coordination level progressing from Near Imbalance to Marginal Coordination. Furthermore, 85% of the counties' EERDD are still in the EDI Behind EEI stage.

The structural composition of the EEI exhibits a pattern of being low in the Dry Hot Valley area and high in other regions, primarily influenced by natural factors, although human activities also significantly impact these interactions. Key natural drivers include temperature, slope, and elevation, while land use and nighttime light reflect human influence. Interaction analysis highlights the combined effects of both natural and human factors, with temperature and nighttime light demonstrating dual-factor enhancement effects. Originating from an impact model primarily driven by economic factors and supplemented by ecological factors, both the EDI and EECCD show a pattern of being higher in the south and lower in the north, with improvements gradually expanding northward from the urban area of Kunming. A-class regions shifted their focus from secondary to tertiary industries and ecological considerations, while B-class regions continued to rely on primary industries and urbanization. Economic restructuring and urbanization played a crucial role, with ecological factors gradually gaining importance. The development gradient gap between the 24 poverty-stricken counties and the 16 non-poverty-stricken counties has narrowed. Simultaneously, policies such as green development, ecological protection, industrial upgrading and transformation, regional coordinated development, targeted poverty alleviation, and poverty alleviation consolidation have played—and will continue to play—a positive role in fostering sustainable development.

Based on their spatiotemporal evolution and corresponding strategies, the development paths of the 40 counties in the study area can be classified into six categories: Economic Priority, Key Economic, Steady Economic, Key Ecological, Steady Ecological, and Continuous Ecological Improvement Regulation Zones. Meanwhile, areas leading in economic development may face challenges such as outdated infrastructure, a limited industrial structure, and the need to balance economic growth with ecological sustainability. Similarly, regions prioritized for ecological protection grapple with issues like fragile ecosystems, insufficient funding, and low public awareness of environmental conservation. It is recommended to increase investments in transportation and water conservancy infrastruc-

ture, strengthen coordinated regional economic development, and promote a diversified industrial structure. Furthermore, efforts should focus on enhancing ecological protection and restoration, boosting financial support, implementing ecological compensation mechanisms, and fostering innovative models for sustainable ecological development.

Author Contributions: Z.N. wrote the paper with contributions from all co-authors. Y.Z. (Yinbing Zhao) conceived and designed the research, and provided funding. J.L. and Y.L. contributed to the data processing. X.X. and Y.Z. (Yang Zhang) contributed to the methodology. All authors have read and agreed to the published version of the manuscript.

Funding: This research was supported by the Soft Science Project of Sichuan Provincial Department of Science and Technology (2022JDR0061), the Open Foundation of the State Key Laboratory of Urban and Regional Ecology of China (SKLURE2022-2-6), the Philosophy and Social Sciences Research Fund Project of Chengdu University of Technology in 2021 (YJ2021-YB023),and the Key Laboratory of Supported by Open Foundation of the Research Center for Human Geography of Tibetan Plateau and Its Eastern Edge (Chengdu University of Technology) (RWDL2022-ZD002 and RWDL2021-ZD002).

Data Availability Statement: Data will be made available on reasonable request.

Conflicts of Interest: The authors declare no conflicts of interest.

Abbreviations of Nouns

LR-Jinsha	The lower reaches of the Jinsha River
16 A-class regions	Sixteen counties in the study area are classified as non-impoverished
24 B-class regions	By 2020, 24 counties in the study area had been lifted out of poverty
MODIS	Moderate-Resolution Imaging Spectroradiometer
NDVI	Normalized Difference Vegetation Index
NDBSI	Normalized Difference Built-up and Bareness Index
LST	Land Surface Temperature
WET	Wetness Index
RSEI	Remote sensing ecological index
BRI	Biodiversity richness index
EEI	Ecological environment index
EDI	Economic development index
EcoESTI	Economic structure index
EcoEEI	Economic environment index
EcoESCI	Economic scale index
EECD	Ecological–economic coupling degree
EECCD	Ecological–economic coupling coordination degree
EERDD	Ecological–economic relative development degree

Appendix A. Supplementary Data

Table A1. Weights of EDI evaluation indicators for the five periods.

Indicator \ Year	Total Primary Industry Output	Total Secondary Industry Output	Total Tertiary Industry Output	Urbanization Rate	Nighttime Light Index	Per Capita Cropland Area	Total GDP	Per Capita GDP	Total Retail Sales of Consumer Goods
2000	0.059	0.119	0.111	0.122	0.181	0.042	0.115	0.092	0.159
2005	0.047	0.117	0.153	0.094	0.157	0.037	0.123	0.116	0.157
2010	0.054	0.114	0.154	0.080	0.164	0.043	0.129	0.106	0.157
2015	0.066	0.115	0.143	0.061	0.163	0.046	0.129	0.106	0.171
2020	0.066	0.131	0.162	0.046	0.163	0.053	0.135	0.086	0.157

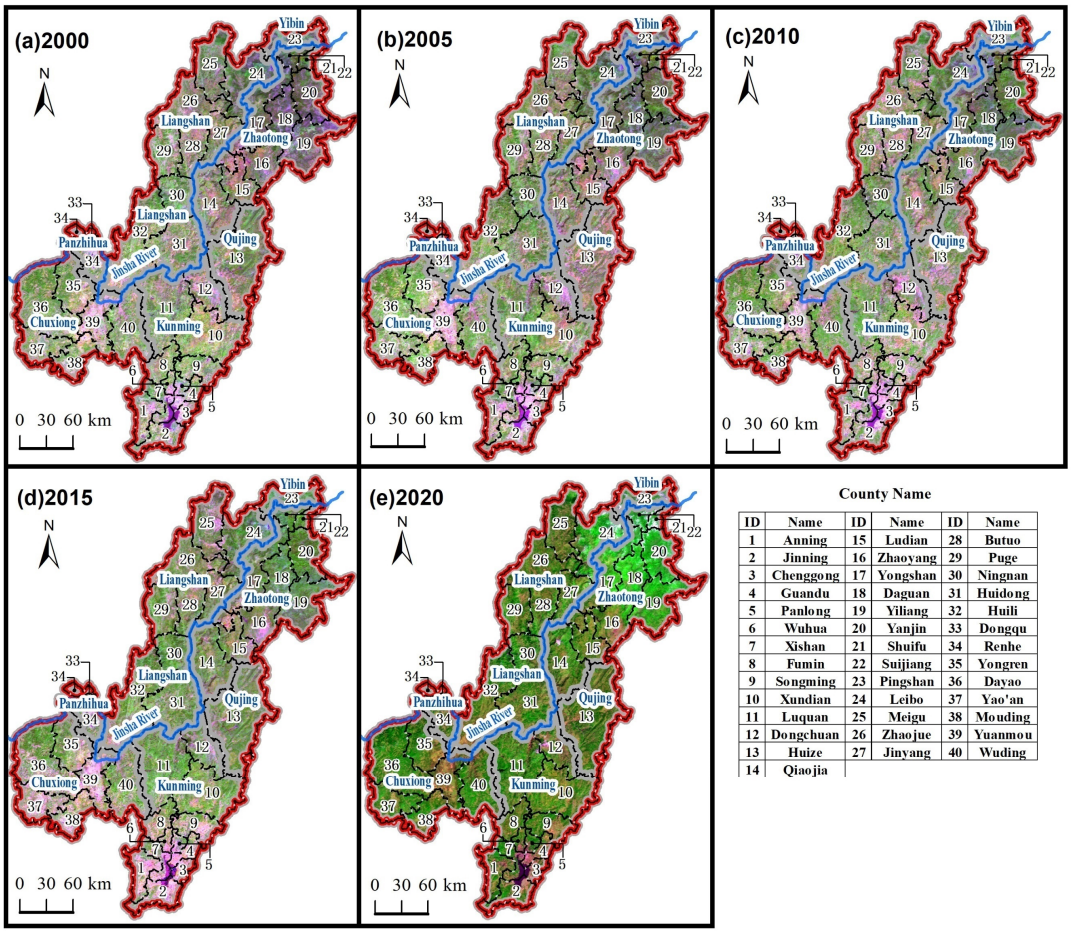


Figure A1. MODIS data for extracting remote sensing ecological indices from five periods.

Table A2. Changes in ecological environment index (EEI) from 2000 to 2020.

County	EEI					County	EEI				
	2000	2005	2010	2015	2020		2000	2005	2010	2015	2020
Suijiang	0.6584	0.6194	0.6491	0.7447	0.7010	Puge	0.4192	0.4237	0.4575	0.4997	0.5213
Shuifu	0.6453	0.5919	0.6278	0.7144	0.6745	Wuhua	0.4140	0.4088	0.4143	0.5088	0.5013
Pingshan	0.6216	0.5949	0.6115	0.6830	0.6600	Yongren	0.4277	0.4392	0.4244	0.4625	0.4865
Yanjin	0.5766	0.5484	0.5760	0.7090	0.6794	Fumin	0.4217	0.4092	0.3903	0.4886	0.4950
Leibo	0.5952	0.5218	0.5614	0.5888	0.6017	Qiaojia	0.3985	0.3952	0.4190	0.4816	0.4949
Daguan	0.4918	0.4793	0.5045	0.5947	0.6299	Huize	0.3891	0.3914	0.3880	0.4866	0.4889
Xishan	0.5054	0.4836	0.5044	0.5599	0.5649	Huidong	0.3924	0.4061	0.3999	0.4510	0.4770
Yao'an	0.5135	0.4872	0.5069	0.5341	0.5509	Xundian	0.3753	0.4086	0.3548	0.4922	0.4791
Yiliang	0.4521	0.4884	0.4789	0.5880	0.5833	Huili	0.3801	0.4039	0.3951	0.4552	0.4706
Dayao	0.5011	0.4983	0.5055	0.5313	0.5504	Zhaojue	0.3649	0.3851	0.4103	0.4434	0.4833
Yongshan	0.4615	0.4608	0.4765	0.5517	0.5616	Butuo	0.3769	0.3871	0.3984	0.4447	0.4762
Panlong	0.4478	0.4511	0.4566	0.5633	0.5520	Guandu	0.4227	0.3980	0.3819	0.4507	0.4270
Anning	0.4352	0.4396	0.4878	0.5427	0.5631	Jinyang	0.3763	0.3912	0.3736	0.4520	0.4413
Wuding	0.4371	0.4604	0.4527	0.5204	0.5510	Zhaoyang	0.3652	0.3668	0.3740	0.4574	0.4549
Meigu	0.4664	0.4565	0.4697	0.4997	0.5167	Chenggong	0.3791	0.3747	0.3658	0.4362	0.4486
Ningnan	0.4608	0.4509	0.4473	0.5091	0.5182	Renhe	0.3781	0.3759	0.3742	0.4108	0.4476
Luquan	0.4275	0.4598	0.4425	0.5173	0.5330	Ludian	0.3502	0.3415	0.3600	0.4353	0.4536
Mouding	0.4453	0.4279	0.4579	0.5027	0.5267	Dongchuan	0.3429	0.3509	0.3249	0.4094	0.4272
Songming	0.4419	0.4500	0.4130	0.5343	0.5190	Dongqu	0.3001	0.3109	0.3154	0.3598	0.4081
Jinning	0.4251	0.4150	0.4533	0.5202	0.5322	Yuanmou	0.2814	0.2903	0.2695	0.3233	0.3615

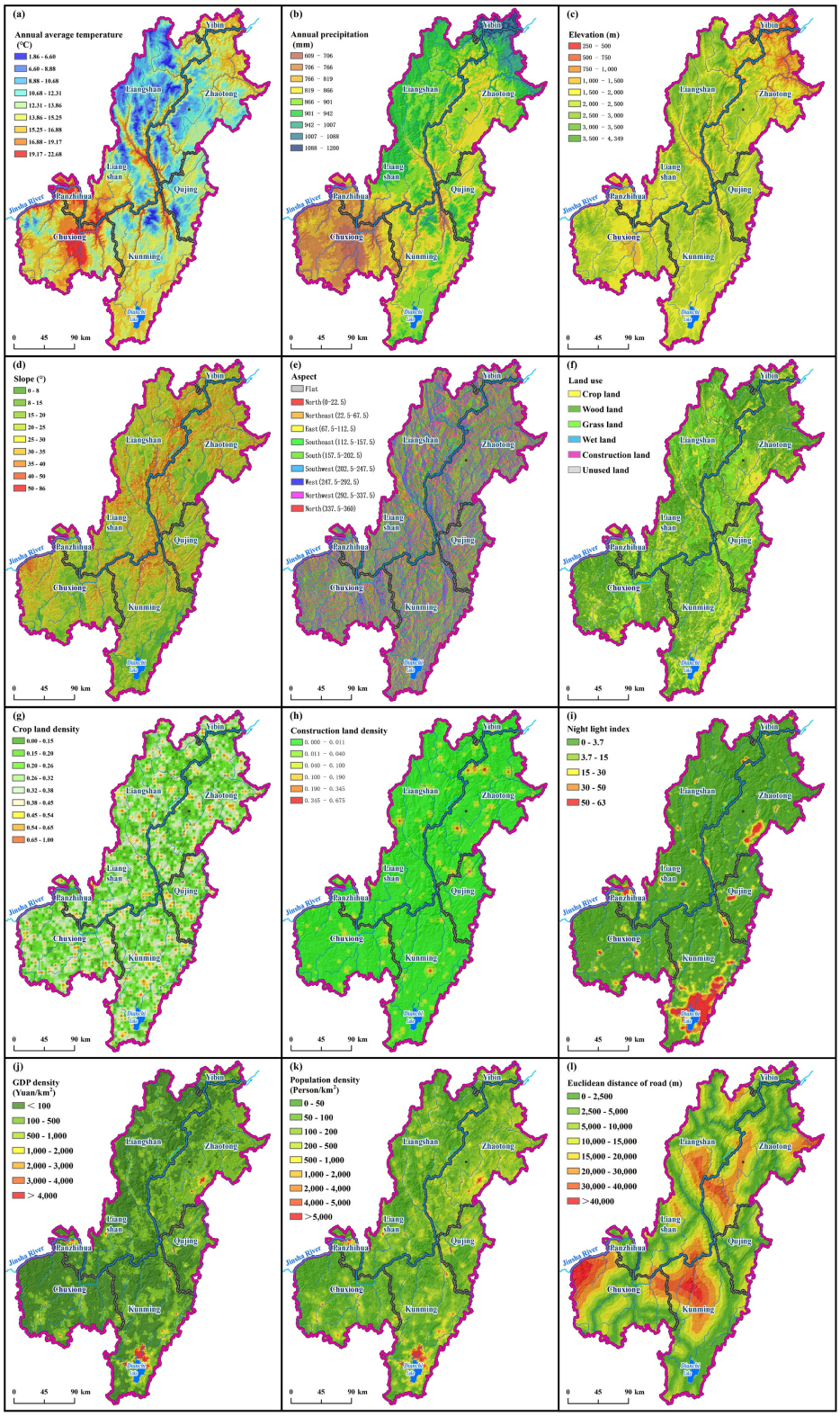


Figure A2. The driving factors of the ecological environment index (EEI):(**a**) Annual average temperature; (**b**) Annual precipitation; (**c**) Elevation; (**d**) Slope; (**e**) Aspect; (**f**) Land use; (**g**) Crop land density; (**h**) Construction land density; (**i**) Night light index; (**j**) GDP density; (**k**) Population density; (**l**) Euclidean distance of road.

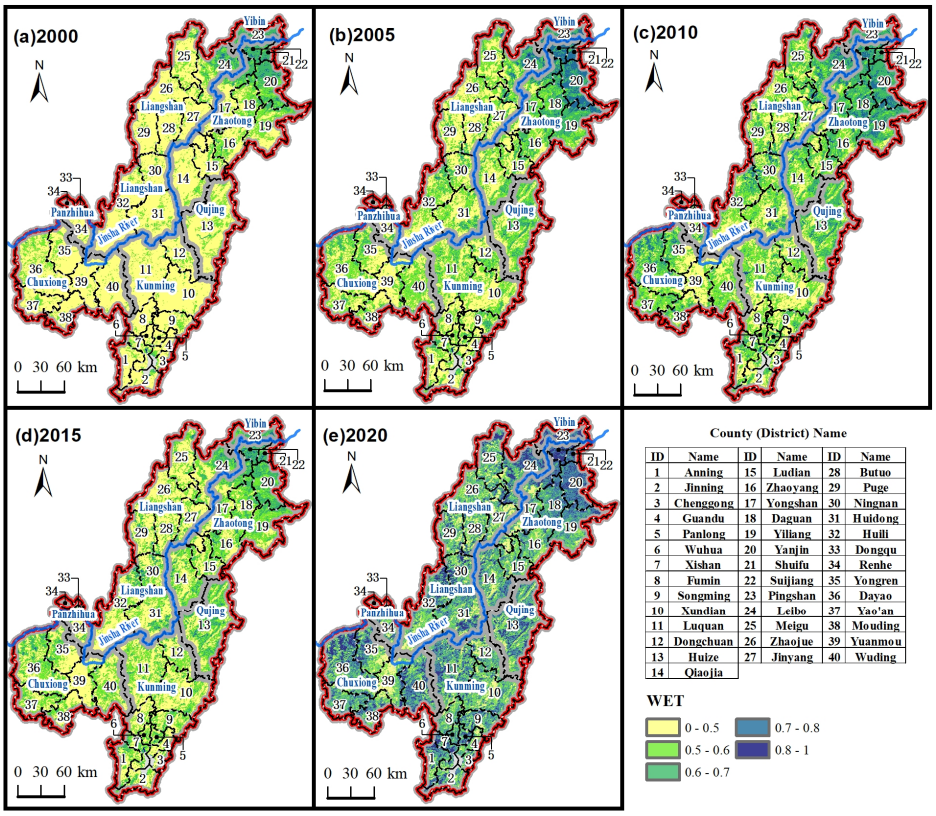


Figure A3. Spatial distribution of WET from 2000 to 2020.

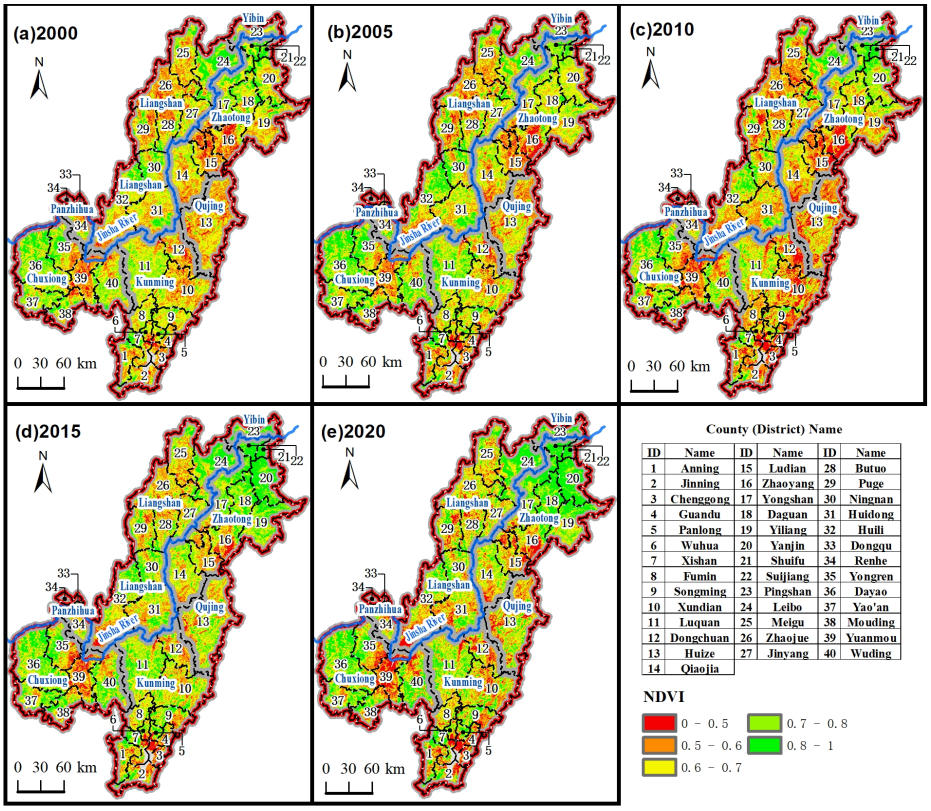


Figure A4. Spatial distribution of NDVI from 2000 to 2020.

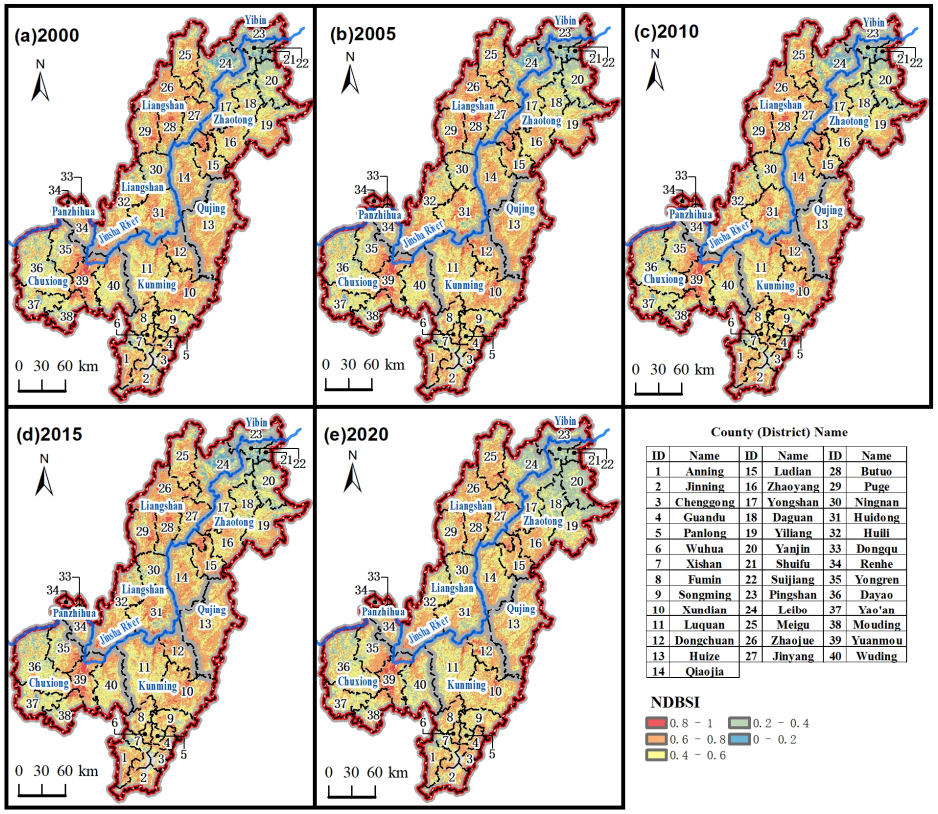


Figure A5. Spatial distribution of NDBSI from 2000 to 2020.

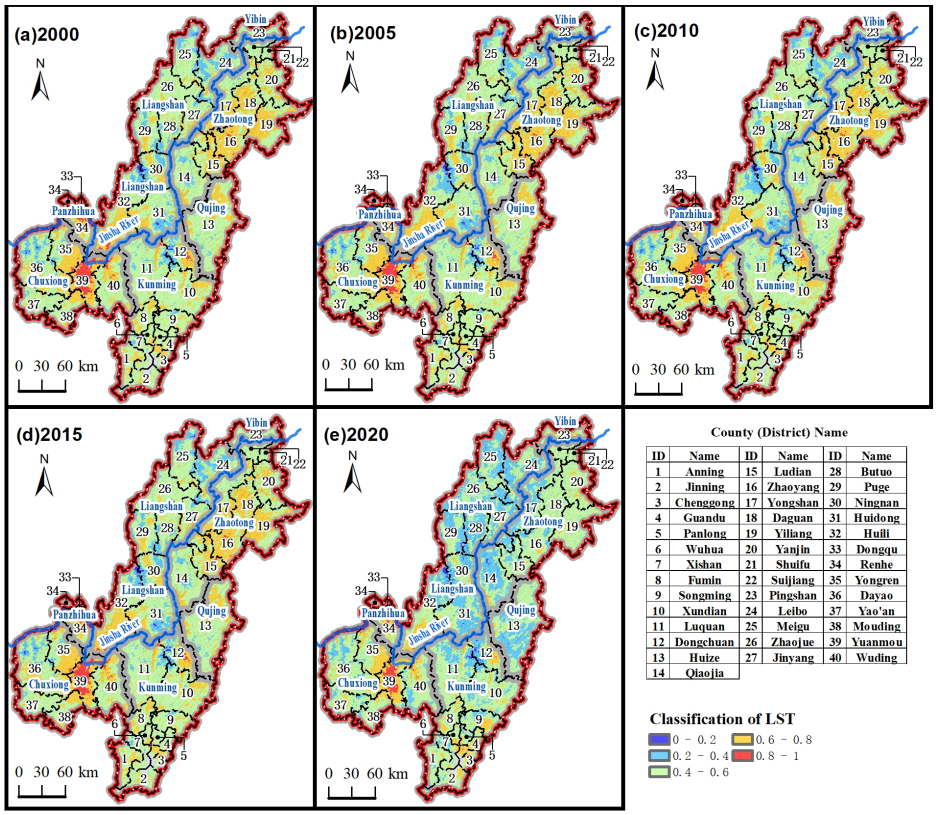


Figure A6. Spatial distribution of LST from 2000 to 2020.

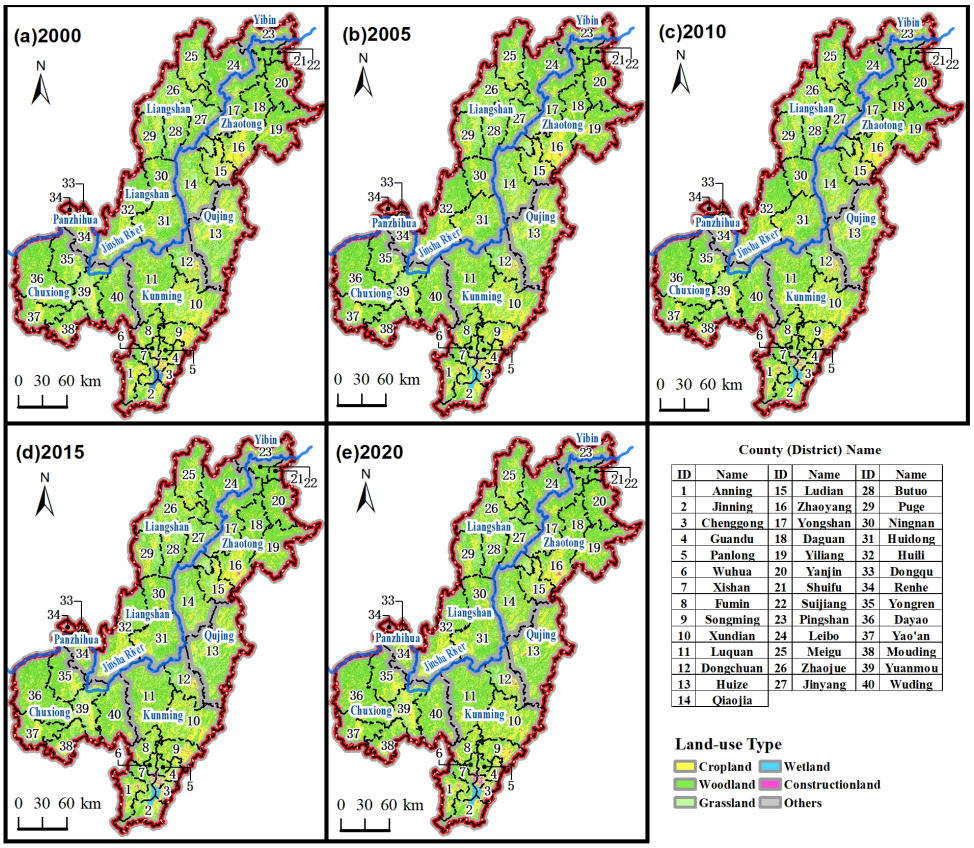


Figure A7. Spatial distribution of land use types from 2000 to 2020.

Table A3. Changes in economic structure index (EcoESTI) from 2000 to 2020.

Name	EcoESTI					Change Rate	Name	EcoESTI					Change Rate
	2000	2005	2010	2015	2020			2000	2005	2010	2015	2020	
Guandu	0.2514	0.2752	0.2692	0.2627	0.3275	0.3026	Yiliang	0.0513	0.0526	0.0530	0.0581	0.0699	0.3624
Wuding	0.0552	0.2883	0.2769	0.2595	0.2999	4.4362	Yuanmou	0.0509	0.0494	0.0530	0.0587	0.0665	0.3070
Xishan	0.1143	0.1573	0.1554	0.1679	0.2103	0.8408	Fumin	0.0447	0.0477	0.0509	0.0650	0.0633	0.4158
Panlong	0.0594	0.1573	0.1616	0.1927	0.2187	2.6813	Dongchuan	0.0454	0.0450	0.0536	0.0637	0.0624	0.3762
Dongqu	0.2004	0.1335	0.1302	0.1329	0.1328	−0.3371	Wuhua	0.0519	0.0521	0.0538	0.0410	0.0702	0.3529
Anning	0.1172	0.1042	0.1010	0.1105	0.1778	0.5174	Ludian	0.0459	0.0456	0.0489	0.0674	0.0587	0.2814
Zhaoyang	0.1391	0.1001	0.1050	0.1196	0.1354	−0.0268	Pingshan	0.0509	0.0477	0.0516	0.0524	0.0636	0.2515
Huili	0.1039	0.1015	0.1283	0.1360	0.1039	−0.0006	Yanjin	0.0467	0.0462	0.0463	0.0721	0.0506	0.0837
Huize	0.0843	0.0853	0.1024	0.0740	0.1428	0.6935	Yao'an	0.0511	0.0493	0.0501	0.0491	0.0608	0.1885
Huidong	0.0851	0.0922	0.1061	0.0581	0.0937	0.1008	Shuifu	0.0417	0.0434	0.0412	0.0747	0.0506	0.2127
Chenggong	0.0677	0.0716	0.0715	0.0726	0.1437	1.1228	Mouding	0.0477	0.0466	0.0482	0.0491	0.0588	0.2341
Jinyang	0.0824	0.0679	0.0729	0.0590	0.0899	0.0919	Leibo	0.0456	0.0483	0.0522	0.0449	0.0553	0.2133
Renhe	0.0678	0.0629	0.0792	0.0503	0.1023	0.5105	Yongren	0.0386	0.0398	0.0406	0.0680	0.0503	0.3046
Dayao	0.0564	0.0551	0.0561	0.1059	0.0732	0.2990	Puge	0.0394	0.0420	0.0434	0.0686	0.0434	0.1037
Luquan	0.0689	0.0620	0.0615	0.0510	0.0863	0.2535	Zhaojue	0.0417	0.0441	0.0447	0.0572	0.0471	0.1293
Xundian	0.0642	0.0647	0.0655	0.0474	0.0838	0.3049	Jinning	0.0381	0.0400	0.0437	0.0572	0.0449	0.1795
Ningnan	0.0511	0.0529	0.0549	0.1011	0.0593	0.1611	Meigu	0.0379	0.0426	0.0426	0.0477	0.0456	0.2027
Songming	0.0659	0.0622	0.0604	0.0517	0.0766	0.1625	Daguan	0.0434	0.0418	0.0407	0.0451	0.0451	0.0384
Qiaojia	0.0546	0.0555	0.0581	0.0545	0.0746	0.3661	Butuo	0.0369	0.0395	0.0420	0.0426	0.0448	0.2144
Yongshan	0.0500	0.0527	0.0511	0.0558	0.0764	0.5279	Suijiang	0.0326	0.0360	0.0376	0.0566	0.0417	0.2773

Table A4. Changes in economic environment index (EcoEEI) from 2000 to 2020.

Name	EcoEEI					Change Rate	Name	EcoEEI					Change Rate
	2000	2005	2010	2015	2020			2000	2005	2010	2015	2020	
Dongqu	0.3375	0.2808	0.2735	0.2490	0.2074	−0.3854	Mouding	0.0757	0.0677	0.0737	0.0658	0.0819	0.0820
Wuding	0.2836	0.2299	0.2265	0.1954	0.1745	−0.3847	Wuhua	0.0744	0.0662	0.0718	0.0711	0.0799	0.0750
Panlong	0.2496	0.2234	0.2169	0.2039	0.1764	−0.2932	Dayao	0.0749	0.0646	0.0704	0.0748	0.0784	0.0467
Guandu	0.1771	0.1668	0.1919	0.2253	0.2361	0.3333	Yao'an	0.0780	0.0683	0.0736	0.0685	0.0728	−0.0659
Chenggong	0.1559	0.1420	0.2057	0.2401	0.2324	0.4907	Huize	0.0697	0.0662	0.0723	0.0701	0.0776	0.1133
Xishan	0.2354	0.1933	0.1927	0.1725	0.1520	−0.3543	Suijiang	0.0764	0.0682	0.0709	0.0616	0.0618	−0.1909
Anning	0.1788	0.1516	0.1530	0.1390	0.1346	−0.2474	Luquan	0.0620	0.0591	0.0708	0.0695	0.0763	0.2294
Renhe	0.1364	0.1346	0.1407	0.1062	0.1105	−0.1899	Ludian	0.0623	0.0579	0.0652	0.0730	0.0785	0.2592
Jinyang	0.0958	0.0893	0.1109	0.1022	0.1086	0.1341	Leibo	0.0676	0.0617	0.0630	0.0691	0.0660	−0.0240
Songming	0.0904	0.0857	0.1093	0.1089	0.1119	0.2380	Puge	0.0777	0.0616	0.0614	0.0613	0.0652	−0.1614
Dongchuan	0.1018	0.0881	0.0959	0.0877	0.0896	−0.1197	Yongshan	0.0609	0.0585	0.0616	0.0622	0.0733	0.2046
Yongren	0.0927	0.0819	0.0919	0.0919	0.0974	0.0511	Jinning	0.0741	0.0629	0.0619	0.0542	0.0622	−0.1612
Zhaoyang	0.0940	0.0803	0.0850	0.0932	0.0963	0.0237	Butuo	0.0731	0.0597	0.0591	0.0587	0.0598	−0.1818
Fumin	0.0872	0.0802	0.0966	0.0858	0.0974	0.1170	Meigu	0.0736	0.0598	0.0576	0.0572	0.0556	−0.2446
Ningnan	0.0906	0.0811	0.0848	0.0811	0.0874	−0.0347	Daguan	0.0606	0.0597	0.0582	0.0584	0.0640	0.0561
Yuanmou	0.0889	0.0746	0.0773	0.0802	0.0966	0.0858	Zhaojue	0.0698	0.0541	0.0558	0.0585	0.0598	−0.1431
Xundian	0.0821	0.0749	0.0894	0.0821	0.0868	0.0577	Pingshan	0.0649	0.0511	0.0518	0.0616	0.0673	0.0359
Huili	0.0735	0.0723	0.0851	0.0855	0.0943	0.2830	Qiaojia	0.0561	0.0507	0.0575	0.0576	0.0701	0.2496
Shuifu	0.0803	0.0807	0.0833	0.0701	0.0756	−0.0586	Yiliang	0.0576	0.0456	0.0453	0.0493	0.0565	−0.0181
Huidong	0.0716	0.0641	0.0684	0.0808	0.0862	0.2051	Yanjin	0.0506	0.0497	0.0510	0.0492	0.0520	0.0285

Table A5. Changes in economic scale index (EcoESCI) from 2000 to 2020.

Name	EcoESCI					Change Rate	Name	EcoESCI					Change Rate
	2000	2005	2010	2015	2020			2000	2005	2010	2015	2020	
Guandu	0.2803	0.3613	0.3401	0.4097	0.3840	0.3696	Xundian	0.0557	0.0566	0.0573	0.0652	0.0762	0.3688
Wuding	0.1255	0.2559	0.4132	0.4341	0.3858	2.0745	Yuanmou	0.0522	0.0513	0.0518	0.0619	0.0786	0.5062
Panlong	0.2161	0.2943	0.2563	0.3130	0.3495	0.6175	Wuhua	0.0505	0.0510	0.0506	0.0635	0.0784	0.5529
Dongqu	0.3045	0.3248	0.2966	0.2563	0.1818	−0.4031	Yao'an	0.0531	0.0538	0.0521	0.0555	0.0723	0.3611
Xishan	0.1401	0.2598	0.2478	0.3274	0.3052	1.1777	Mouding	0.0499	0.0502	0.0515	0.0561	0.0774	0.5499
Anning	0.1510	0.1550	0.1370	0.1708	0.2146	0.4216	Yongren	0.0471	0.0478	0.0479	0.0607	0.0748	0.5886
Renhe	0.0881	0.1014	0.1398	0.1474	0.1265	0.4367	Pingshan	0.0525	0.0479	0.0526	0.0563	0.0655	0.2459
Chenggong	0.0944	0.0959	0.0896	0.1251	0.1786	0.8915	Yongshan	0.0454	0.0497	0.0482	0.0600	0.0710	0.5642
Zhaoyang	0.1241	0.1079	0.1058	0.1169	0.1285	0.0355	Leibo	0.0444	0.0504	0.0583	0.0658	0.0548	0.2335
Huili	0.0816	0.0929	0.1313	0.1263	0.0943	0.1558	Qiaojia	0.0465	0.0474	0.0463	0.0490	0.0537	0.1564
Jinyang	0.0913	0.0744	0.0798	0.0951	0.1032	0.1314	Yiliang	0.0450	0.0480	0.0475	0.0485	0.0526	0.1679
Huidong	0.0701	0.0854	0.1037	0.0952	0.0825	0.1772	Ludian	0.0413	0.0438	0.0464	0.0496	0.0543	0.3161
Shuifu	0.0732	0.0898	0.0745	0.0873	0.0933	0.2743	Puge	0.0445	0.0503	0.0492	0.0489	0.0413	−0.0717
Huize	0.0742	0.0766	0.0759	0.0812	0.1005	0.3534	Jinning	0.0407	0.0436	0.0505	0.0513	0.0465	0.1404
Songming	0.0660	0.0707	0.0686	0.0852	0.0879	0.3325	Yanjin	0.0457	0.0457	0.0444	0.0464	0.0437	−0.0423
Fumin	0.0561	0.0649	0.0689	0.0818	0.0994	0.7697	Butuo	0.0399	0.0437	0.0469	0.0465	0.0409	0.0261
Dongchuan	0.0515	0.0525	0.0708	0.0748	0.0830	0.6118	Daguan	0.0449	0.0425	0.0402	0.0452	0.0443	−0.0131
Ningnan	0.0567	0.0603	0.0660	0.0706	0.0639	0.1274	Suijiang	0.0365	0.0413	0.0448	0.0443	0.0497	0.3630
Luquan	0.0555	0.0529	0.0596	0.0673	0.0812	0.4636	Zhaojue	0.0415	0.0431	0.0430	0.0438	0.0402	−0.0318
Dayao	0.0566	0.0582	0.0556	0.0650	0.0783	0.3844	Meigu	0.0388	0.0437	0.0423	0.0412	0.0385	−0.0062

Table A6. Changes in the economic development index (EDI) from 2000 to 2020.

Name	EDI					Change Rate	Name	EDI					Change Rate
	2000	2005	2010	2015	2020			2000	2005	2010	2015	2020	
Guandu	0.6110	0.7026	0.7009	0.7977	0.8482	0.3880	Yuanmou	0.0924	0.0750	0.0816	0.1010	0.1423	0.5405
Wuhua	0.3656	0.6734	0.8162	0.7891	0.7608	1.0809	Luquan	0.0866	0.0738	0.0913	0.0880	0.1442	0.6649
Dongqu	0.7442	0.6383	0.6000	0.5385	0.4227	−0.4320	Yongren	0.0788	0.0691	0.0797	0.1207	0.1231	0.5629
Panlong	0.4282	0.5746	0.5343	0.6098	0.6451	0.5065	Wuding	0.0770	0.0691	0.0757	0.0758	0.1289	0.6738
Xishan	0.3905	0.5101	0.4953	0.5682	0.5680	0.4544	Yao'an	0.0825	0.0712	0.0753	0.0733	0.1063	0.2881
Anning	0.3474	0.3105	0.2905	0.3205	0.4276	0.2309	Mouding	0.0737	0.0642	0.0729	0.0711	0.1186	0.6095
Chenggong	0.2183	0.2091	0.2666	0.3381	0.4552	1.0849	Yongshan	0.0566	0.0606	0.0605	0.0780	0.1212	1.1399
Zhaoyang	0.2577	0.1881	0.1954	0.2296	0.2606	0.0112	Leibo	0.0579	0.0602	0.0730	0.0800	0.0764	0.3195
Renhe	0.1926	0.1985	0.2592	0.2042	0.2400	0.2457	Ludian	0.0498	0.0470	0.0601	0.0900	0.0919	0.8454
Huili	0.1592	0.1664	0.2439	0.2477	0.1930	0.2123	Pingshan	0.0687	0.0464	0.0557	0.0703	0.0967	0.4084
Jinning	0.1697	0.1313	0.1632	0.1565	0.2022	0.1913	Qiaojia	0.0575	0.0533	0.0615	0.0611	0.0988	0.7186
Huize	0.1287	0.1278	0.1500	0.1253	0.2213	0.7201	Puge	0.0621	0.0536	0.0535	0.0788	0.0503	−0.1895

Table A6. *Cont.*

Name	EDI					Change Rate	Name	EDI					Change Rate
	2000	2005	2010	2015	2020			2000	2005	2010	2015	2020	
Huidong	0.1271	0.1413	0.1774	0.1342	0.1630	0.2827	Yiliang	0.0542	0.0460	0.0454	0.0559	0.0793	0.4636
Songming	0.1226	0.1184	0.1378	0.1460	0.1768	0.4418	Jinyang	0.0533	0.0462	0.0556	0.0627	0.0539	0.0103
Fumin	0.0884	0.0925	0.1159	0.1326	0.1605	0.8160	Suijiang	0.0457	0.0454	0.0529	0.0625	0.0534	0.1689
Dongchuan	0.0989	0.0854	0.1199	0.1264	0.1354	0.3688	Zhaojue	0.0533	0.0410	0.0430	0.0596	0.0474	−0.1123
Ningnan	0.0987	0.0939	0.1052	0.1527	0.1111	0.1253	Yanjin	0.0433	0.0414	0.0414	0.0676	0.0466	0.0774
Shuifu	0.0956	0.1136	0.0987	0.1322	0.1198	0.2530	Daguan	0.0493	0.0437	0.0387	0.0488	0.0538	0.0900
Xundian	0.1024	0.0958	0.1115	0.0949	0.1473	0.4387	Butuo	0.0502	0.0426	0.0475	0.0479	0.0458	−0.0884
Dayao	0.0882	0.0776	0.0816	0.1456	0.1304	0.4783	Meigu	0.0506	0.0458	0.0421	0.0461	0.0400	−0.2111

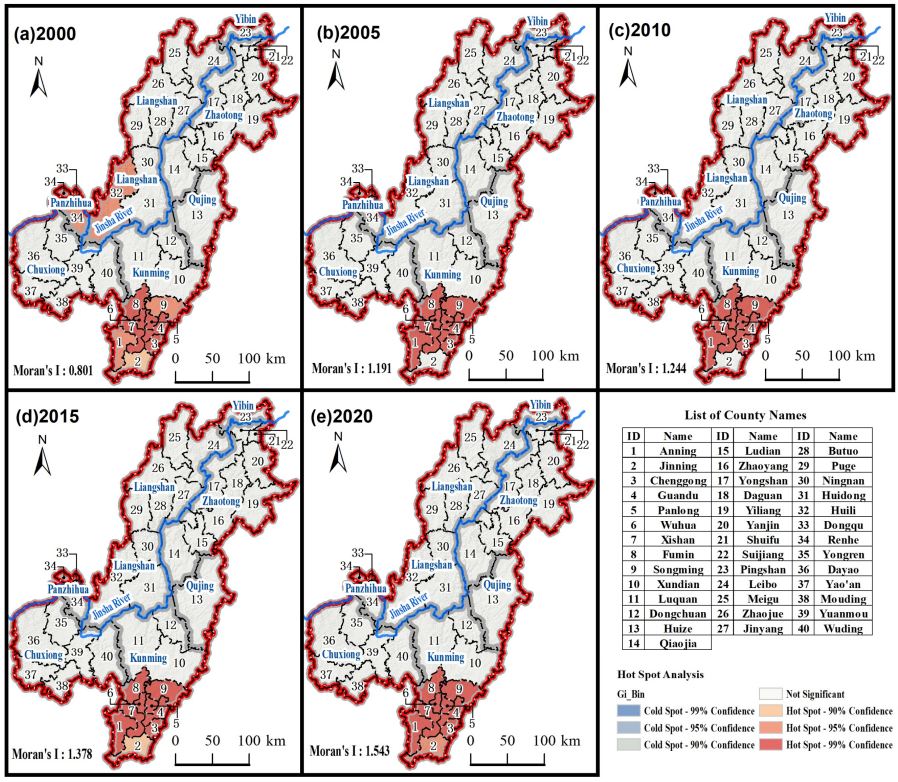


Figure A8. Hotspot analysis of economic development index (EDI).

Table A7. Changes in ecological–economic coupling degree (EECD) from 2000 to 2020.

Name	EECD					Name	EECD				
	2000	2005	2010	2015	2020		2000	2005	2010	2015	2020
Xishan	0.9918	0.9996	1.0000	1.0000	1.0000	Luquan	0.7486	0.6906	0.7532	0.7050	0.8188
Panlong	0.9998	0.9927	0.9969	0.9992	0.9970	Dayao	0.7136	0.6828	0.6918	0.8218	0.7871
Anning	0.9937	0.9851	0.9673	0.9663	0.9906	Wuding	0.7138	0.6736	0.7008	0.6662	0.7840
Chenggong	0.9631	0.9590	0.9876	0.9919	1.0000	Shuifu	0.6706	0.7350	0.6853	0.7259	0.7158
Wuhua	0.9981	0.9697	0.9452	0.9764	0.9786	Ludian	0.6603	0.6521	0.7004	0.7536	0.7486
Guandu	0.9833	0.9609	0.9556	0.9606	0.9439	Mouding	0.6981	0.6735	0.6884	0.6589	0.7747
Zhaoyang	0.9850	0.9467	0.9495	0.9434	0.9624	Yao'an	0.6908	0.6670	0.6713	0.6515	0.7365
Renhe	0.9457	0.9511	0.9834	0.9419	0.9533	Qiaojia	0.6638	0.6474	0.6680	0.6322	0.7448
Dongqu	0.9050	0.9387	0.9505	0.9800	0.9998	Yongshan	0.6240	0.6410	0.6325	0.6587	0.7641
Huili	0.9123	0.9092	0.9716	0.9554	0.9084	Jinyang	0.6595	0.6147	0.6718	0.6543	0.6228
Jinning	0.9032	0.8545	0.8823	0.8433	0.8933	Puge	0.6703	0.6313	0.6124	0.6860	0.5666
Huidong	0.8597	0.8753	0.9228	0.8409	0.8714	Leibo	0.5685	0.6091	0.6383	0.6489	0.6324
Huize	0.8643	0.8616	0.8968	0.8070	0.9263	Zhaojue	0.6671	0.5899	0.5862	0.6463	0.5702

Table A7. *Cont.*

Name	EECD					Name	EECD				
	2000	2005	2010	2015	2020		2000	2005	2010	2015	2020
Yuanmou	0.8627	0.8079	0.8446	0.8518	0.9004	Butuo	0.6443	0.5978	0.6172	0.5926	0.5659
Dongchuan	0.8337	0.7936	0.8875	0.8492	0.8550	Yiliang	0.6183	0.5610	0.5626	0.5632	0.6492
Songming	0.8246	0.8121	0.8662	0.8211	0.8706	Pingshan	0.5987	0.5181	0.5530	0.5817	0.6678
Fumin	0.7570	0.7755	0.8404	0.8196	0.8600	Meigu	0.5945	0.5755	0.5493	0.5561	0.5163
Xundian	0.8207	0.7845	0.8531	0.7363	0.8482	Daguan	0.5756	0.5536	0.5147	0.5294	0.5383
Ningnan	0.7623	0.7554	0.7851	0.8425	0.7625	Yanjin	0.5096	0.5108	0.5000	0.5639	0.4902
Yongren	0.7249	0.6854	0.7297	0.8103	0.8030	Suijiang	0.4927	0.5047	0.5281	0.5345	0.5131

Table A8. Average EECCD and its change rate from 2000 to 2020.

County	Average EECCD	Change Rate	County	Average EECCD	Change Rate
Guandu	0.7418	0.0884	Yao'an	0.4530	0.0837
Wuhua	0.7386	0.2596	Pingshan	0.4526	0.1055
Panlong	0.7234	0.1662	Dongchuan	0.4512	0.1422
Xishan	0.7166	0.1289	Yongren	0.4510	0.1565
Dongqu	0.6642	−0.0626	Wuding	0.4484	0.2056
Anning	0.6386	0.1234	Leibo	0.4462	0.0743
Chenggong	0.5832	0.2537	Mouding	0.4390	0.1737
Zhaoyang	0.5484	0.0596	Yongshan	0.4378	0.2711
Renhe	0.5420	0.1021	Suijiang	0.4324	0.0552
Huili	0.5380	0.1069	Yuanmou	0.4144	0.1841
Jinning	0.5260	0.1062	Yanjin	0.4136	0.0630
Shuifu	0.5186	0.0703	Yiliang	0.4114	0.1717
Songming	0.5056	0.1411	Qiaojia	0.4110	0.2082
Huize	0.5016	0.2135	Puge	0.4066	0.0000
Huidong	0.5004	0.1163	Ludian	0.4000	0.2452
Ningnan	0.4800	0.0606	Daguan	0.3984	0.0861
Dayao	0.4796	0.1285	Jinyang	0.3852	0.0452
Fumin	0.4754	0.2096	Meigu	0.3832	−0.0332
Xundian	0.4628	0.1625	Zhaojue	0.3772	0.0401
Luquan	0.4610	0.2005	Butuo	0.3732	0.0350

Table A9. EECCD in 40 counties from 2000 to 2020.

County	2000	2005	2010	2015	2020	County	2000	2005	2010	2015	2020
Guandu	0.7130	0.7270	0.7190	0.7740	0.7760	Pingshan	0.4550	0.4080	0.4290	0.4680	0.5030
Wuhua	0.6240	0.7240	0.7630	0.7960	0.7860	Yao'an	0.4540	0.4320	0.4420	0.4450	0.4920
Panlong	0.6620	0.7140	0.7030	0.7660	0.7720	Dongchuan	0.4290	0.4160	0.4440	0.4770	0.4900
Xishan	0.6670	0.7050	0.7070	0.7510	0.7530	Yongren	0.4280	0.4170	0.4290	0.4860	0.4950
Dongqu	0.6870	0.6670	0.6600	0.6630	0.6440	Wuding	0.4280	0.4220	0.4300	0.4460	0.5160
Anning	0.6240	0.6080	0.6140	0.6460	0.7010	Leibo	0.4310	0.4210	0.4500	0.4660	0.4630
Chenggong	0.5360	0.5290	0.5590	0.6200	0.6720	Mouding	0.4260	0.4070	0.4270	0.4350	0.5000
Zhaoyang	0.5540	0.5120	0.5200	0.5690	0.5870	Yongshan	0.4020	0.4090	0.4120	0.4550	0.5110
Renhe	0.5190	0.5230	0.5580	0.5380	0.5720	Suijiang	0.4170	0.4100	0.4310	0.4640	0.4400
Huili	0.4960	0.5090	0.5570	0.5790	0.5490	Yanjin	0.3970	0.3880	0.3930	0.4680	0.4220
Jinning	0.5180	0.4830	0.5220	0.5340	0.5730	Yuanmou	0.4020	0.3840	0.3850	0.4250	0.4760
Shuifu	0.4980	0.5090	0.4990	0.5540	0.5330	Qiaojia	0.3890	0.3810	0.4010	0.4140	0.4700
Songming	0.4820	0.4800	0.4880	0.5280	0.5500	Yiliang	0.3960	0.3870	0.3840	0.4260	0.4640
Huize	0.4730	0.4730	0.4910	0.4970	0.5740	Puge	0.4020	0.3880	0.3960	0.4450	0.4020
Huidong	0.4730	0.4890	0.5160	0.4960	0.5280	Ludian	0.3630	0.3560	0.3840	0.4450	0.4520
Ningnan	0.4620	0.4540	0.4660	0.5280	0.4900	Daguan	0.3950	0.3810	0.3740	0.4130	0.4290
Dayao	0.4590	0.4430	0.4510	0.5270	0.5180	Jinyang	0.3760	0.3670	0.3800	0.4100	0.3930
Fumin	0.4390	0.4410	0.4610	0.5050	0.5310	Meigu	0.3920	0.3800	0.3750	0.3900	0.3790
Xundian	0.4430	0.4450	0.4460	0.4650	0.5150	Zhaojue	0.3740	0.3550	0.3650	0.4030	0.3890
Luquan	0.4390	0.4290	0.4480	0.4620	0.5270	Butuo	0.3710	0.3580	0.3710	0.3820	0.3840

Table A10. Ranking of ecological–economic relative development degree (EERDD).

County	EERDD					Average Value	Ranking	County	EERDD					Average Value	Ranking
	2000	2005	2010	2015	2020				2000	2005	2010	2015	2020		
Dongqu	2.4802	2.0527	1.9020	1.4969	1.0358	1.7935	1	Luquan	0.2027	0.1606	0.2064	0.1701	0.2706	0.2021	21
Guandu	1.4456	1.7655	1.8355	1.7701	1.9863	1.7606	2	Dayao	0.1761	0.1557	0.1614	0.2740	0.2370	0.2008	22
Wuhua	0.8832	1.6470	1.9701	1.5507	1.5175	1.5137	3	Wuding	0.1762	0.1501	0.1673	0.1456	0.2340	0.1746	23
Panlong	0.9563	1.2738	1.1701	1.0825	1.1686	1.1303	4	Shuifu	0.1482	0.1918	0.1572	0.1850	0.1776	0.1720	24
Xishan	0.7728	1.0548	0.9820	1.0149	1.0054	0.9660	5	Ludian	0.1422	0.1376	0.1670	0.2067	0.2026	0.1712	25
Chenggong	0.5759	0.5582	0.7289	0.7751	1.0147	0.7305	6	Mouding	0.1655	0.1500	0.1592	0.1414	0.2252	0.1683	26
Anning	0.7984	0.7062	0.5956	0.5906	0.7594	0.6900	7	Yao'an	0.1607	0.1461	0.1486	0.1372	0.1930	0.1571	27
Zhaoyang	0.7055	0.5127	0.5223	0.5020	0.5728	0.5631	8	Qiaojia	0.1442	0.1350	0.1467	0.1269	0.1996	0.1505	28
Renhe	0.5095	0.5281	0.6926	0.4971	0.5361	0.5527	9	Yongshan	0.1227	0.1315	0.1270	0.1413	0.2157	0.1477	29
Huili	0.4189	0.4120	0.6173	0.5441	0.4102	0.4805	10	Jinyang	0.1417	0.1181	0.1489	0.1388	0.1221	0.1339	30
Jinning	0.3993	0.3163	0.3599	0.3008	0.3799	0.3512	11	Puge	0.1481	0.1264	0.1170	0.1577	0.0965	0.1291	31
Huidong	0.3238	0.3480	0.4437	0.2977	0.3418	0.3510	12	Leibo	0.0973	0.1154	0.1301	0.1358	0.1270	0.1211	32
Huize	0.3308	0.3266	0.3865	0.2575	0.4527	0.3508	13	Zhaojue	0.1462	0.1065	0.1049	0.1344	0.0980	0.1180	33
Yuanmou	0.3283	0.2584	0.3026	0.3124	0.3936	0.3191	14	Butuo	0.1333	0.1101	0.1193	0.1077	0.0962	0.1133	34
Dongchuan	0.2885	0.2435	0.3691	0.3089	0.3170	0.3054	15	Yiliang	0.1198	0.0942	0.0949	0.0951	0.1360	0.1080	35
Songming	0.2774	0.2630	0.3337	0.2733	0.3406	0.2976	16	Pingshan	0.1105	0.0780	0.0910	0.1029	0.1466	0.1058	36
Fumin	0.2096	0.2260	0.2970	0.2715	0.3243	0.2657	17	Meigu	0.1086	0.1003	0.0896	0.0922	0.0773	0.0936	37
Xundian	0.2728	0.2344	0.3143	0.1929	0.3074	0.2644	18	Daguan	0.1003	0.0912	0.0768	0.0820	0.0853	0.0871	38
Ningnan	0.2142	0.2083	0.2351	0.2998	0.2144	0.2344	19	Yanjin	0.0750	0.0754	0.0718	0.0954	0.0686	0.0772	39
Yongren	0.1842	0.1573	0.1878	0.2611	0.2531	0.2087	20	Suijiang	0.0694	0.0734	0.0816	0.0839	0.0762	0.0769	40

Table A11. Average ecological–economic relative development degree (EERDD) and its change rate in 40 counties from 2000 to 2020.

County	Average EERDD	Change Rate	County	Average EERDD	Change Rate
Guandu	1.7597	0.3740	Luquan	0.2034	0.3353
Dongqu	1.7374	−0.5824	Dayao	0.2024	0.3459
Wuhua	1.5152	0.7182	Wuding	0.1761	0.3277
Panlong	1.1300	0.2220	Ludian	0.1746	0.4249
Xishan	0.9672	0.3010	Shuifu	0.1721	0.1987
Chenggong	0.7421	0.7620	Mouding	0.1697	0.3608
Anning	0.6873	−0.0488	Yao'an	0.1576	0.2007
Zhaoyang	0.5605	−0.1882	Qiaojia	0.1517	0.3838
Renhe	0.5509	0.0523	Yongshan	0.1500	0.7583
Huili	0.4800	−0.0207	Jinyang	0.1336	−0.1385
Huize	0.3513	0.3688	Puge	0.1285	−0.3482
Jinning	0.3508	−0.0485	Leibo	0.1211	0.3052
Huidong	0.3495	0.0554	Zhaojue	0.1171	−0.3297
Yuanmou	0.3226	0.1992	Butuo	0.1124	−0.2784
Dongchuan	0.3052	0.0986	Yiliang	0.1084	0.1344
Songming	0.2975	0.2277	Pingshan	0.1065	0.3264
Fumin	0.2676	0.5470	Meigu	0.0932	−0.2878
Xundian	0.2616	0.1269	Daguan	0.0868	−0.1490
Ningnan	0.2353	0.0007	Yanjin	0.0778	−0.0856
Yongren	0.2104	0.3741	Suijiang	0.0771	0.0980

References

1. Tian, Y.; Huang, P.; Zhao, X. Spatial analysis, coupling coordination, and efficiency evaluation of green innovation: A case study of the Yangtze River Economic Belt. *PLoS ONE* **2020**, *15*, e0243459. [CrossRef] [PubMed]
2. An, S.; Zhang, S.; Hou, H.; Zhang, Y.; Xu, H.; Liang, J. Coupling coordination analysis of the ecology and economy in the Yellow River Basin under the background of high-quality development. *Land* **2022**, *11*, 1235. [CrossRef]
3. Ekins, P. The Kuznets curve for the environment and economic growth: Examining the evidence. *Environ. Plan. A* **1997**, *29*, 805–830. [CrossRef]
4. Leal, P.H.; Marques, A.C. The evolution of the environmental Kuznets curve hypothesis assessment: A literature review under a critical analysis perspective. *Heliyon* **2022**, *8*, e11521. [CrossRef]
5. Sagar, A.D.; Najam, A. The human development index: A critical review. *Ecol. Econ.* **1998**, *25*, 249–264. [CrossRef]
6. Phillips, J. Determining sustainability using the Environmental Performance Index and Human Development Index–An alternative approach to the Environmental Human Index through a holistic quantitative dynamic framework. *Sci. Total Environ.* **2023**, *884*, 163752. [CrossRef]
7. Zheng, X.; Chen, Y. A better strategy: Using green GDP to measure economic health. *Front. Environ. Sci.* **2024**, *12*, 1459764. [CrossRef]

8. Zheng, Y.; Chen, M. Promoting Green GDP for more balanced development. *Envtl. Pol'y L.* **2007**, *37*, 416.
9. Ahmed, Z.; Asghar, M.M.; Malik, M.N.; Nawaz, K. Moving towards a sustainable environment: The dynamic linkage between natural resources, human capital, urbanization, economic growth, and ecological footprint in China. *Resour. Policy* **2020**, *67*, 101677. [CrossRef]
10. Desli, E.; Gkoulgkoutsika, A.; Sdrolia, E.; Zarotiadis, G. Eco-efficiency: A methodological framework and assessment. *Clean. Environ. Syst.* **2021**, *3*, 100049. [CrossRef]
11. Coluccia, B.; Valente, D.; Fusco, G.; De Leo, F.; Porrini, D. Assessing agricultural eco-efficiency in Italian Regions. *Ecol. Indic.* **2020**, *116*, 106483. [CrossRef]
12. Babcicky, P. Rethinking the foundations of sustainability measurement: The limitations of the Environmental Sustainability Index (ESI). *Social. Indic. Res.* **2013**, *113*, 133–157. [CrossRef]
13. Cucchiella, F.; D'Adamo, I.; Gastaldi, M.; Koh, S.L.; Rosa, P. A comparison of environmental and energetic performance of European countries: A sustainability index. *Renew. Sustain. Energy Rev.* **2017**, *78*, 401–413. [CrossRef]
14. Mora, F. The use of ecological integrity indicators within the natural capital index framework: The ecological and economic value of the remnant natural capital of México. *J. Nat. Conserv.* **2019**, *47*, 77–92. [CrossRef]
15. Czúcz, B.; Molnár, Z.; Horváth, F.; Nagy, G.G.; Botta-Dukát, Z.; Török, K. Using the natural capital index framework as a scalable aggregation methodology for regional biodiversity indicators. *J. Nat. Conserv.* **2012**, *20*, 144–152. [CrossRef]
16. Han, X.; Cao, T.; Yan, X. Comprehensive evaluation of ecological environment quality of mining area based on sustainable development indicators: A case study of Yanzhou Mining in China. *Environ. Dev. Sustain.* **2021**, *23*, 7581–7605. [CrossRef]
17. Li, F.; Wang, F.; Liu, H.; Huang, K.; Yu, Y.; Huang, B. A comparative analysis of ecosystem service valuation methods: Taking Beijing, China as a case. *Ecol. Indic.* **2023**, *154*, 110872. [CrossRef]
18. Kang, N.; Hou, L.; Huang, J.; Liu, H. Ecosystem services valuation in China: A meta-analysis. *Sci. Total Environ.* **2022**, *809*, 151122. [CrossRef]
19. Li, L.; Fan, Z.; Feng, W.; Yuxin, C.; Keyu, Q. Coupling coordination degree spatial analysis and driving factor between socio-economic and eco-environment in northern China. *Ecol. Indic.* **2022**, *135*, 108555. [CrossRef]
20. Wang, Y.; Song, C.; Cheng, C.; Wang, H.; Wang, X.; Gao, P. Modelling and evaluating the economy-resource-ecological environment system of a third-polar city using system dynamics and ranked weights-based coupling coordination degree model. *Cities* **2023**, *133*, 104151. [CrossRef]
21. Shi, T.; Yang, S.; Zhang, W.; Zhou, Q. Coupling coordination degree measurement and spatiotemporal heterogeneity between economic development and ecological environment----Empirical evidence from tropical and subtropical regions of China. *J. Clean. Prod.* **2020**, *244*, 118739. [CrossRef]
22. Jiang, H.-N.; Zhang, W.-Z.; Yu, J.-H.; Zhang, J.-W. Spatial coupling of innovative milieu and industrial structure transformation of resource-based cities in Shanxi province. *J. Nat. Resour.* **2020**, *35*, 269–283. [CrossRef]
23. Guan, D.; Gao, W.; Su, W.; Li, H.; Hokao, K. Modeling and dynamic assessment of urban economy–resource–environment system with a coupled system dynamics–geographic information system model. *Ecol. Indic.* **2011**, *11*, 1333–1344. [CrossRef]
24. Fang, W.; An, H.; Li, H.; Gao, X.; Sun, X.; Zhong, W. Accessing on the sustainability of urban ecological-economic systems by means of a coupled emergy and system dynamics model: A case study of Beijing. *Energy Policy* **2017**, *100*, 326–337. [CrossRef]
25. Moffatt, I.; Hanley, N. Modelling sustainable development: Systems dynamic and input–ouput approaches. *Environ. Model. Softw.* **2001**, *16*, 545–557. [CrossRef]
26. Long, X.; Wu, S.; Wang, J.; Wu, P.; Wang, Z. Urban water environment carrying capacity based on VPOSR-coefficient of variation-grey correlation model: A case of Beijing, China. *Ecol. Indic.* **2022**, *138*, 108863. [CrossRef]
27. Ke, S.; Qiao, D.; Chen, Z. Analysis of the influencing factors on China's forestry economic growth based on grey correlation model. *For. Econ. Rev.* **2019**, *1*, 17–31. [CrossRef]
28. Wang, Z.; Yang, L.; Yin, J.; Zhang, B. Assessment and prediction of environmental sustainability in China based on a modified ecological footprint model. *Resour. Conserv. Recycl.* **2018**, *132*, 301–313. [CrossRef]
29. Sabir, S.; Gorus, M.S. The impact of globalization on ecological footprint: Empirical evidence from the South Asian countries. *Environ. Sci. Pollut. Res.* **2019**, *26*, 33387–33398. [CrossRef]
30. Zuo, Z.; Guo, H.; Cheng, J.; Li, Y. How to achieve new progress in ecological civilization construction?–Based on cloud model and coupling coordination degree model. *Ecol. Indic.* **2021**, *127*, 107789. [CrossRef]
31. Tomal, M. Evaluation of coupling coordination degree and convergence behaviour of local development: A spatiotemporal analysis of all Polish municipalities over the period 2003–2019. *Sustain. Cities Soc.* **2021**, *71*, 102992. [CrossRef]
32. Zhu, X.; Zuo, X.; Li, H. The dual effects of heterogeneous environmental regulation on the technological innovation of Chinese steel enterprises—Based on a high-dimensional fixed effects model. *Ecol. Econ.* **2021**, *188*, 107113. [CrossRef]
33. Cheng, J.; Zhang, X.; Gao, Q. Analysis of the spatio-temporal changes and driving factors of the marine economic–ecological–social coupling coordination: A case study of 11 coastal regions in China. *Ecol. Indic.* **2023**, *153*, 110392. [CrossRef]
34. Zhang, Q.; Shen, J.; Sun, F. Spatiotemporal differentiation of coupling coordination degree between economic development and water environment and its influencing factors using GWR in China's province. *Ecol. Model.* **2021**, *462*, 109794. [CrossRef]
35. Lv, L.; Chen, C.; Wang, Z. Spatiotemporal differentiation and the obstacle factors influencing the coupling coordination between economic development and water pollution control capability in the Yangtze River Economic Belt. *Environ. Sci. Pollut. Res.* **2022**, *29*, 75681–75698. [CrossRef]

36. Sun, Q.; Sui, Y.-J. Agricultural Green Ecological Efficiency Evaluation Using BP Neural Network–DEA Model. *Systems* **2023**, *11*, 291. [CrossRef]
37. Wu, M.; Wei, Y.; Lam, P.T.; Liu, F.; Li, Y. Is urban development ecologically sustainable? Ecological footprint analysis and prediction based on a modified artificial neural network model: A case study of Tianjin in China. *J. Clean. Prod.* **2019**, *237*, 117795. [CrossRef]
38. Chang, C.-P.; Dong, M.; Sui, B.; Chu, Y. Driving forces of global carbon emissions: From time-and spatial-dynamic perspectives. *Econ. Model.* **2019**, *77*, 70–80. [CrossRef]
39. Duan, C.; Zhu, W.; Wang, S.; Chen, B. Drivers of global carbon emissions 1990–2014. *J. Clean. Prod.* **2022**, *371*, 133371. [CrossRef]
40. Sueyoshi, T.; Yuan, Y. Social sustainability measured by intermediate approach for DEA environmental assessment: Chinese regional planning for economic development and pollution prevention. *Energy Econ.* **2017**, *66*, 154–166. [CrossRef]
41. Wu, X.; Liu, S.; Cheng, F.; Hou, X.; Zhang, Y.; Dong, S.; Liu, G. A regional strategy for ecological sustainability: A case study in Southwest China. *Sci. Total Environ.* **2018**, *616*, 1224–1234. [CrossRef] [PubMed]
42. Han, Z.; Jiao, S.; Zhang, X.; Xie, F.; Ran, J.; Jin, R.; Xu, S. Seeking sustainable development policies at the municipal level based on the triad of city, economy and environment: Evidence from Hunan province, China. *J. Environ. Manag.* **2021**, *290*, 112554. [CrossRef] [PubMed]
43. Artmann, M.; Inostroza, L.; Fan, P. Urban sprawl, compact urban development and green cities. How much do we know, how much do we agree? *Ecol. Indic.* **2019**, *96*, 3–9. [CrossRef]
44. Yuan, L.; Li, R.; He, W.; Wu, X.; Kong, Y.; Degefu, D.M.; Ramsey, T.S. Coordination of the industrial-ecological economy in the Yangtze River Economic Belt, China. *Front. Environ. Sci.* **2022**, *10*, 882221. [CrossRef]
45. Liu, L.; Yang, Y.; Liu, S.; Gong, X.; Zhao, Y.; Jin, R.; Duan, H.; Jiang, P. A comparative study of green growth efficiency in Yangtze River Economic Belt and Yellow River Basin between 2010 and 2020. *Ecol. Indic.* **2023**, *150*, 110214. [CrossRef]
46. Song, Y.-S.; Du, C.; Yang, C.; Qin, C. Ecological Environmental Quality Evaluation of Yellow River Basin. *Procedia Eng.* **2012**, *28*, 754–758. [CrossRef]
47. Zhang, Z.; Li, H.; Cao, Y. Research on the coordinated development of economic development and ecological environment of nine Provinces (regions) in the Yellow River Basin. *Sustainability* **2022**, *14*, 13102. [CrossRef]
48. Zhang, S.; Yang, P.; Xia, J.; Qi, K.; Wang, W.; Cai, W.; Chen, N. Research and analysis of ecological environment quality in the Middle Reaches of the Yangtze River Basin between 2000 and 2019. *Remote Sens.* **2021**, *13*, 4475. [CrossRef]
49. Zhang, Y.; Sun, M.; Yang, R.; Li, X.; Zhang, L.; Li, M. Decoupling water environment pressures from economic growth in the Yangtze River Economic Belt, China. *Ecol. Indic.* **2021**, *122*, 107314. [CrossRef]
50. Sun, J.; Zhou, L.; Zong, H. Landscape pattern vulnerability of the eastern Hengduan Mountains, China and response to elevation and artificial disturbance. *Land* **2022**, *11*, 1110. [CrossRef]
51. Qin, Y.; Wang, F.; Zhang, S.; Tu, Y.; Chen, C.; Yang, Y. Impacts of cascade hydropower development on aquatic environment in middle and lower reaches of Jinsha River, China: A review. *Environ. Sci. Pollut. Res.* **2024**, *31*, 54363–54380. [CrossRef] [PubMed]
52. Liu, Y.; Xu, Y. A geographic identification of multidimensional poverty in rural China under the framework of sustainable livelihoods analysis. *Appl. Geogr.* **2016**, *73*, 62–76. [CrossRef]
53. Huang, X.-R.; Gao, L.-Y.; Yang, P.-P.; Xi, Y.-Y. Cumulative impact of dam constructions on streamflow and sediment regime in lower reaches of the Jinsha River, China. *J. Mt. Sci.* **2018**, *15*, 2752–2765. [CrossRef]
54. Zhang, X.-F.; Yan, H.-C.; Yue, Y.; Xu, Q.-X. Quantifying natural and anthropogenic impacts on runoff and sediment load: An investigation on the middle and lower reaches of the Jinsha River Basin. *J. Hydrol. Reg. Stud.* **2019**, *25*, 100617. [CrossRef]
55. Li, B.; Pan, B.; Cheng, W.; Han, J.; Qi, D.; Zhu, C. Research on geomorphological regionalization of China. *Acta Geogr. Sin.* **2013**, *68*, 291–306. [CrossRef]
56. Zheng, J.; Bian, J.J.; Ge, Q.; Hao, Z.; Yin, Y.; Liao, Y. The climate regionalization in China for 1981–2010. *Chin. Sci. Bull* **2013**, *58*, 3088–3099.
57. Gorelick, N.; Hancher, M.; Dixon, M.; Ilyushchenko, S.; Thau, D.; Moore, R. Google Earth Engine: Planetary-scale geospatial analysis for everyone. *Remote Sens. Environ.* **2017**, *202*, 18–27. [CrossRef]
58. Deng, M.; Chen, J.; Tao, F.; Zhu, J.; Wang, M. On the coupling and coordination development between environment and economy: A case study in the Yangtze River Delta of China. *Int. J. Environ. Res. Public Health* **2022**, *19*, 586. [CrossRef]
59. Li, W.; Yi, P.; Zhang, D.; Zhou, Y. Assessment of coordinated development between social economy and ecological environment: Case study of resource-based cities in Northeastern China. *Sustain. Cities Soc.* **2020**, *59*, 102208. [CrossRef]
60. Fan, W.; Wang, H.; Liu, Y.; Liu, H. Spatio-temporal variation of the coupling relationship between urbanization and air quality: A case study of Shandong Province. *J. Clean. Prod.* **2020**, *272*, 122812. [CrossRef]
61. Chen, J.; Li, Z.; Dong, Y.; Song, M.; Shahbaz, M.; Xie, Q. Coupling coordination between carbon emissions and the eco-environment in China. *J. Clean. Prod.* **2020**, *276*, 123848. [CrossRef]
62. Cheng, X.; Long, R.; Chen, H.; Li, Q. Coupling coordination degree and spatial dynamic evolution of a regional green competitiveness system–A case study from China. *Ecol. Indic.* **2019**, *104*, 489–500. [CrossRef]
63. Liao, S.; Wu, Y.; Wong, S.W.; Shen, L. Provincial perspective analysis on the coordination between urbanization growth and resource environment carrying capacity (RECC) in China. *Sci. Total Environ.* **2020**, *730*, 138964. [CrossRef] [PubMed]
64. Li, Y.F.; Li, Y.; Zhou, Y.; Shi, Y.L.; Zhu, X.D. Investigation of a coupling model of coordination between urbanization and the environment. *J. Environ. Manag.* **2012**, *98*, 127–133. [CrossRef]

65. Xu, H. A remote sensing urban ecological index and its application. *Acta Ecol. Sin.* **2013**, *33*, 7853–7862.
66. Xu, H.; Wang, Y.; Guan, H.; Shi, T.; Hu, X. Detecting Ecological Changes with a Remote Sensing Based Ecological Index (RSEI) Produced Time Series and Change Vector Analysis. *Remote Sens.* **2019**, *11*, 2345. [CrossRef]
67. Zhou, J.X.; Chen, J.; Chen, X.H.; Zhu, X.L.; Qiu, Y.A.; Song, H.H.; Rao, Y.H.; Zhang, C.S.; Cao, X.; Cui, X.H. Sensitivity of six typical spatiotemporal fusion methods to different influential factors: A comparative study for a normalized difference vegetation index time series reconstruction. *Remote Sens. Environ.* **2021**, *252*, 112130. [CrossRef]
68. Solomos, S.; Abuelgasim, A.; Spyrou, C.; Binietoglou, I.; Nickovic, S. Development of a dynamic dust source map for NMME-DREAM v1.0 model based on MODIS Normalized Difference Vegetation Index (NDVI) over the Arabian Peninsula. *Geosci. Model Dev.* **2019**, *12*, 979–988. [CrossRef]
69. Nguyen, C.T.; Chidthaisong, A.; Diem, P.K.; Huo, L.Z. A Modified Bare Soil Index to Identify Bare Land Features during Agricultural Fallow-Period in Southeast Asia Using Landsat 8. *Land* **2021**, *10*, 231. [CrossRef]
70. Suharyadi, R.; Umarhadi, D.A.; Awanda, D.; Widyatmanti, W. Exploring Built-Up Indices and Machine Learning Regressions for Multi-Temporal Building Density Monitoring Based on Landsat Series. *Sensors* **2022**, *22*, 4716. [CrossRef]
71. Nanjam, R.; Ahmadi, F.F. A New Spatiotemporal Model for Analyzing the Variations of Urban Heat Islands Using Remotely Sensed Multi Spectral Images: The Case of Mashhad City, Iran. *J. Indian. Soc. Remote* **2021**, *49*, 2489–2502. [CrossRef]
72. Xie, F.; Fan, H. Deriving drought indices from MODIS vegetation indices (NDVI/EVI) and Land Surface Temperature (LST): Is data reconstruction necessary? *Int. J. Appl. Earth Obs.* **2021**, *101*, 102352. [CrossRef]
73. Jolliffe, I.T.; Cadima, J. Principal component analysis: A review and recent developments. *Philos. Trans. R. Soc. A* **2016**, *374*, 20150202. [CrossRef] [PubMed]
74. Dos Santos, P.H.; Neves, S.M.; Sant'Anna, D.O.; de Oliveira, C.H.; Carvalho, H.D. The analytic hierarchy process supporting decision making for sustainable development: An overview of applications. *J. Clean. Prod.* **2019**, *212*, 119–138. [CrossRef]
75. Zhu, Y.X.; Tian, D.Z.; Yan, F. Effectiveness of Entropy Weight Method in Decision-Making. *Math. Probl. Eng.* **2020**, *2020*, 3564835. [CrossRef]
76. Dou, S.; Zhu, Y.; Xu, D.; Amuakwa-Mensah, F. Ecological challenges in the economic recovery of resource-depleted cities in China. *J. Environ. Manag.* **2023**, *333*, 117406. [CrossRef]
77. Xu, Y.; Dai, Q.-Y.; Lu, Y.-G.; Zhao, C.; Huang, W.-T.; Xu, M.; Feng, Y.-X. Identification of ecologically sensitive zones affected by climate change and anthropogenic activities in Southwest China through a NDVI-based spatial-temporal model. *Ecol. Indic.* **2024**, *158*, 111482. [CrossRef]
78. Praveen, B.; Talukdar, S.; Shahfahad; Mahato, S.; Mondal, J.; Sharma, P.; Islam, A.M.T.; Rahman, A. Analyzing trend and forecasting of rainfall changes in India using non-parametrical and machine learning approaches. *Sci. Rep.* **2020**, *10*, 10342. [CrossRef]
79. Zhang, M.M.; Kafy, A.A.; Ren, B.; Zhang, Y.W.; Tan, S.K.; Li, J.X. Application of the Optimal Parameter Geographic Detector Model in the Identification of Influencing Factors of Ecological Quality in Guangzhou, China. *Land* **2022**, *11*, 1303. [CrossRef]
80. Wei, W.; Jin, C.G.; Han, Y.; Huang, Z.H.; Niu, T.; Li, J.K. The Coordinated Development and Regulation Research on Public Health, Ecological Environment and Economic Development: Evidence from the Yellow River Basin of China. *Int. J. Environ. Res. Public Health* **2022**, *19*, 6927. [CrossRef]
81. Park, Y.S.; Lek, S. Chapter 7—Artificial Neural Networks: Multilayer Perceptron for Ecological Modeling. In *Developments in Environmental Modelling*; Jørgensen, S.E., Ed.; Elsevier: Amsterdam, The Netherlands, 2016; Volume 28, pp. 123–140.
82. Chen, Q.; Chen, H.; Zhang, J.; Hou, Y.; Shen, M.; Chen, J.; Xu, C. Impacts of climate change and LULC change on runoff in the Jinsha River Basin. *J. Geogr. Sci.* **2020**, *30*, 85–102. [CrossRef]
83. Zhou, Y.; Yi, Y.-J.; Liu, H.-X.; Tang, C.-H.; Zhu, Y.-l.; Zhang, S.-H. Effect of geomorphologic features and climate change on vegetation distribution in the arid hot valleys of Jinsha River, Southwest China. *J. Mt. Sci.* **2022**, *19*, 2874–2885. [CrossRef]
84. Zhou, J.; Lu, T. Long-Term Spatial and Temporal Variation of Near Surface Air Temperature in Southwest China During 1969–2018. *Front. Earth Sci.* **2021**, *9*, 753757. [CrossRef]
85. Yetemen, O.; Istanbulluoglu, E.; Flores-Cervantes, J.H.; Vivoni, E.R.; Bras, R.L. Ecohydrologic role of solar radiation on landscape evolution. *Water Resour. Res.* **2015**, *51*, 1127–1157. [CrossRef]
86. Yang, J.; El-Kassaby, Y.A.; Guan, W. The effect of slope aspect on vegetation attributes in a mountainous dry valley, Southwest China. *Sci. Rep.* **2020**, *10*, 16465. [CrossRef]
87. Li, J.; Dong, S.; Yang, Z.; Peng, M.; Liu, S.; Li, X. Effects of cascade hydropower dams on the structure and distribution of riparian and upland vegetation along the middle-lower Lancang-Mekong River. *For. Ecol. Manag.* **2012**, *284*, 251–259. [CrossRef]
88. Zhou, Y.; Yi, Y.; Liu, H.; Tang, C.; Zhang, S. Spatiotemporal dynamic of soil erosion and the key factors impact processes over semi-arid catchments in Southwest China. *Ecol. Eng.* **2024**, *201*, 107217. [CrossRef]
89. Liu, S.; Wang, C.; Wang, P.; Chen, J.; Wang, X.; Yuan, Q. Anthropogenic disturbances on distribution and sources of pharmaceuticals and personal care products throughout the Jinsha River Basin, China. *Environ. Res.* **2021**, *198*, 110449. [CrossRef]
90. Schmidt, A.H.; Denn, A.R.; Hidy, A.J.; Bierman, P.R.; Tang, Y. Human and natural controls on erosion in the Lower Jinsha River, China. *J. Asian Earth Sci.* **2019**, *170*, 351–359. [CrossRef]
91. Liu, F.; Yang, L.; Wang, S. Spatial and temporal evolution and correlation analysis of landscape ecological risks and ecosystem service values in the Jinsha River Basin. *J. Resour. Ecol.* **2023**, *14*, 914–927. [CrossRef]

92. Zhang, Y.; Shang, K.; Shi, Z.; Wang, H.; Li, X. Spatial pattern of the vitality of Chinese characteristic towns: A perspective from nighttime lights. *Land* **2022**, *11*, 85. [CrossRef]
93. Yuan, J.; Li, R.; Huang, K. Driving factors of the variation of ecosystem service and the trade-off and synergistic relationships in typical karst basin. *Ecol. Indic.* **2022**, *142*, 109253. [CrossRef]
94. Lian, Y.; You, G.J.-Y.; Lin, K.; Jiang, Z.; Zhang, C.; Qin, X. Characteristics of climate change in southwest China karst region and their potential environmental impacts. *Environ. Earth Sci.* **2015**, *74*, 937–944. [CrossRef]
95. Soga, M.; Gaston, K.J. The ecology of human–nature interactions. *Proc. R. Soc. B* **2020**, *287*, 20191882. [CrossRef] [PubMed]
96. Liu, Q.; Hao, Y.; Stebler, E.; Tanaka, N.; Zou, C.B. Impact of plant functional types on coherence between precipitation and soil moisture: A wavelet analysis. *Geophys. Res. Lett.* **2017**, *44*, 12197–112207. [CrossRef]
97. Ding, X.; Shao, X.; Wang, J.; Peng, S.; Shi, J. Research on the Spatial-Temporal Pattern Evolution and Driving Force of Ecological Environment Quality in Kunming City Based on Remote Sensing Ecological Environment Index in the Past 25 Years. *Pol. J. Environ. Stud.* **2023**, *33*, 1073–1089. [CrossRef]
98. Li, W.; Xie, S.; Wang, Y.; Huang, J.; Cheng, X. Effects of urban expansion on ecosystem health in Southwest China from a multi-perspective analysis. *J. Clean. Prod.* **2021**, *294*, 126341. [CrossRef]
99. Yao, S.; Jiang, Y.; Su, X.; Wang, R. Evaluation of Regional Eco-Efficiency and Improvement Paths in the Yangtze River Economic Belt under the "Double Carbon" Target. *Pol. J. Environ. Stud.* **2024**, *33*, 4879–4892. [CrossRef]
100. Dai, X.; Li, W.; Liu, Z.; Tong, C.; Li, C.; Zeng, J.; Ye, Y.; Li, W.; Shan, Y.; Zhou, J.; et al. Effects of Mining on Urban Environmental Change: A Case Study of Panzhihua. *Remote Sens.* **2022**, *14*, 6004. [CrossRef]
101. Yang, R.Y.; Zhong, C.B. Land Suitability Evaluation of Sorghum Planting in Luquan County of Jinsha River Dry and Hot Valley Based on the Perspective of Sustainable Development of Characteristic Poverty Alleviation Industry. *Agriculture* **2022**, *12*, 1852. [CrossRef]
102. Ma, L.; Chung, J.; Thorson, S. E-government in China: Bringing economic development through administrative reform. *Gov. Inf. Q.* **2005**, *22*, 20–37. [CrossRef]
103. Qi, Y.; Yang, Y.; Jin, F. China's economic development stage and its spatio-temporal evolution: A prefectural-level analysis. *J. Geogr. Sci.* **2013**, *23*, 297–314. [CrossRef]
104. Sun, M.; Yang, R.; Li, X.; Zhang, L.; Liu, Q. Designing a path for the sustainable development of key ecological function zones: A case study of southwest China. *Glob. Ecol. Conserv.* **2021**, *31*, e01840. [CrossRef]
105. Zhao, L. Spatial Pattern Evolution and Spatial Transformation Trend of Industry in China. *Sci. Geogr. Sin.* **2021**, *41*, 387–396. [CrossRef]
106. Sang, Y.-F.; Wang, Z.; Liu, C. Spatial and temporal variability of daily temperature during 1961–2010 in the Yangtze River Basin, China. *Quat. Int.* **2013**, *304*, 33–42. [CrossRef]
107. Ning, Y.; Liu, S.G.; Zhao, S.Q.; Liu, M.C.; Gao, H.Q.; Gong, P. Urban growth rates, trajectories, and multi-dimensional disparities in China. *Cities* **2022**, *126*, 103717. [CrossRef]
108. Ge, Y.; Yuan, Y.; Hu, S.; Ren, Z.; Wu, Y. Space–time variability analysis of poverty alleviation performance in China's poverty-stricken areas. *Spat. Stat.* **2017**, *21*, 460–474. [CrossRef]
109. Teng, Y.; Yang, J.; Zuo, R.; Wang, J. Impact of urbanization and industrialization upon surface water quality: A pilot study of Panzhihua mining town. *J. Earth Sci.* **2011**, *22*, 658–668. [CrossRef]
110. Liu, M.; Zhang, Z.; Zhang, H.; Yang, M.; Song, D.; Ou, X. Spatial-Temporal Monitoring of Urban Growth: A Case in Kunming, Southwest China. In Proceedings of the Geo-Informatics in Resource Management and Sustainable Ecosystem, Hong Kong, China, 18–20 November 2016; pp. 116–127.
111. Liu, T.; Yu, L.; Chen, X.; Li, X.; Du, Z.; Yan, Y.; Peng, D.; Gong, P. Utilizing nighttime light datasets to uncover the spatial patterns of county-level relative poverty-returning risk in China and its alleviating factors. *J. Clean. Prod.* **2024**, *448*, 141682. [CrossRef]
112. Li, H.B.; Jin, X.B.; McCormick, B.P.; Tittonell, P.; Liu, J.; Han, B.; Sun, R.; Zhou, Y.K. Analysis of the contribution of land consolidation to sustainable poverty alleviation under various natural conditions. *Land Use Policy* **2023**, *133*, 106871. [CrossRef]
113. Deng, Y.; Wang, S.; Bai, X.; Tian, Y.; Wu, L.; Xiao, J.; Chen, F.; Qian, Q. Relationship among land surface temperature and LUCC, NDVI in typical karst area. *Sci. Rep.* **2018**, *8*, 641. [CrossRef] [PubMed]
114. Chen, X.; Li, X. The Imbalanced Pattern of Population and Economy and Its Influencing Factors in the Wumeng Mountain Area. *J. Resour. Ecol.* **2024**, *15*, 937–950. [CrossRef]
115. Yang, Y.; Fang, Y.-p.; Xu, Y.; Zhang, Y. Assessment of urban resilience based on the transformation of resource-based cities: A case study of Panzhihua, China. *Ecol. Soc.* **2021**, *26*, 20. [CrossRef]
116. Emran, M.S.; Hou, Z. Access to markets and rural poverty: Evidence from household consumption in China. *Rev. Econ. Stat.* **2013**, *95*, 682–697. [CrossRef]
117. Su, J.; Shen, T.; Jin, S. Ecological efficiency evaluation and driving factor analysis of the coupling coordination of the logistics industry and manufacturing industry. *Environ. Sci. Pollut. Res.* **2022**, *29*, 62458–62474. [CrossRef]
118. Wang, J.; Han, Q.; Wu, K.; Xu, Z.; Liu, P. Spatial-temporal patterns and evolution characteristics of the coordinated development of industrial economy, natural resources and environment in China. *Resour. Policy* **2022**, *75*, 102463. [CrossRef]

119. Jiang, S.; Chen, X.; Smettem, K.; Wang, T. Climate and land use influences on changing spatiotemporal patterns of mountain vegetation cover in southwest China. *Ecol. Indic.* **2021**, *121*, 107193. [CrossRef]
120. Li, W.; Wang, Y.; Xie, S.; Cheng, X. Spatiotemporal evolution scenarios and the coupling analysis of ecosystem health with land use change in Southwest China. *Ecol. Eng.* **2022**, *179*, 106607. [CrossRef]

Disclaimer/Publisher's Note: The statements, opinions and data contained in all publications are solely those of the individual author(s) and contributor(s) and not of MDPI and/or the editor(s). MDPI and/or the editor(s) disclaim responsibility for any injury to people or property resulting from any ideas, methods, instructions or products referred to in the content.